Lectures on spintronics

Master 2 Univ. Grenoble Alpes

Vincent Baltz
CNRS Researcher at SPINTEC

Lecture 1	–	04 Dec.
Lecture 2	–	07 Dec.
Lecture 3	–	11 Dec.
Lecture 4	–	14 Dec.
Exercises 1 & 2	–	21 Dec.

vincent.baltz@cea.fr
https://fr.linkedin.com/in/vincentbaltz
www.spintec.fr/af-spintronics/

Lectures on spintronics

Master 2 Univ. Grenoble Alpes

Vincent Baltz
CNRS Researcher at SPINTEC

Lecture 1	–	04 Dec.
Lecture 2	–	07 Dec.
Lecture 3	–	11 Dec.
Lecture 4	–	14 Dec.
Exercises 1 & 2	–	21 Dec.

spintec
SPIN IN ELECTRONICS

vincent.baltz@cea.fr
https://fr.linkedin.com/in/vincentbaltz
www.spintec.fr/af-spintronics/

Note about the delivery of these lectures:

- Incomplete slides distributed at the beginning of each lecture
- Mix of slideshow and writing down on the blackboard
- Complete slides posted online at the end of the 5 lectures
- Although the timing is very tight, asking/sending questions is encouraged
- 'Quiz Test' on the lectures: December 21

vincent.baltz@cea.fr
https://fr.linkedin.com/in/vincentbaltz
www.spintec.fr/af-spintronics/

Outline

1h30

I. **Brief overview of the field of spintronics and its applications**

II. **First notions to describe electron and spin transport – AMR, CIP-GMR**

1h30

III. Spin accumulation – CPP-GMR

1h30

IV. Transfer of angular momentum – STT

1h30

V. Berry curvature, parity and time symmetries – AHE

VI. Brief non-exhaustive introduction to current topics

1h30

Exercise 1 - Anisotropic magnetoresistance (AMR)

Exercise 2 – The spin pumping (SP) and inverse spin Hall effects (ISHE)

I. Brief overview of the field of spintronics and its applications

$\mathbf{s} \propto (m_e \mathbf{r} \times \mathbf{v})$ / $\mathbf{m} \propto (-\frac{e}{2} \mathbf{r} \times \mathbf{v})$

Spin angular momentum / Spin magnetic moment

Internal quantum properties of the electron

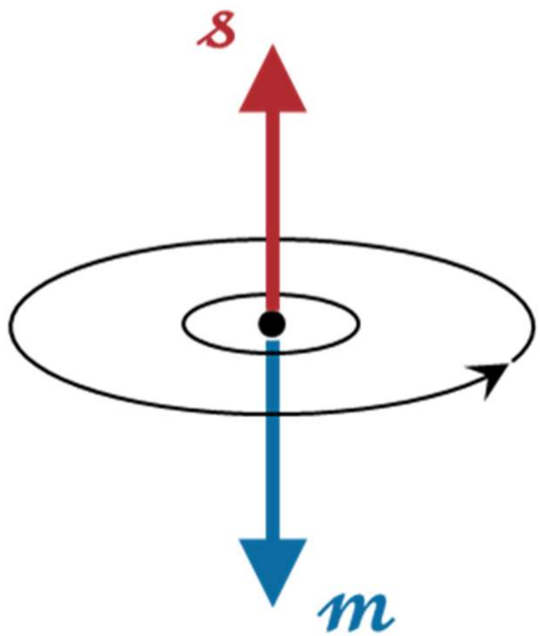

DOI: 10.1051/978-2-7598-2917-0.c002

Notation: moment (↓)-spin(⇑) electron

spin projection quantum number

$$s = m_s \hbar \text{ with } m_s = \pm \frac{1}{2}$$

$$\mathbf{m} = -\frac{e}{2m_e} g \mathbf{s}$$

Landé factor

$$\Rightarrow m \simeq \mp \mu_B \text{ with } \mu_B = \frac{e\hbar}{2m_e}$$

and $g \simeq 2$

$$\boxed{\mathbf{m} = -|\gamma| \mathbf{s}}$$

where $\gamma = -\frac{e}{2m_e} g < 0$ is the gyromagnetic ratio

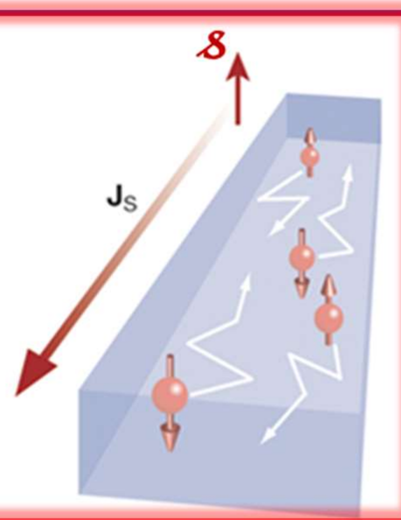

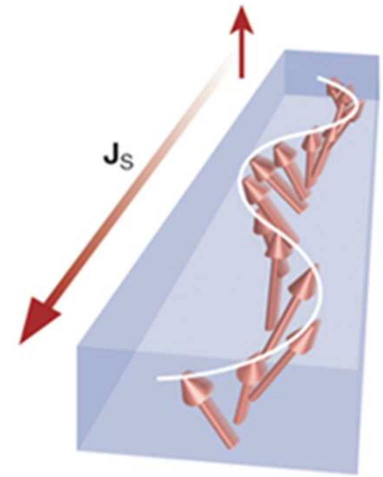

Nature 464, 262 (2010)

Electronics exploits charge transport

Unpolarized currents

Spin electronics exploits spin transport

- on top of moving charges: **electronic transport**

Polarized currents in magnetic materials

Pure spin current in magnetic & non-magnetic materials

- via exchange interactions: **magnonic transport/spin waves**

Pure spin current in magnetic materials

This series of lectures:

- **focuses on the electronic transport of spin**
- **introduces some key underlying physical principles of spintronics**

First, brief introduction to:

- some of the flagship applications of spintronics

Success story #1

1988
Discovery of **the GMR effect**

1991
Practical implementation in spin-valves

1997-now
Commercial product (sensor), in billions of HDD

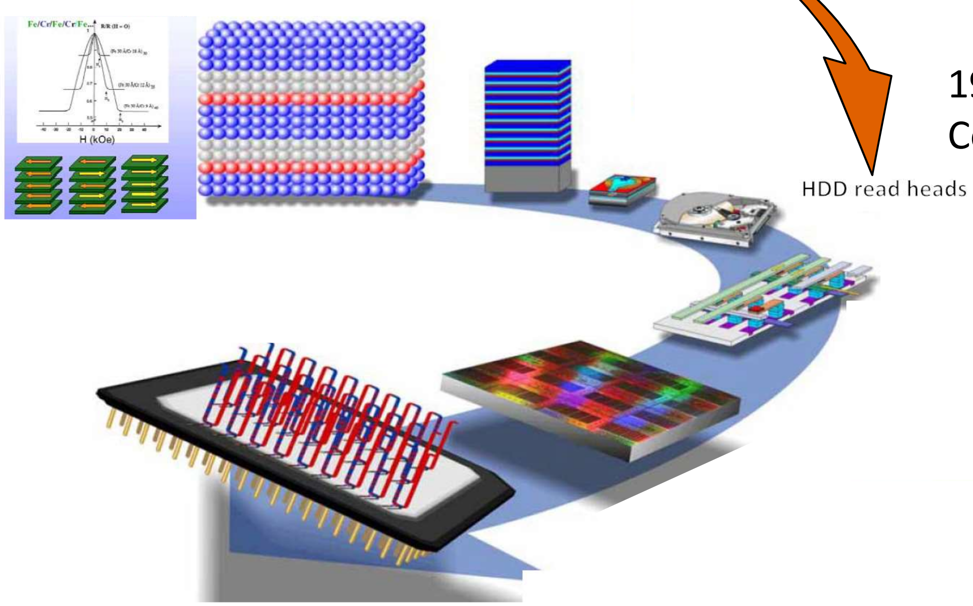

Nobel Prize 2007

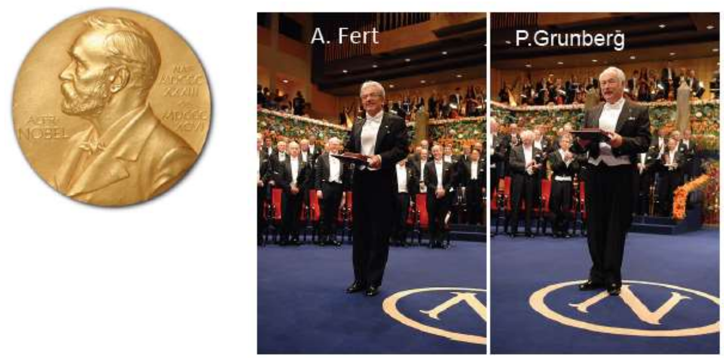

Success story #2

MRAM is not the best in each category but it scores everywhere

1995
Discovery of **the STT effect**

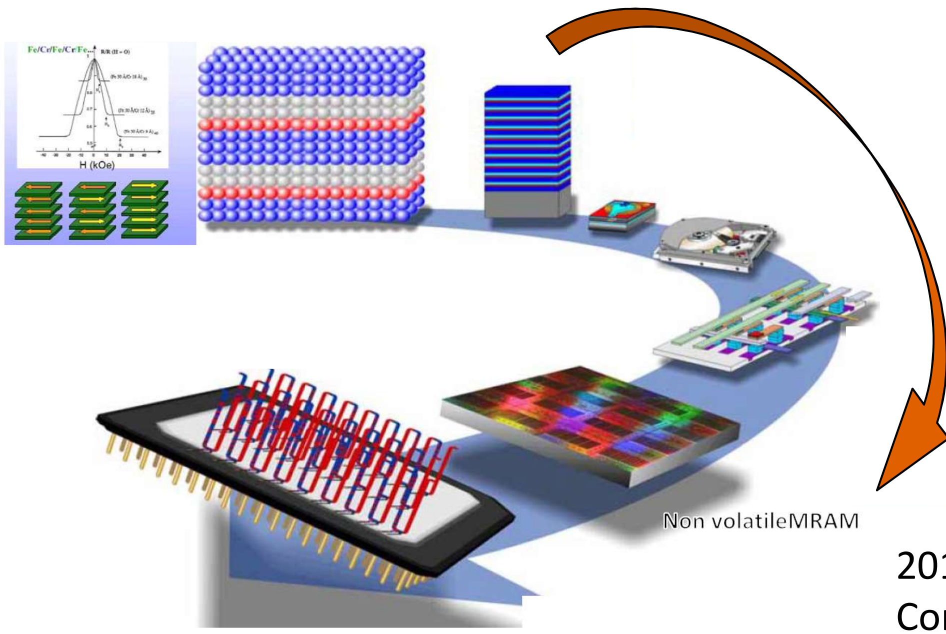

2005
Practical implementation in TMR junctions

2013-now
Commercial product (MRAM / non-volatile memory)

Many more success stories to come

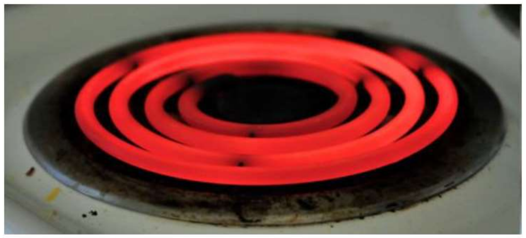

Kitchen Stove

≈ 10 W/cm²

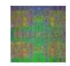

Microprocessor Die

≈ 100 W/cm²

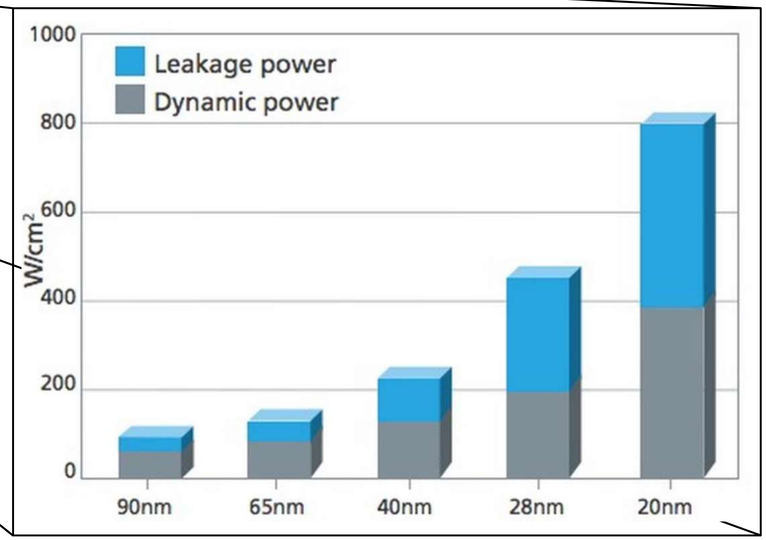

Energy harvesting:

- Miniaturization of electronics is hampered by energy consumption issues
- **Spin (currents)** may circumvent such issues

Numerous fields of applications:

- Information technology - IT (e.g. memory, processors, data security)
- Biomedical (e.g. sensors)
- Telecommunication (e.g. transceiver)
- Artificial intelligence - AI (e.g. neuromorphic computing)

Many more success stories to come

'More transistors and magnets are produced in fabs than grains of rice are grown in paddy fields' (tcd Dublin)

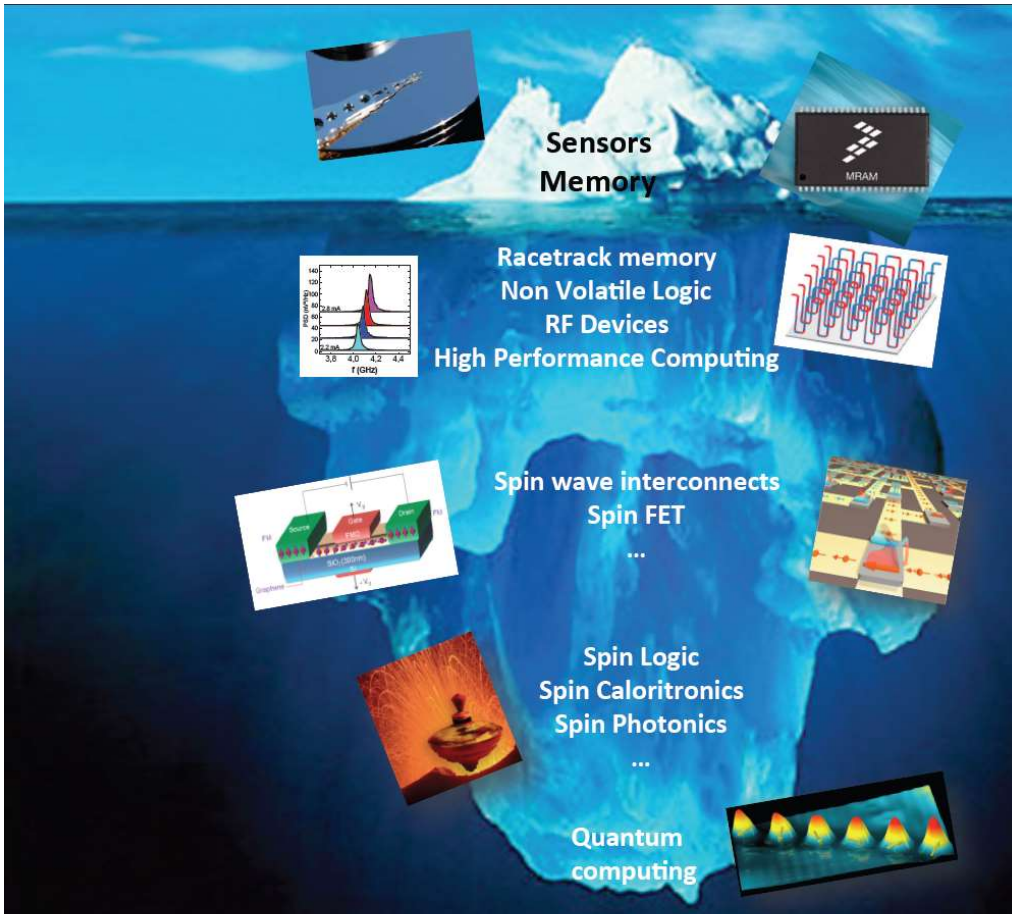

The goal of this series of lectures is: **to give you the basic knowledge to understand most of the underlying physical principles of spintronics**

II. First notions to describe electron and spin transport – AMR, CIP-GMR

Different transport regimes

Quantum	$\psi(\boldsymbol{r}, t)$	AMR 'CFJ', STT 'Slonczewski', Berry curvature …
Semiclassical	$f(\boldsymbol{r}, \boldsymbol{k}, t)$	GMR drift-diffusion 'Valet&Fert'…
Classical	$n(\boldsymbol{r}, t)$	Drift-diffusion 'Drude'…
Phenomenological		All: AMR, GMR, TMR …

$\psi(\boldsymbol{r}, t)$: wavefunction
$f(\boldsymbol{r}, \boldsymbol{k}, t)$: distribution function
$n(\boldsymbol{r}, t)$: density

Notation: **bold** is used for vectors, e.g. $\boldsymbol{r} = \vec{r}$

Majority moment (↑)-spin(⇓) and minority moment (↓)-spin(⇑) electrons are considered to flow in separate channels. This is known as the two current model. It was introduced in 1936 by N. F. Mott.

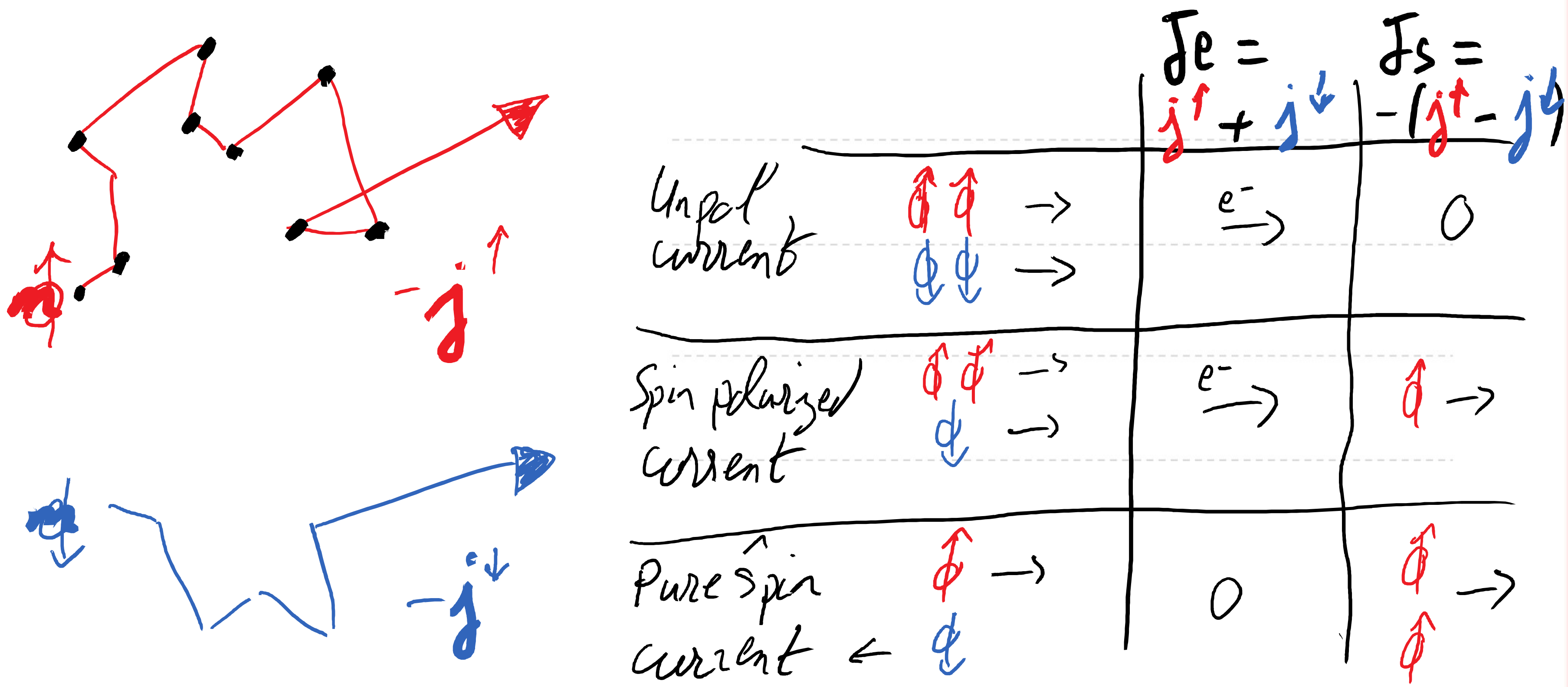

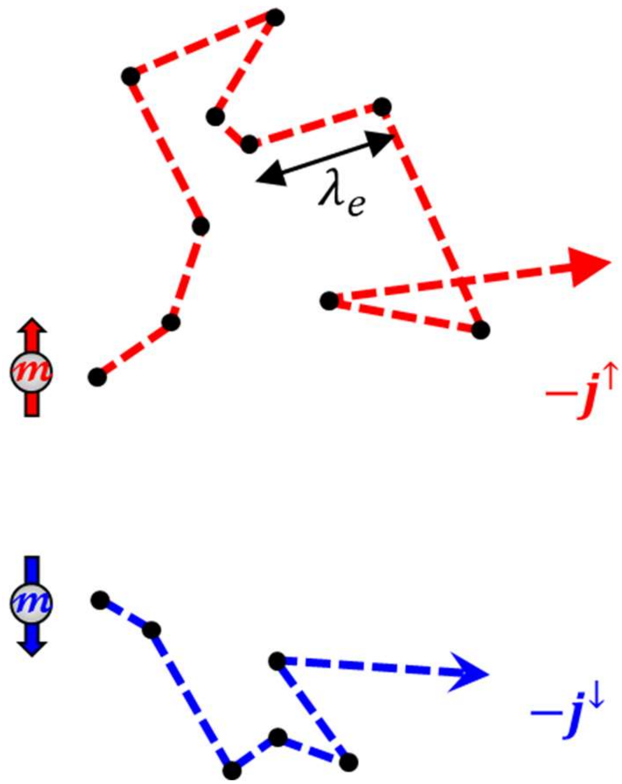

DOI: 10.1051/978-2-7598-2917-0.c002

Drude model of electronic transport

$$j = \sigma E \qquad \sigma = \frac{N(\varepsilon_F)\, e^2 D}{m_e}$$

$$j = \frac{\sigma \nabla \mu}{e} \qquad E = -\nabla V$$

$$\mu = \mu_e = -eV$$

μ_e: electrostatic potential (energy); V: electric potential

Electron mean free path

$$\lambda_e = v_F \tau_e$$

v_F: Fermi velocity; τ_e: scattering time

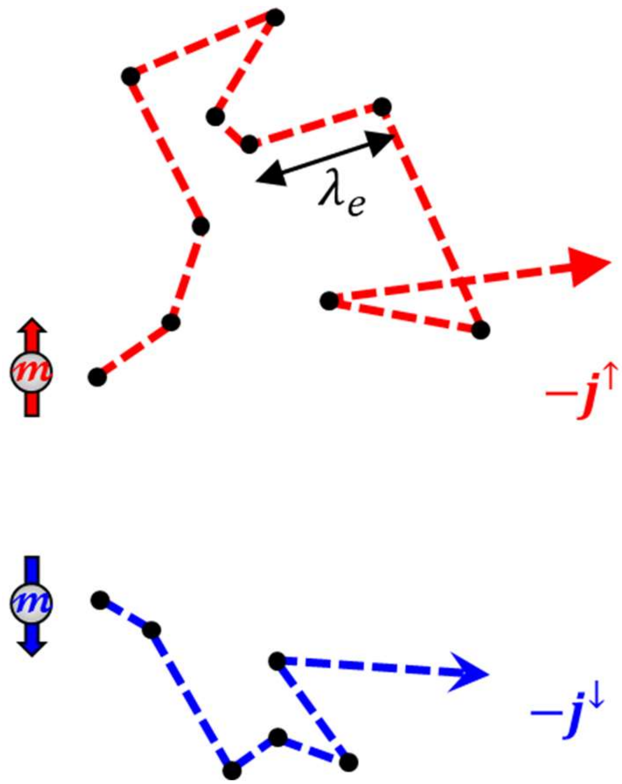

DOI: 10.1051/978-2-7598-2917-0.c002

In the next slides, we will explain why τ_e is spin-dependent, making $\boldsymbol{j}^{\uparrow} \neq \boldsymbol{j}^{\downarrow}$

Spin-dependent generalized Ohm's law

$$j^{\uparrow(\downarrow)} = \sigma^{\uparrow(\downarrow)} \frac{\nabla \mu^{\uparrow(\downarrow)}}{e}$$

(2 equations)

In metals, conduction processes occur at or near the Fermi surface (for $\varepsilon = \varepsilon_F$)

Copper

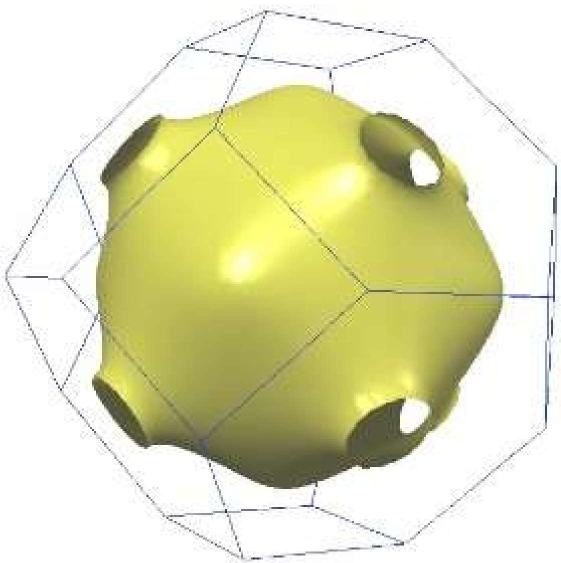

$3d^{10}4s^1$

Aluminium

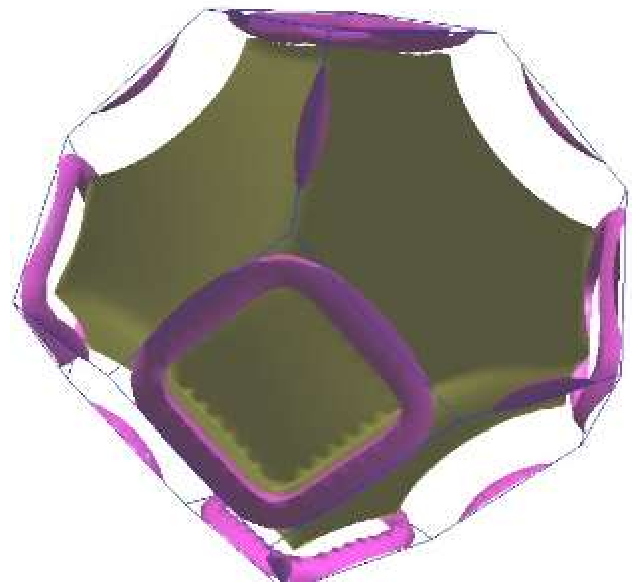

$3s^2 4p^1$

http://www.phys.ufl.edu/fermisurface/

Ferromagnets have different Fermi surfaces for majority moment (↑)-spin(⇓) and minority moment (↓)-spin(⇑) electrons => spin-dependent conduction processes

bcc iron | fcc nickel

majority (↑)

minority (↓)

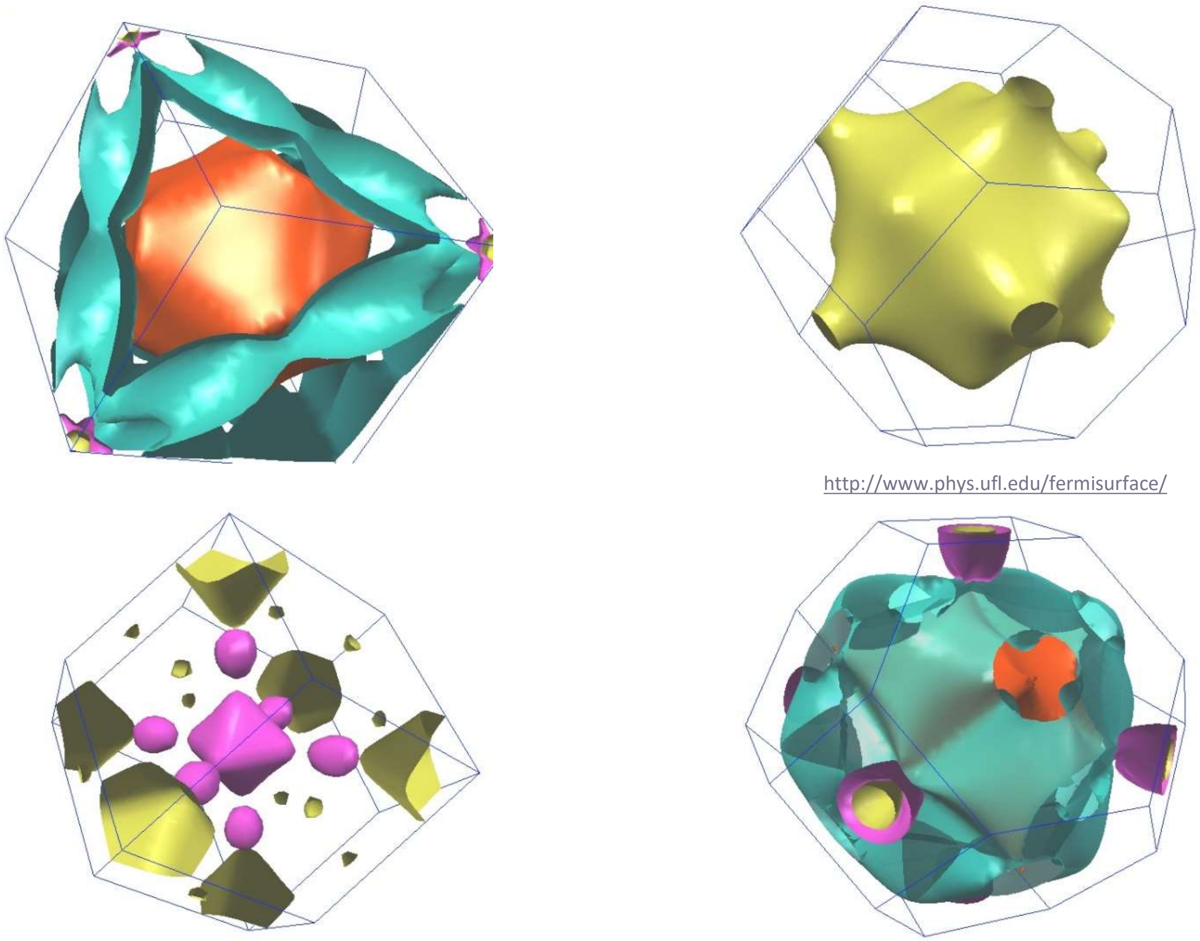

http://www.phys.ufl.edu/fermisurface/

$3d^6 4s^2$ | $3d^8 4s^2$

Partial density of state (DOS) of *3d* transition metals
for majority moment (↑)-spin(⇓) and minority moment (↓)-spin(⇑) electrons

DOS = number of continuum states in an infinitesimally small energy interval $\varepsilon + d\varepsilon$

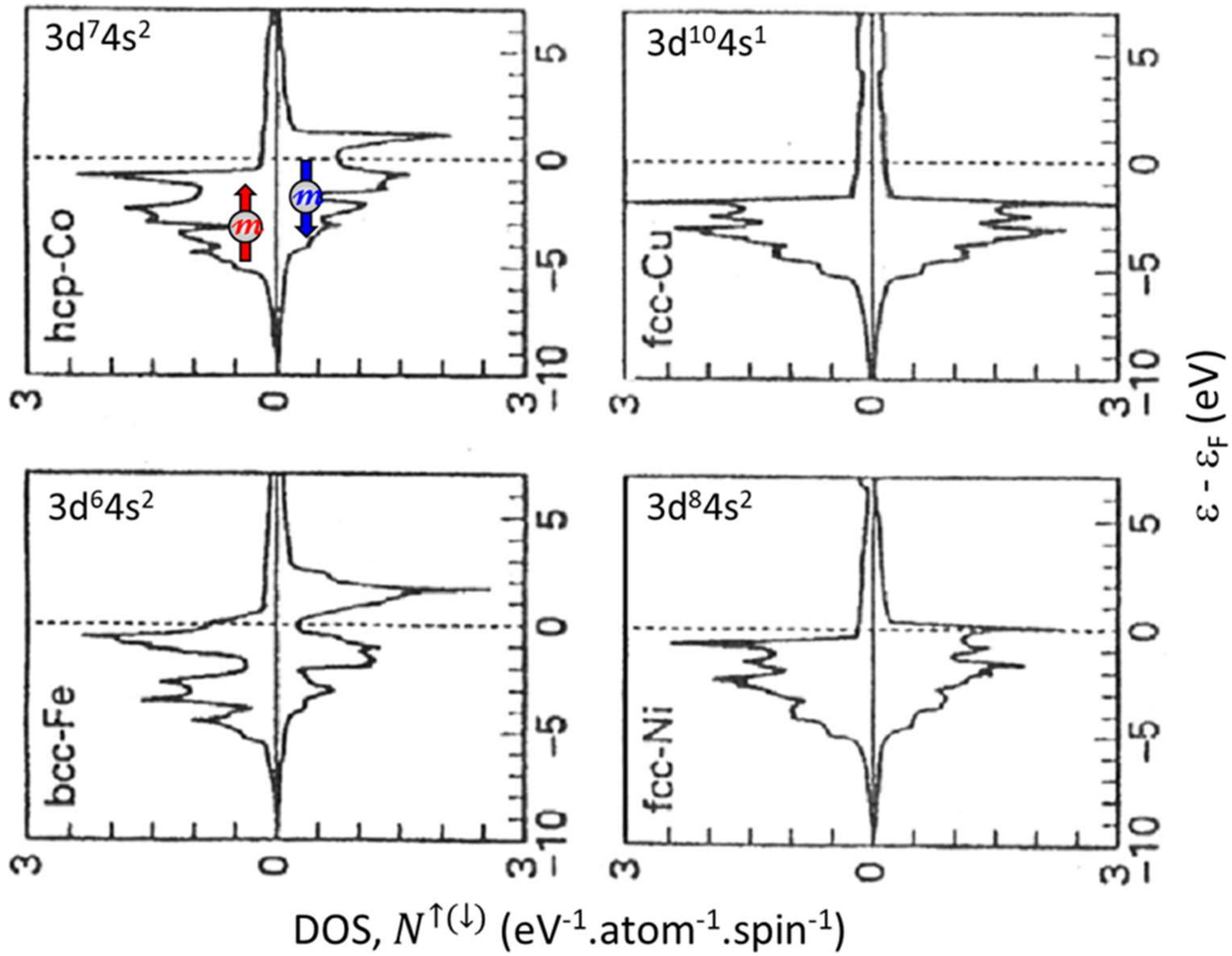

Physics of Low Dimensional Systems, Springer, Boston

In transition metals, spins contributing to transport are split in two types:

- localized spins carried by heavy 3*d*-electrons
- itinerant spins carried by light 4*s*-electrons

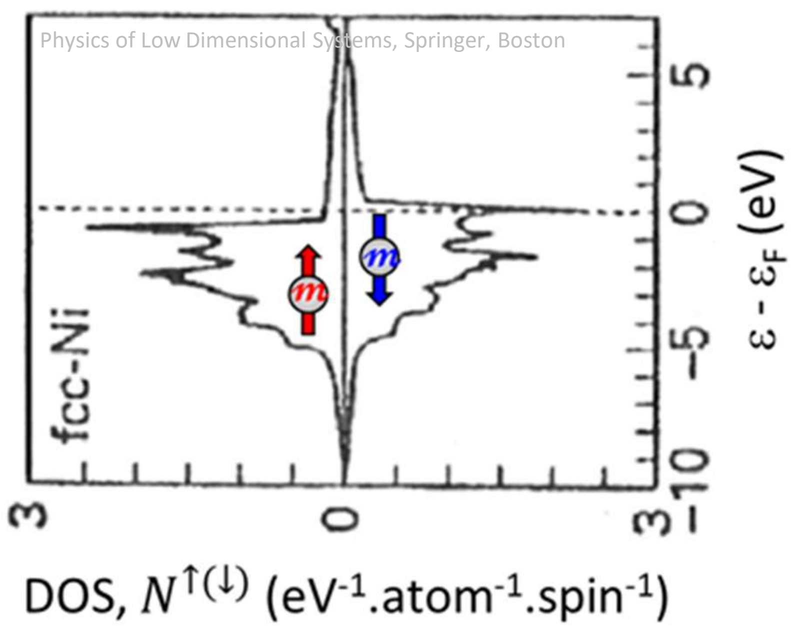

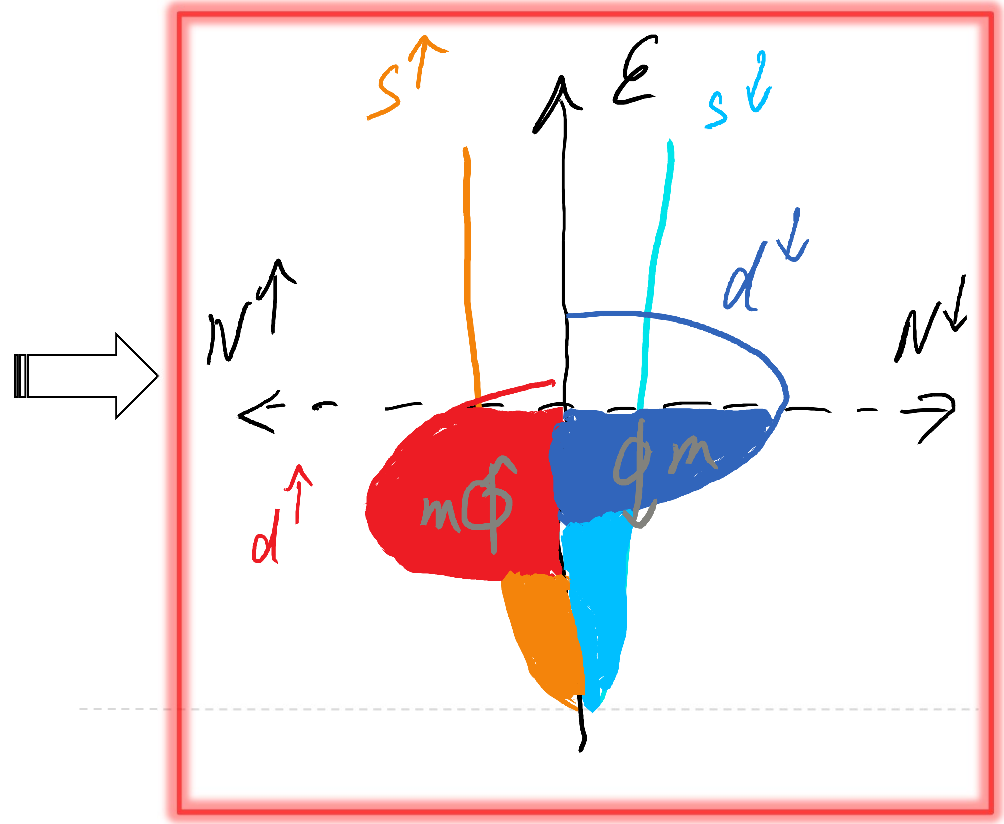

Elastic scattering between itinerant *s*-electrons and localized *d*-electrons is considered. This is known as the *s*-*d* model.

Because m*(*d*) >> m*(*s*), *J* is mostly carried by *s*-electrons

Scattering of electrons is determined by $N^{\uparrow(\downarrow)}(\varepsilon_F)$

Fermi's golden rule:

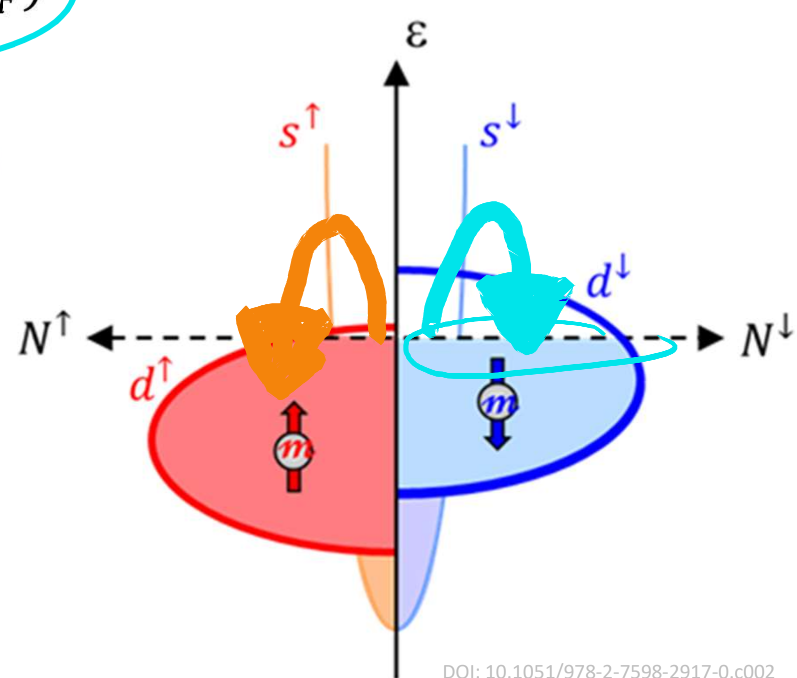

Electronic scattering rate, τ_e, is therefore spin-dependent: $\tau_e^\uparrow > \tau_e^\downarrow$

Example for Co: $\tau_e^\uparrow \simeq 10\,\tau_e^\downarrow$ i.e. $l_e^\uparrow \simeq 10$ nm and $l_e^\downarrow \simeq 1$ nm

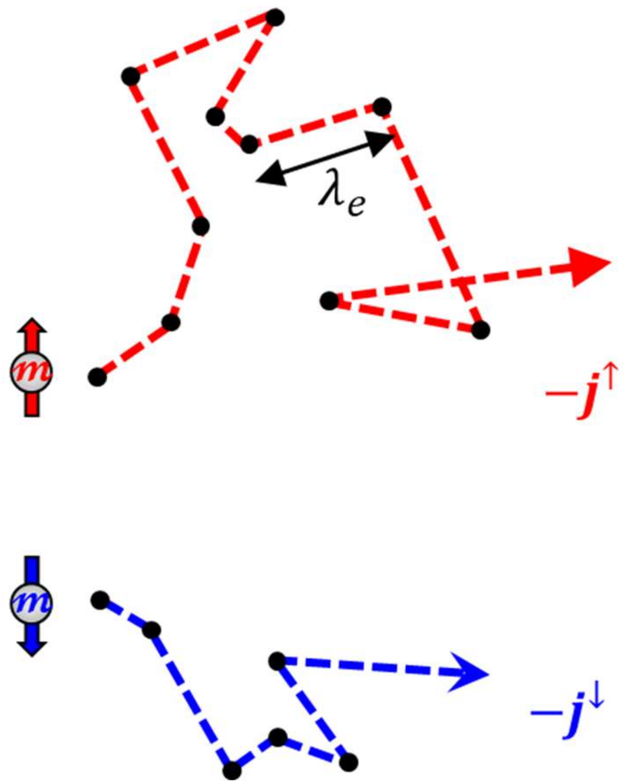

DOI: 10.1051/978-2-7598-2917-0.c002

τ_e is spin-dependent, making $\boldsymbol{j}^{\uparrow} \neq \boldsymbol{j}^{\downarrow}$

Spin-dependent generalized Ohm's law

$$\boldsymbol{j}^{\uparrow(\downarrow)} = \sigma^{\uparrow(\downarrow)} \frac{\boldsymbol{\nabla}\mu^{\uparrow(\downarrow)}}{e}$$

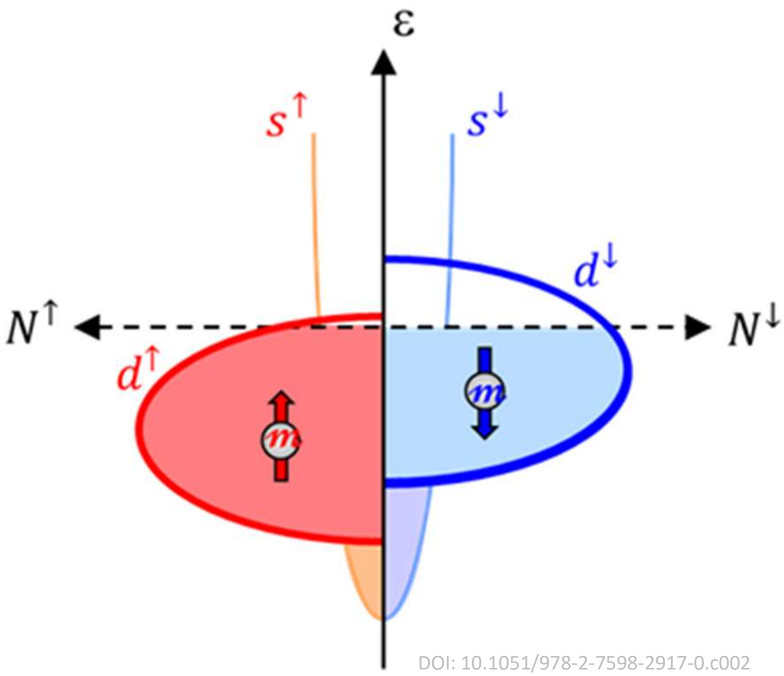

Equivalent circuit

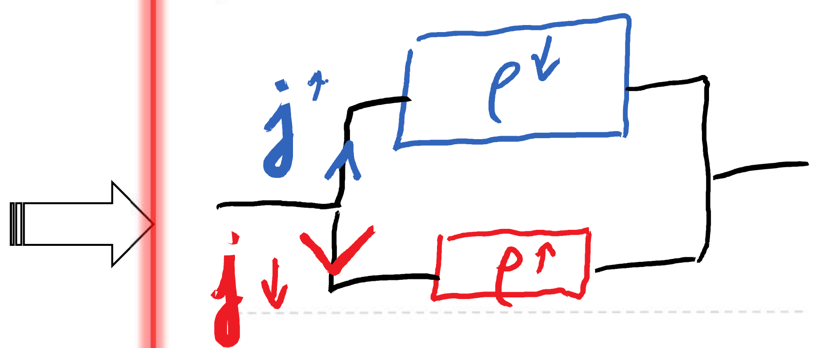

Spin-dependent generalized Ohm's law

$$j^{\uparrow(\downarrow)} = \sigma^{\uparrow(\downarrow)} \frac{\nabla\mu^{\uparrow(\downarrow)}}{e}$$

Some numbers

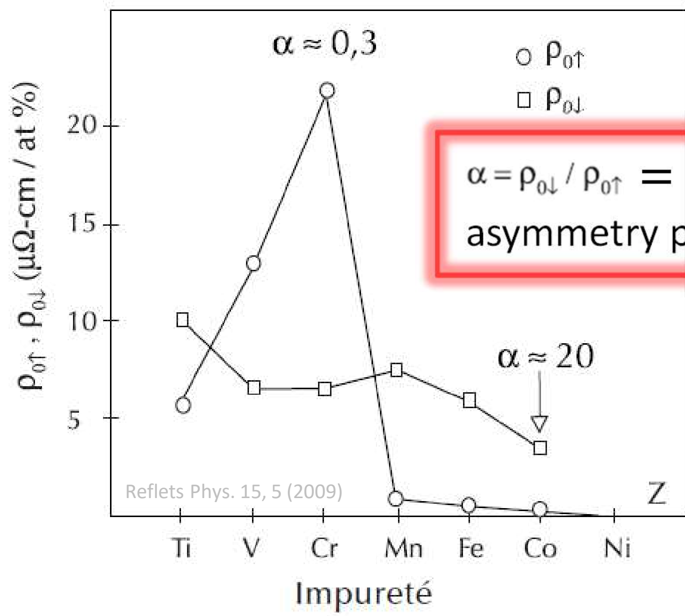

$\alpha = \rho_{0\downarrow} / \rho_{0\uparrow} = \sigma^{\uparrow}/\sigma^{\downarrow}$
asymmetry parameter

Impurity control over a layer's resistance – the case of a ternary alloy

Type 1: e.g. the Ni(Co-Rh) alloy
Electrons flow is altered in the two spin-channels ⇒ **High resistance**

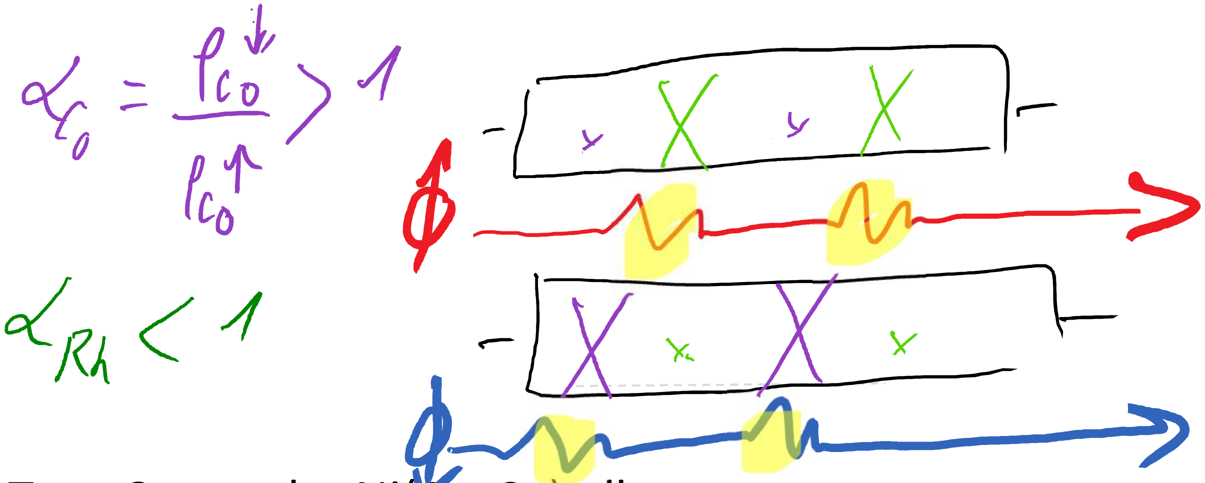

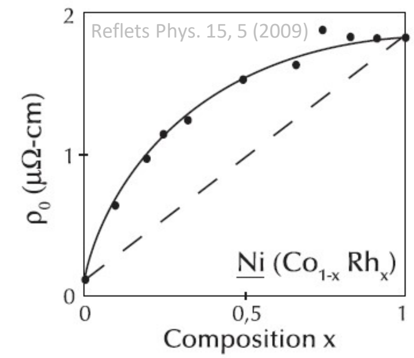

$\alpha_{Co} > 1$, $\alpha_{Rh} < 1$

Type 2: e.g. the Ni(Au-Co) alloy
Electrons flow is altered in one spin-channel only ⇒ **Low resistance**

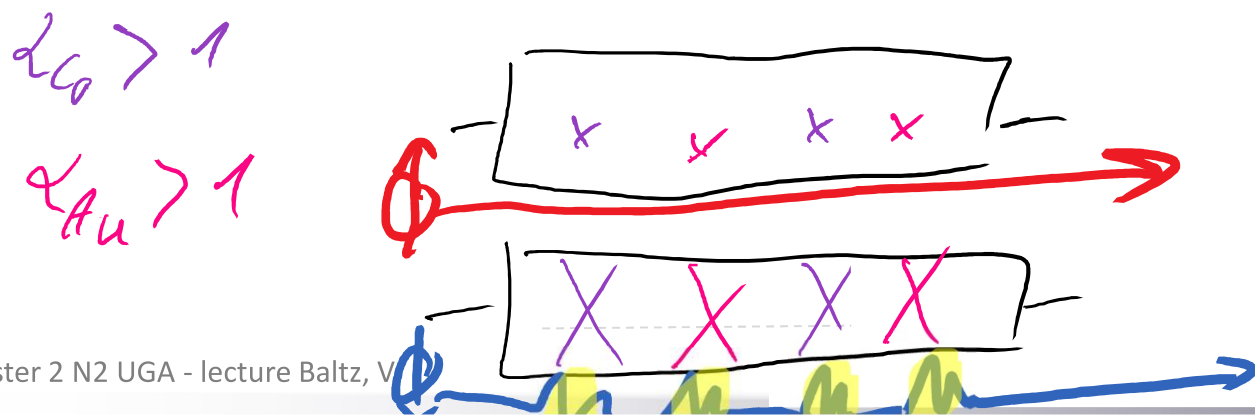

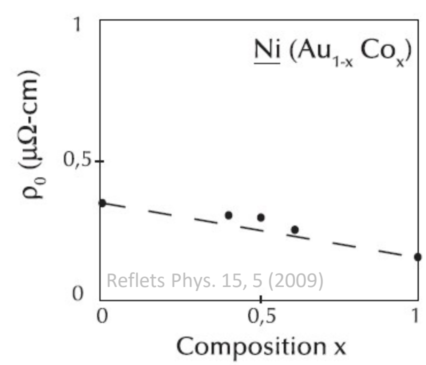

$\alpha_{Co} > 1$, $\alpha_{Au} > 1$

Relative direction of magnetization control over a stack's resistance – CIP-GMR

The initial idea underlying the giant magnetoresistance effect (GMR) is to replace the two types of impurities by two ferromagnetic layers (Fs)

Antiparallel (AP) state = type 1:
Electrons flow is altered
in the two spin-channels

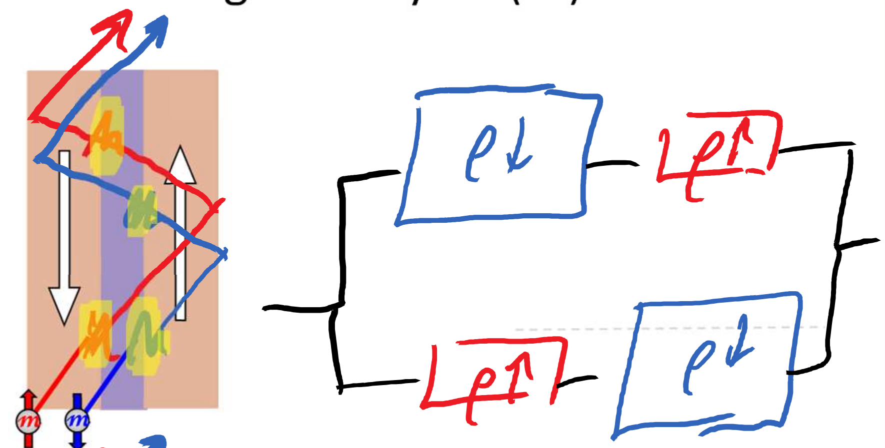

Parallel (P) state = type 2:
Electrons flow is altered
in one spin-channel only

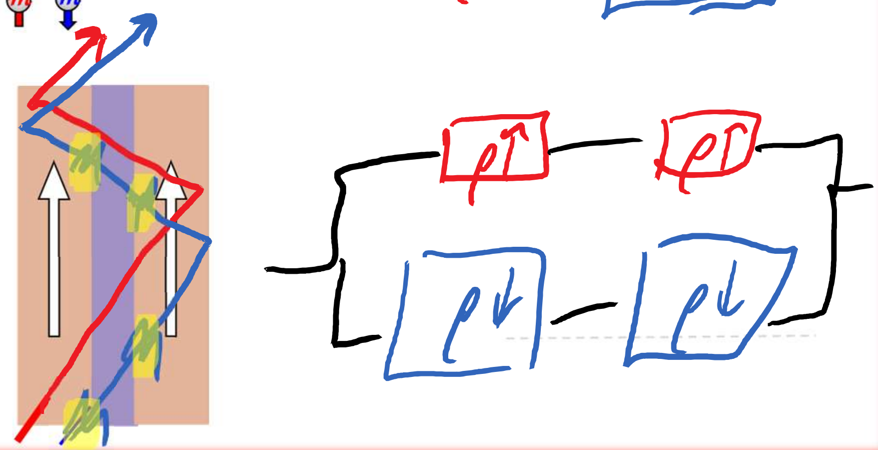

Equivalent circuits

(AP)

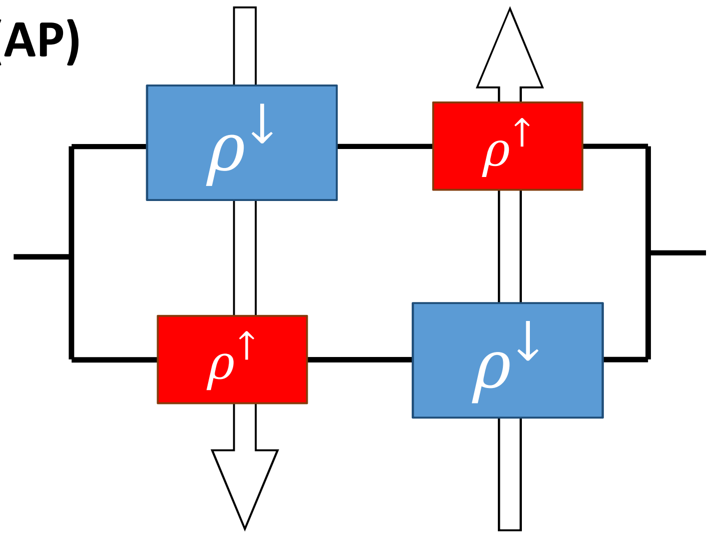

$$\rho^{AP} = \frac{\rho^{\uparrow} + \rho^{\downarrow}}{2}$$

$$\Rightarrow \quad \text{GMR} = \frac{\Delta\rho}{\rho^{AP}} = \left(\frac{\rho^{\uparrow} - \rho^{\downarrow}}{\rho^{\uparrow} + \rho^{\downarrow}}\right)^2 = \left(\frac{\alpha - 1}{\alpha + 1}\right)^2$$

(P)

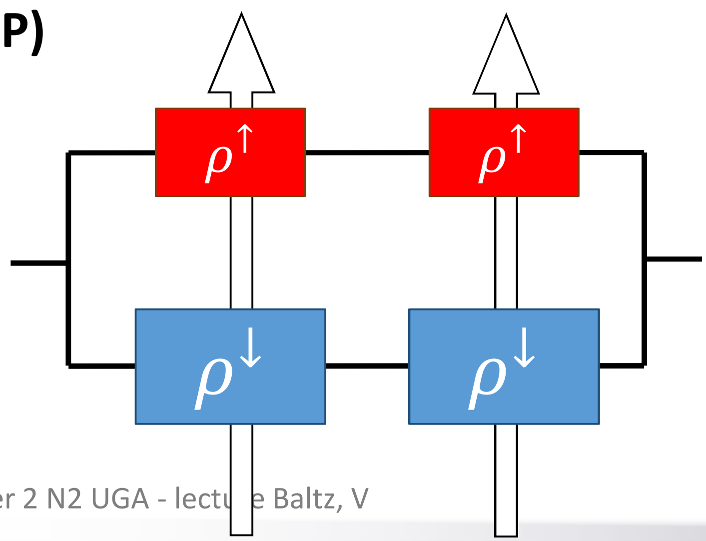

$$\rho^{P} = \frac{2\rho^{\uparrow}\rho^{\downarrow}}{\rho^{\uparrow} + \rho^{\downarrow}}$$

with $\alpha = \dfrac{\rho^{\downarrow}}{\rho^{\uparrow}}$

asymmetry parameter

Notes:

- The relative orientation of the layers'magnetization can for example be controlled by field and spin-torques (see lecture 3).

- An important effect sharing similarities with CIP-GMR is known as the interlayer exchange coupling (IEC) (next set of slides), closely related to Ruderman–Kittel–Kasuya–Yosida (RKKY) interactions between magnetic impurities.

GMR: - the thickess of the non-magnetic (N) spacer-layer, d_N is fixed
- the relative alignement of the magnetic layers (M_1, M_2) is varied by the user (eg with an external magnetic field, a current), leading to a change in resistance

Antiparallel (AP) state

High resistance

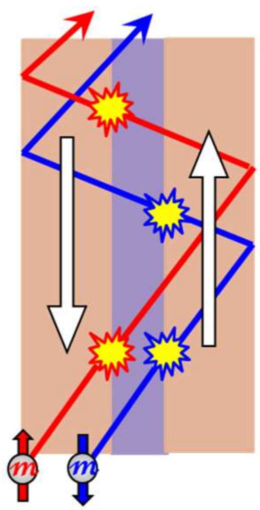

Electrons flow is altered
in the two spin-channels

Parallel (P) state

Low resistance

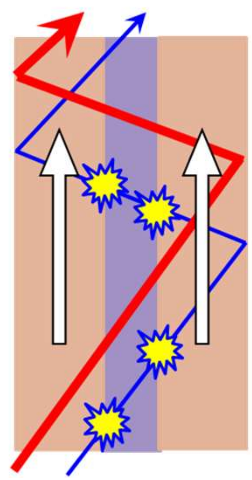

Electrons flow is altered
in ~one spin-channel only
(the spin down channel)

DOI: 10.1051/978-2-7598-2917-0.c002
Adapted from Handbook of Spintronics, Springer, Dordrecht (2015)

IEC: - the thickess of the non-magnetic (N) spacer-layer, d_N is varied, directly leading to a change in resistance

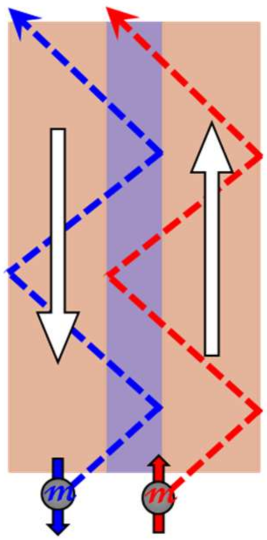

'Classical' behavior

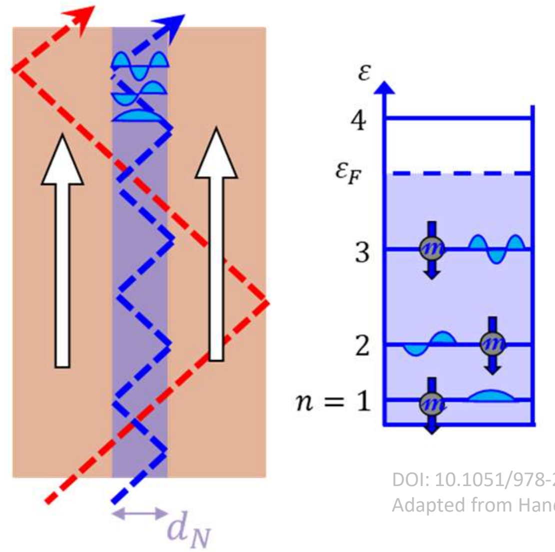

$$\varepsilon_n = \frac{\hbar^2 k_\perp^2}{2\mathrm{m_e}} = \frac{\hbar^2 n^2 \pi^2}{2\mathrm{m_e} d_N^2}$$

DOI: 10.1051/978-2-7598-2917-0.c002
Adapted from Handbook of Spintronics, Springer, Dordrecht (2015)

1D electron quantum well behavior for the minority moment(↓)–spin(⇑) electrons with d_N-dependent quantized energy levels (ε_n)

IEC: - the thickess of the non-magnetic (N) spacer-layer, d_N is varied, directly leading to a change in resistance

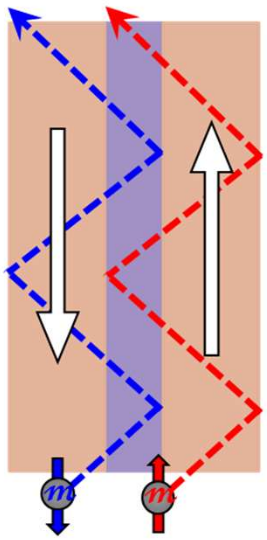

'Classical' behavior

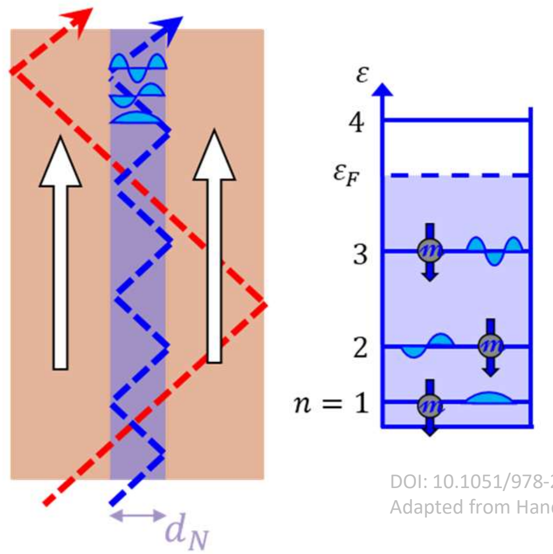

$$\varepsilon_n = \frac{\hbar^2 k_\perp^2}{2m_e} = \frac{\hbar^2 n^2 \pi^2}{2m_e d_N^2}$$

DOI: 10.1051/978-2-7598-2917-0.c002
Adapted from Handbook of Spintronics, Springer, Dordrecht (2015)

1D electron quantum well behavior for the minority moment(↓)–spin(⇑) electrons with d_N-dependent quantized energy levels (ε_n)

'For increasing d_N, the levels move downward. When a level crosses the Fermi energy E_F, the QWS is populated, and the total energy increases. When the QWS level moves further below E_F, the energy again decreases until the next level approaches E_F.'

IEC: - the thickess of the non-magnetic (N) spacer-layer, d_N is varied, directly leading to a change in resistance

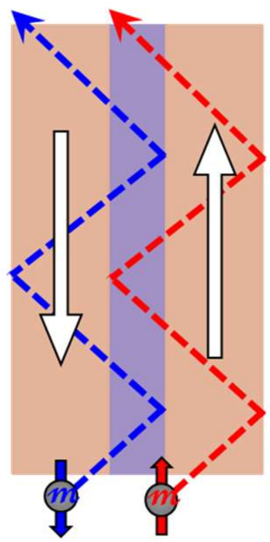

'Classical' behavior

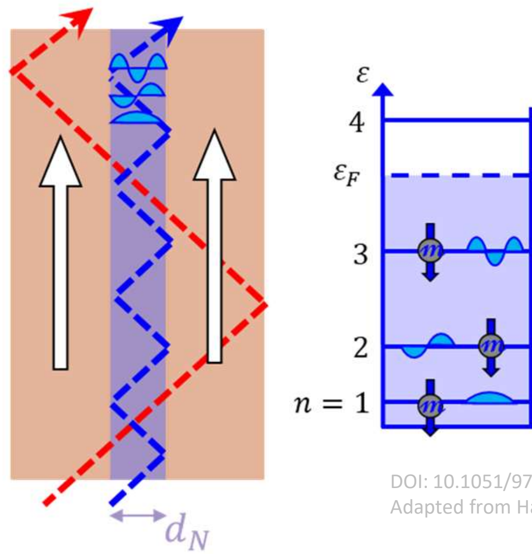

$$\varepsilon_n = \frac{\hbar^2 k_\perp^2}{2m_e} = \frac{\hbar^2 n^2 \pi^2}{2m_e d_N^2}$$

DOI: 10.1051/978-2-7598-2917-0.c002
Adapted from Handbook of Spintronics, Springer, Dordrecht (2015)

1D electron quantum well behavior for the minority moment(↓)–spin(⇑) electrons with d_N-dependent quantized energy levels (ε_n)

Thus, for the P alignment, the energy oscillates with d_N.

In contrast, for the AP alignment (no QWS) the energy stays still.

To always take the configuration with the lowest energy, the alignment switches between P and AP when d_N increases, and hence the coupling oscillates between + and – and the GMR oscillates between high and low R.

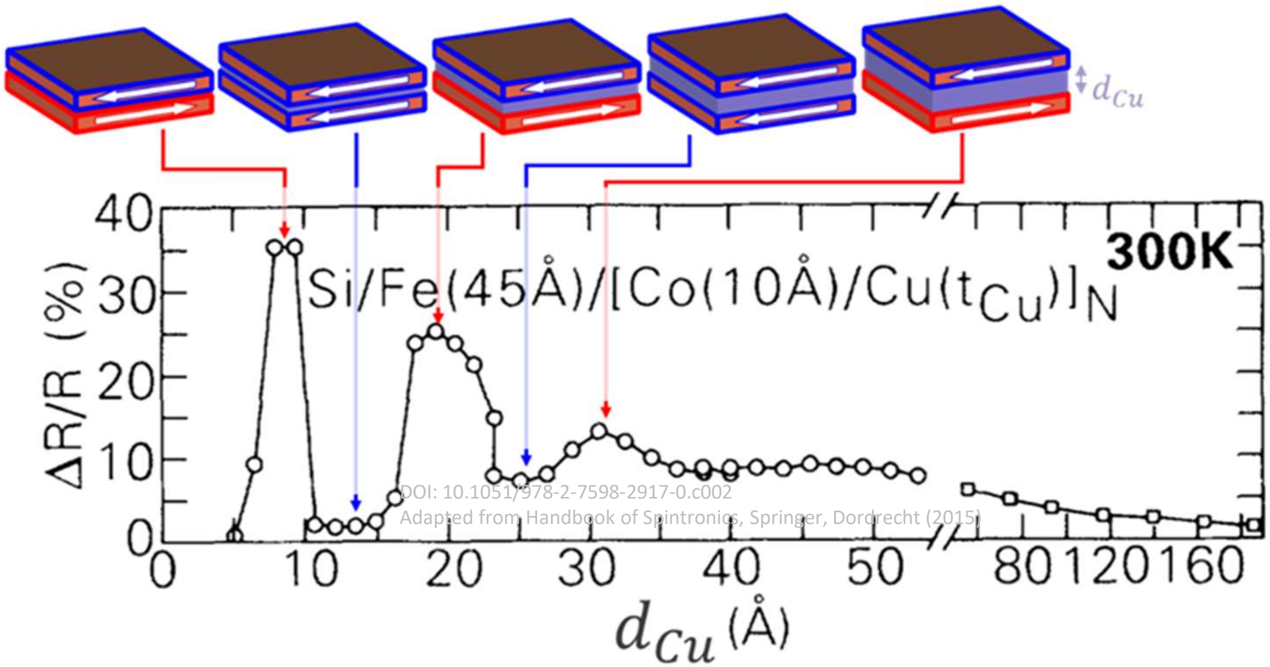

DOI: 10.1051/978-2-7598-2917-0.c002
Adapted from Handbook of Spintronics, Springer, Dordrecht (2015)

Some numbers

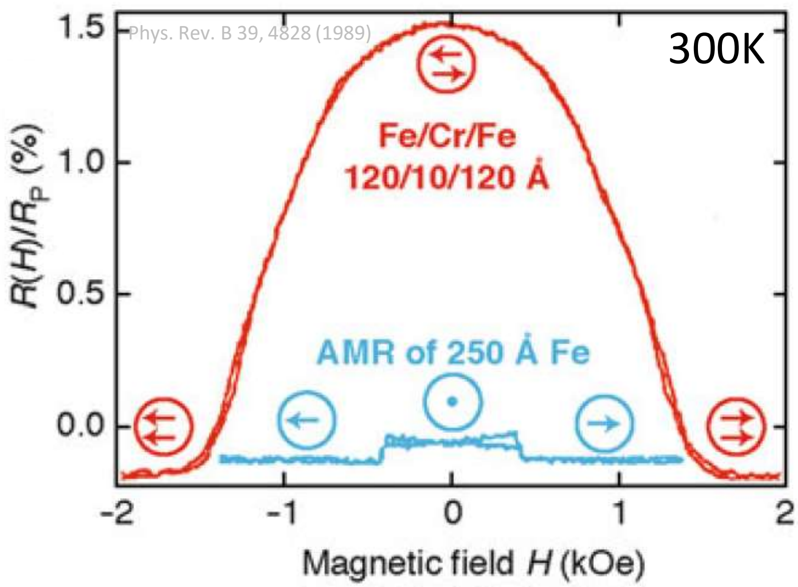

CIP-GMR, 1st experiments (1988-1989)

A. Fert and P. Grünberg
Nobel Prize 2007

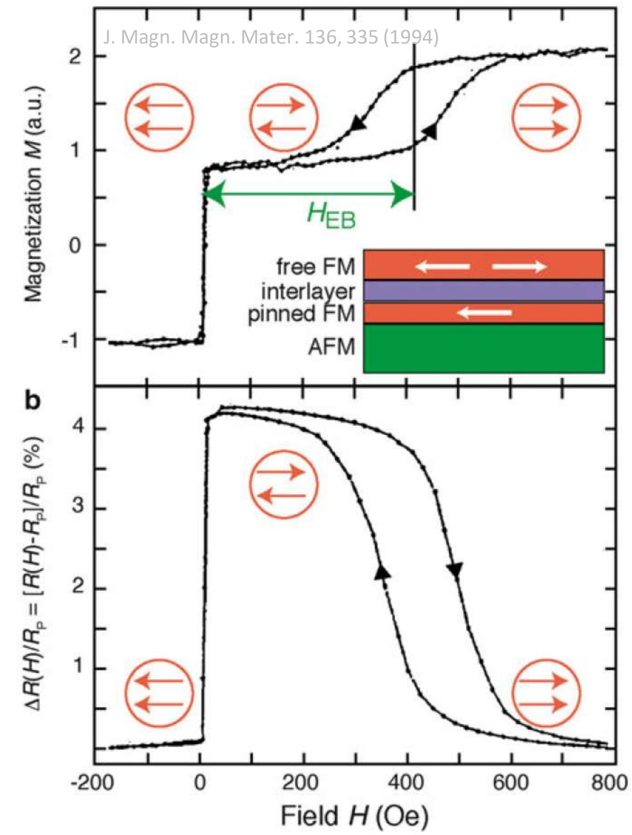

Spin-valve, 1st experiment (1991)
see lecture 2 for CPP-GMR,
typical best values for GMR: few 10th of % at 300K
(see M1 for TMR of few 100th of %)

⇨ Several billions of sensors,
e. g. in hard disk drives

Note:

- Remember that the important characteristic length in CIP-GMR is the (spin-dependent) electron mean free path ($\lambda_e^{\uparrow(\downarrow)}$), as opposed to current perpendicular-to-plane (CPP)-GMR, where spin diffusion length (l_{sf}^*) is the one to consider (see lecture 2), with $l_{sf}^* > \lambda_e$.

The example of MR in read-heads of hard-disk drives for data storage

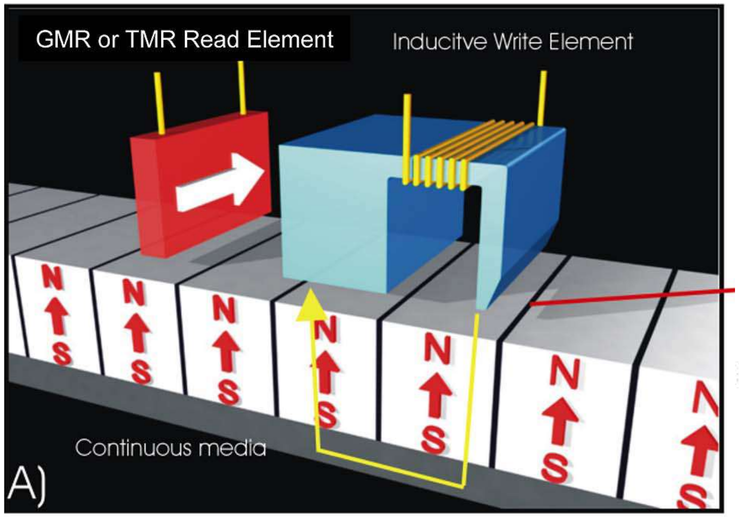

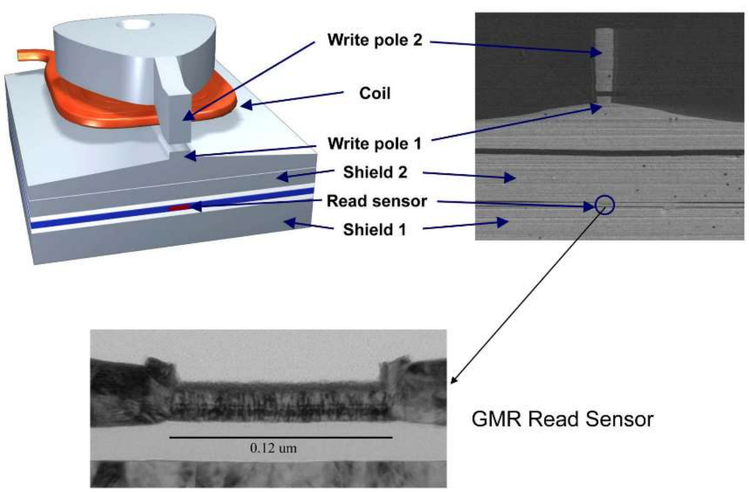

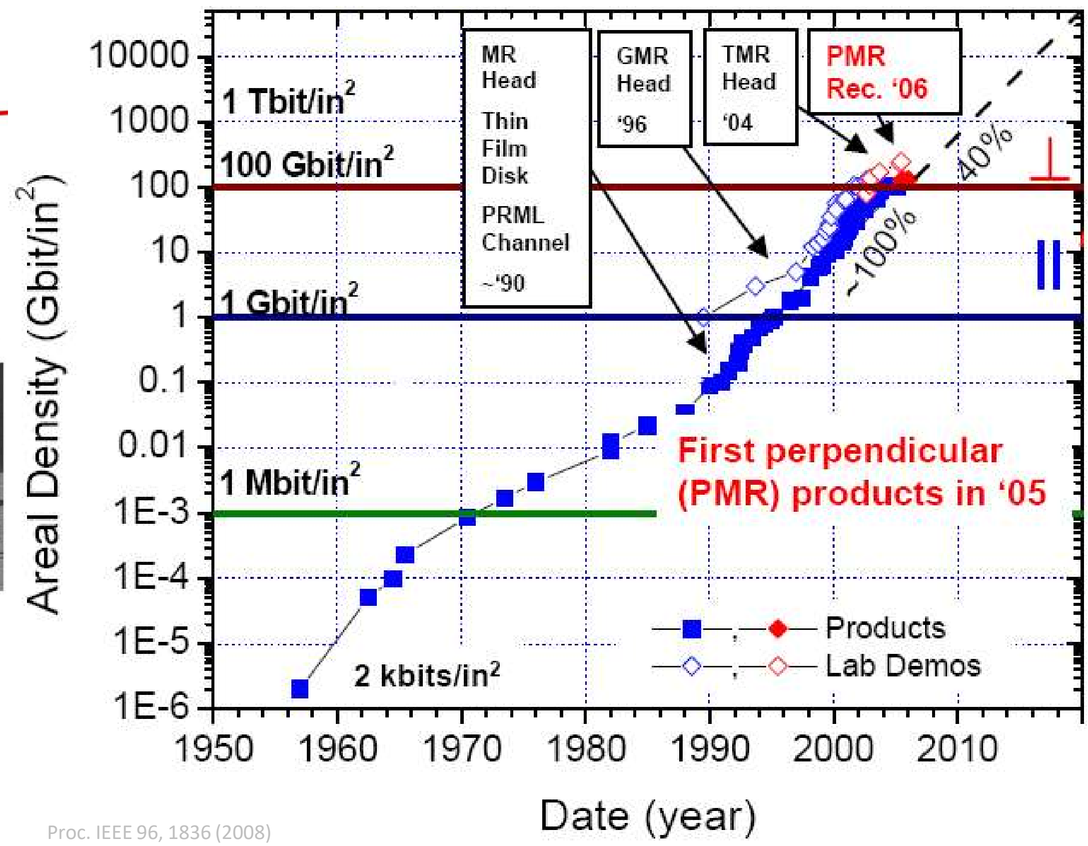

Proc. IEEE 96, 1836 (2008)

Reminder

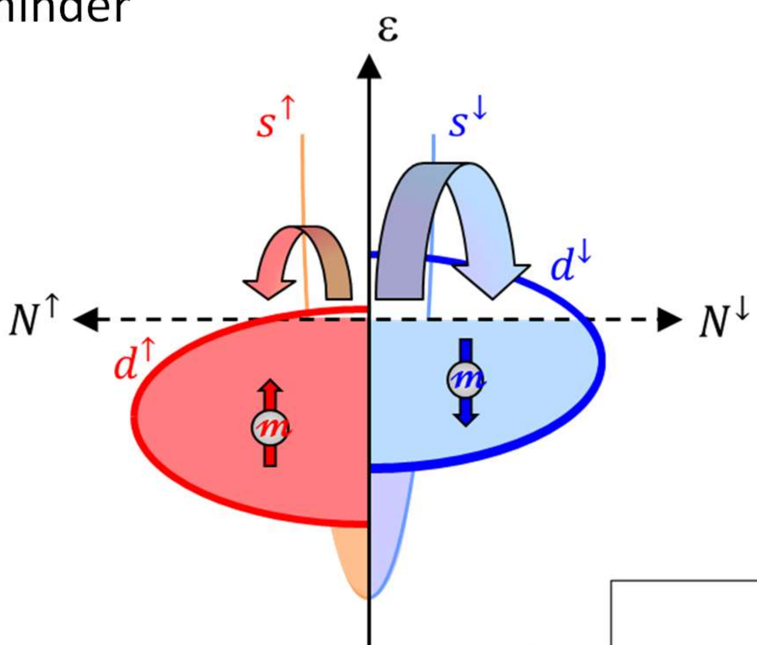

DOI: 10.1051/978-2-7598-2917-0.c002

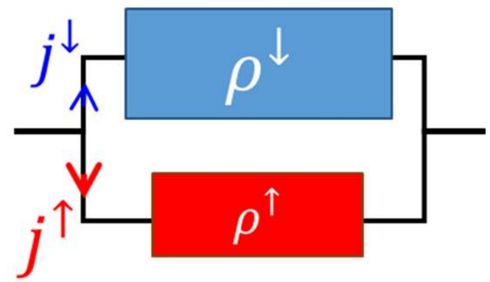

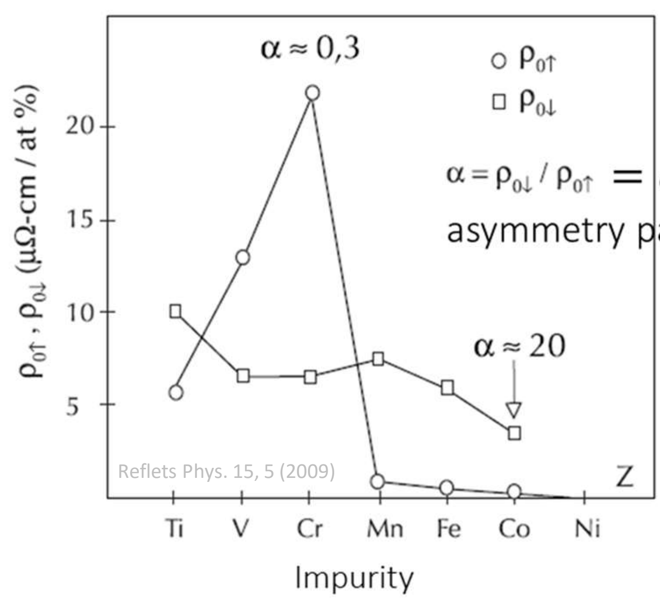

Reflets Phys. 15, 5 (2009)

$\alpha = \rho_{0\downarrow}/\rho_{0\uparrow} = \sigma^{\uparrow}/\sigma^{\downarrow}$

asymmetry parameter

No mixing between the two spin-channels

$$\rho = \frac{\rho^{\uparrow}\rho^{\downarrow}}{\rho^{\uparrow} + \rho^{\downarrow}}$$

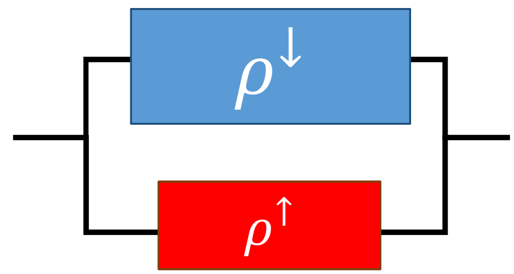

Mixing between the two spin-channels, $\rho^{\uparrow\downarrow}$,
e.g. due to spin-orbit interactions

$$\rho = \frac{\rho^{\uparrow}\rho^{\downarrow} + \rho^{\uparrow\downarrow}(\rho^{\uparrow} + \rho^{\downarrow})}{\rho^{\uparrow} + \rho^{\downarrow} + 4\rho^{\uparrow\downarrow}}$$

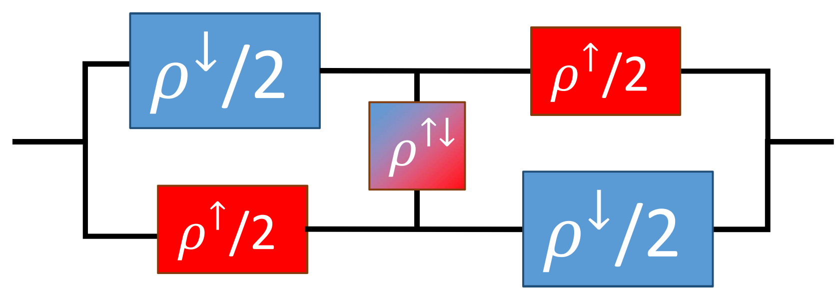

Spin-orbit interaction couples the spin, ***S***, and the orbital, ***L***, angular momentum of an electron. In 3*d* transition metals, this results in:

- a lift of the degeneracy of the energy states of majority- and minority-spins
- a 'mix/reorientation' of the *d* orbitals ($l = 2;\ m_l = -2, -1, 0, +1, +2$)

$$\boldsymbol{H} = \xi_{SO}\boldsymbol{L}.\boldsymbol{S}$$

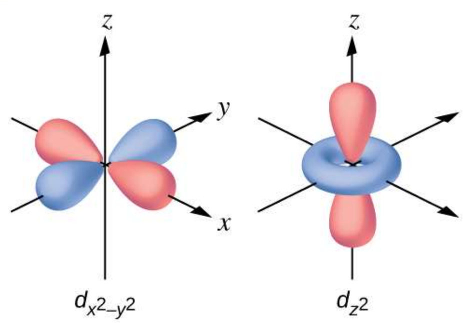

https://openstax.org/books/chemistry/pages/1-introduction

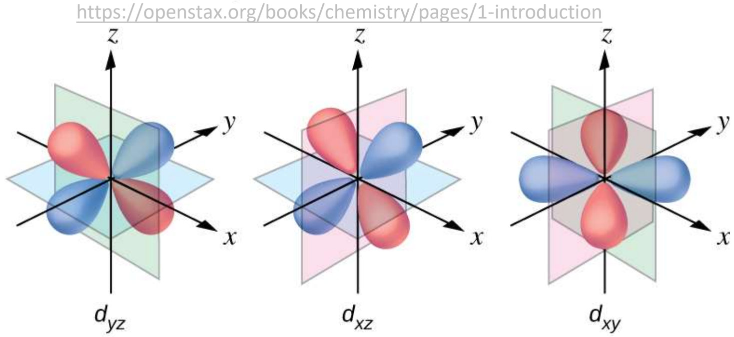

with $\boldsymbol{L}.\boldsymbol{S} = L_x S_x + L_y S_y + L_z S_z = L_z S_z + \frac{1}{2}(L^+ S^- + L^- S^+)$

The ladder operators depend on the quantum numbers as follows:

$$\boldsymbol{L}^{+(-)}|l, m_l\rangle = \sqrt{l(l+1) - m(m+(-)1)}\hbar|l, m_l + (-)1$$

$$\boldsymbol{S}^{+(-)}|s, m_s\rangle = \hbar|s, m_s + (-)1\rangle$$

$$3d^{\uparrow(\downarrow)}(m_l) \rightarrow 3d^{\downarrow(\uparrow)}\ (m_l + (-)1)$$

Numbers: $\xi_{SO} \sim 1$ meV in Ni

Partial density of state (DOS) of *3d* transition metals
for majority moment (↑)-spin(⇓) and minority moment (↓)-spin(⇑) electrons

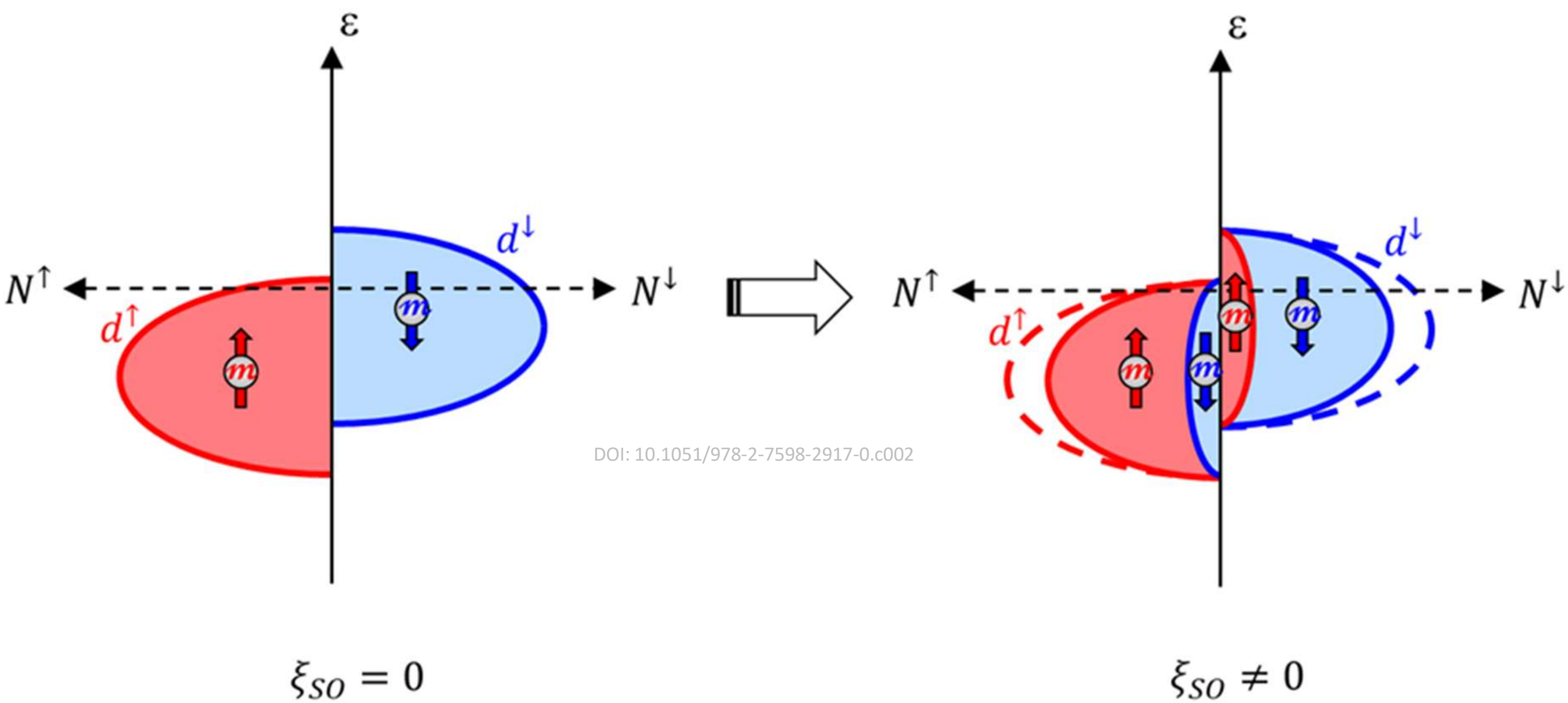

Simplistic illustration of mixing of *d*-bands due to spin-orbit interactions.
The majority moment (↑)-spin(⇓) *d*-band acquires a minority moment (↓)-spin(⇑) character and vice versa.

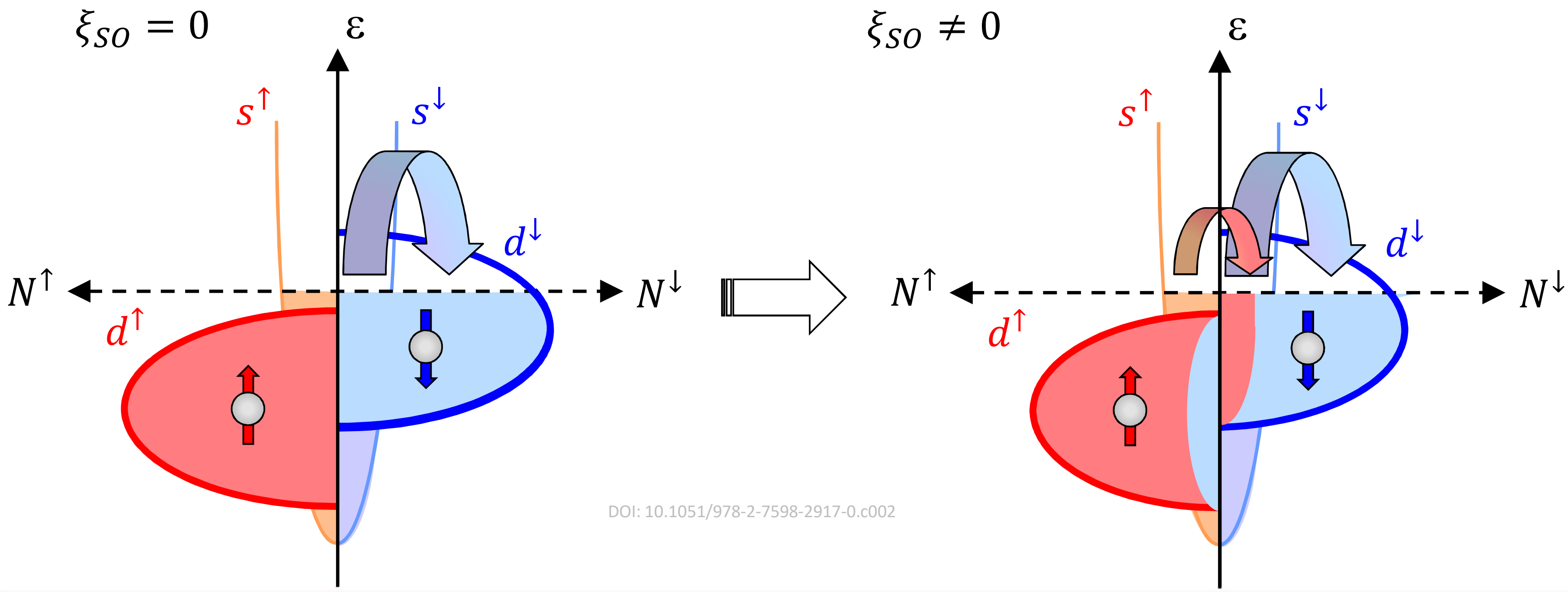

DOI: 10.1051/978-2-7598-2917-0.c002

Mixing of d-bands modifies the spin dependent scattering rates, as it opens a new channel for scattering $s^{\uparrow} \rightarrow d^{\uparrow}$

As a result, we have:

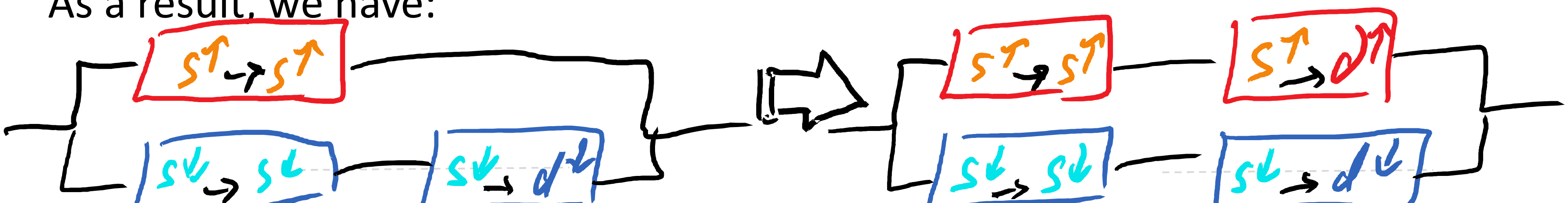

Spin-orbit interactions will depend on the direction of the angular momentum of *s*-electrons (parallel to the wavevector $\hbar\boldsymbol{k}$) relative to that of the *d*-electrons (parallel to ***M***).

Phenomenological picture:
- ***I*** ∥ ***M*** : the electronic orbits are ⊥ to ***I***, offering a large cross section for the *s*-electrons to scatter (high resistivity, $\rho_{\parallel}$)
- when ***I*** ⊥ ***M*** : the electronic orbits are ∥ to ***I*** and thus offer a smaller cross section for scattering (low resistivity, $\rho_{\perp}$).

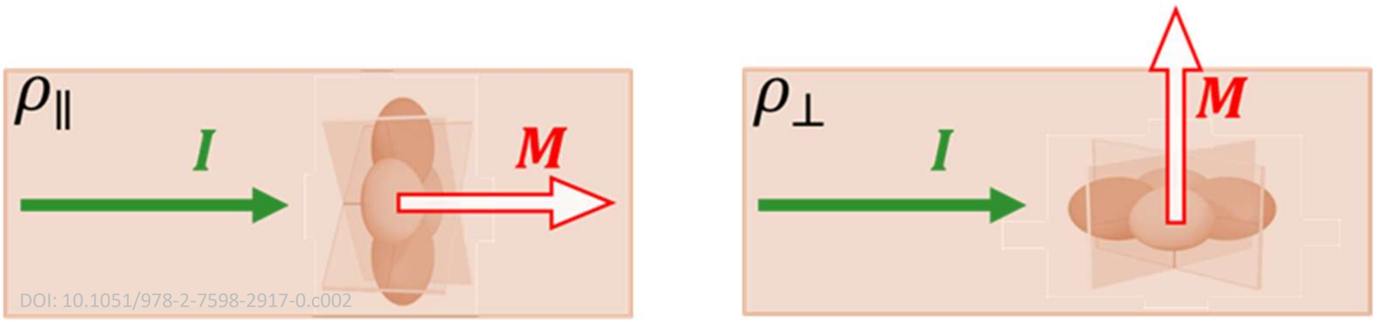

This is known as the anisotropic magnetoresistance (AMR) effect. It was demonstrated experimentally by W. Thomson (Lord Kelvin) in 1857 and explained theoretically e. g. by the Campbell, Fert and Jaoul model (CFJ) in 1970.

Some numbers

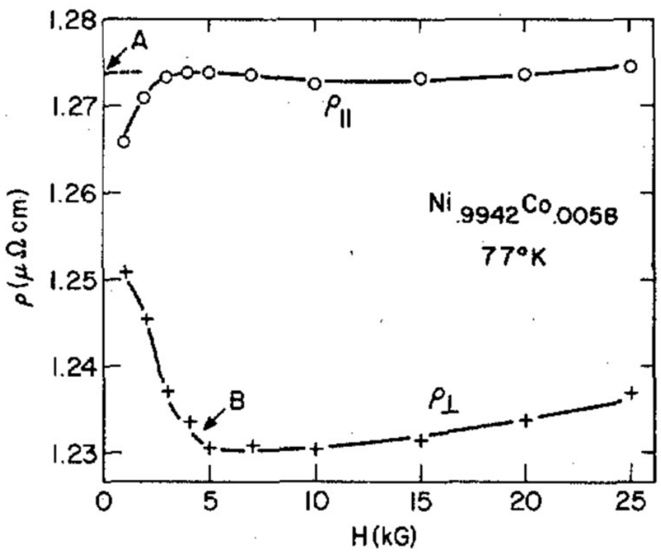

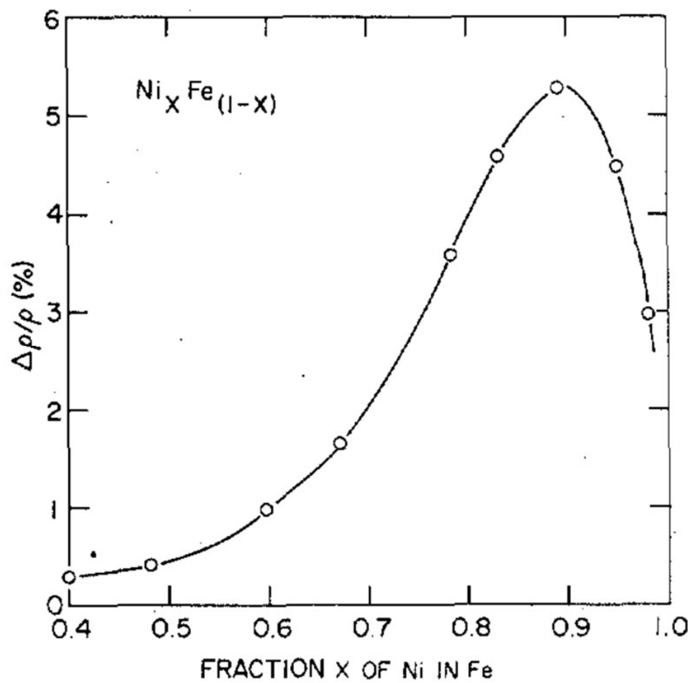

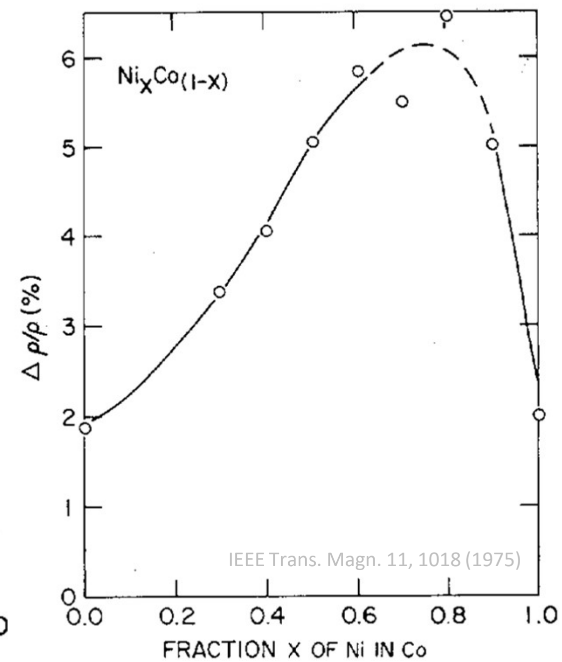

Note: $\rho^{\uparrow\downarrow}$~10 μΩ.cm in Ni and Fe

Angular dependence of AMR, cf. Exercice 1

⇒ Billions of sensors

- **Models and their degree of 'Quantumness'**
  - Phenomenological vs. classical vs ½classical vs quantum
- **Electronic transport**
  - Drude, Band structures, DOS and Fermi level
- **Electronic spin-dependent transport**
  - The two current / s-d models and spin-dependent relaxation (electron mean free path)
  - Spin-orbit interactions and spin mixing, the example of the AMR effect
  - Spin-dependent scattering in heterostructures, the example of the CIP-GMR effect
- **References:**

  - A. Fert, Reflets Phys. **15**, 5 (2009) and references therein
  - P. S. Bechthtold **B7**, in S. Blügel *et al* (eds) Spintronics - from GMR to quantum information (2009)
  - P. Grünberg *et al*, Metallic Multilayers, in Y. Xu Y. *et al* (eds) Handbook of Spintronics, Springer (2015)
  - AMR, CFJ model: I. A. Campbell *et al*, J. Phys. C: Solid State Phys. **3**, S95 (1970)
  - AMR, a review: T. R. McGuire *et al*, IEEE Trans. Magn. **11**, 1018 (1975)
  - CIP-GMR: M. N. Baibich *et al*, Phys. Rev. Lett. **61**, 2472 (1988), G. Binasch *et al*, Phys. Rev. B **39**, 4828 (1989)
  - Spin-valve: B. Dieny, J. Magn. Magn. Mater. **136**, 335 (1994)
  - MR in HDDs: E. Dobisz *et al*, Proc. IEEE **96**, 1836 (2008)

Lectures on spintronics

Master 2 Univ. Grenoble Alpes

Vincent Baltz
CNRS Researcher at SPINTEC

Lecture 1	–	04 Dec.
Lecture 2	–	07 Dec.
Lecture 3	–	11 Dec.
Lecture 4	–	14 Dec.
Exercises 1 & 2	–	21 Dec.

vincent.baltz@cea.fr
https://fr.linkedin.com/in/vincentbaltz
www.spintec.fr/af-spintronics/

1h30
- I. Brief overview of the field of spintronics and its applications
- II. First notions to describe electron and spin transport – AMR, CIP-GMR

1h30
- **III. Spin accumulation – CPP-GMR**

1h30
- IV. Transfer of angular momentum – STT

1h30
- V. Berry curvature, parity and time symmetries – AHE
- VI. Brief non-exhaustive introduction to current topics

1h30
- Exercise 1 - Anisotropic magnetoresistance (AMR)
- Exercise 2 – The spin pumping (SP) and inverse spin Hall effects (ISHE)

III. Spin accumulation – CPP-GMR

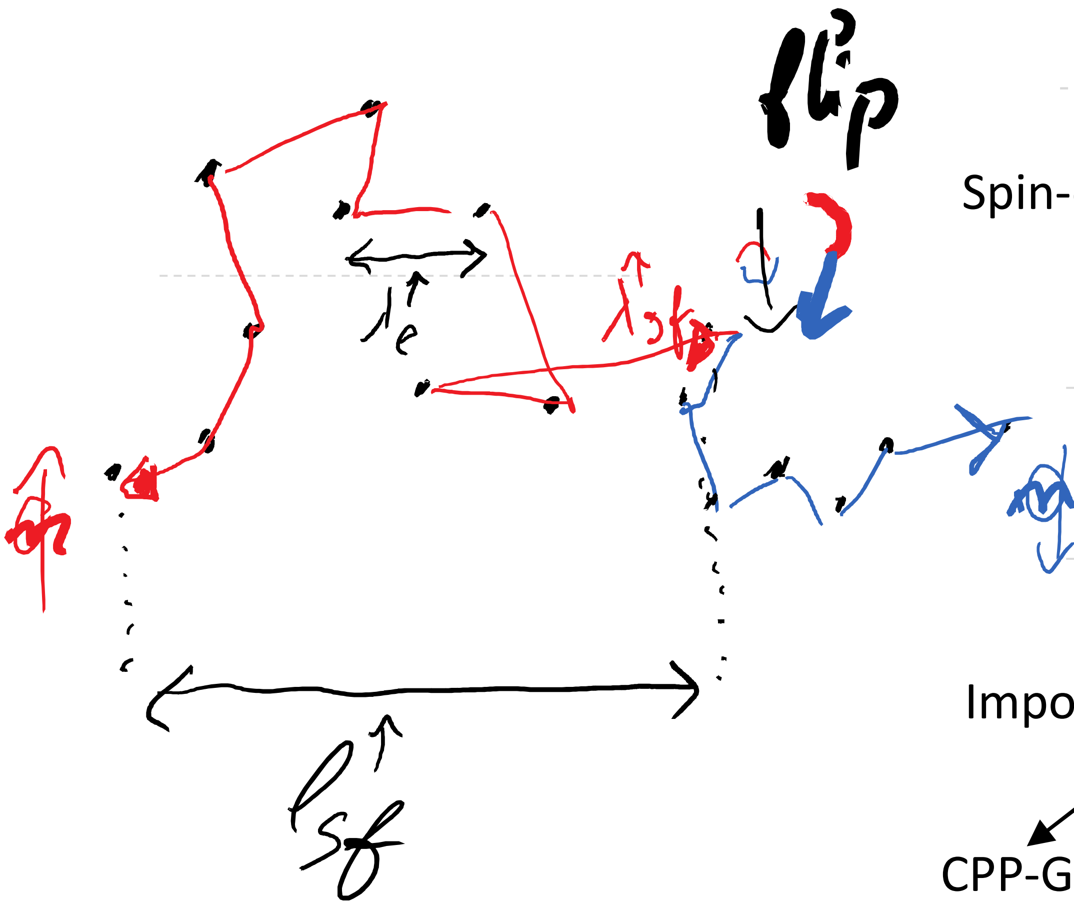

Electron mean free path

$$\lambda_e = v_F \tau_e$$

Spin-flip length

$$\lambda_{sf} = v_F \tau_{sf}$$

Spin-diffusion length *(geometrical mean)*

$$l_{sf} = \sqrt{D \tau_{sf}}$$ ↑ Einstein relation

with $D = \frac{1}{3} v_F \lambda_e$ Fick

$$\Rightarrow l_{sf} = \sqrt{\frac{\lambda_e \lambda_{sf}}{3}}$$

Important note

$l_{sf} > \lambda_e$

↙ CPP-GMR ↘ AMR, CIP-GMR

Spin-flip events are scarce: 1/1000 in some non-magnets

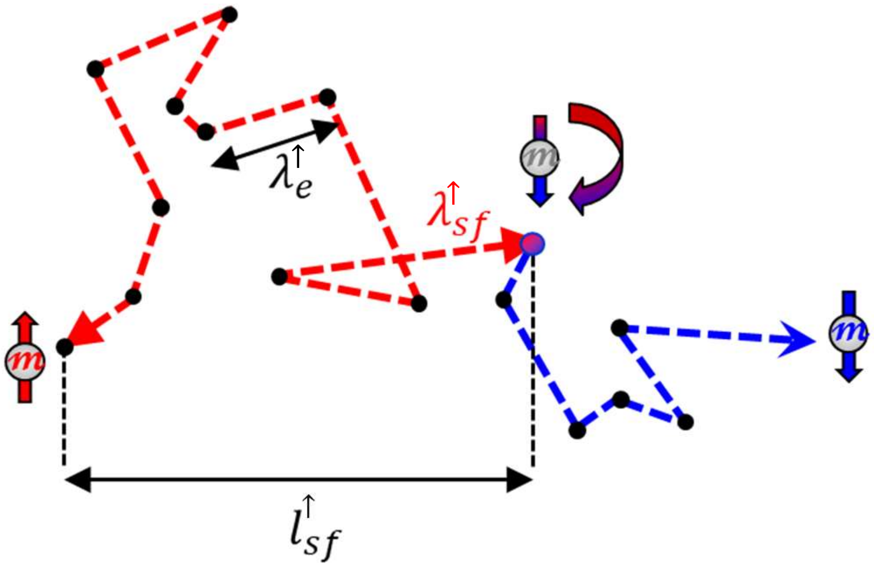

DOI: 10.1051/978-2-7598-2917-0.c002

Spin-dependent electron mean free path

$$\lambda_e^{\uparrow(\downarrow)} = \sqrt{3D^{\uparrow(\downarrow)}\tau_e^{\uparrow(\downarrow)}}$$

Spin-dependent spin-diffusion length

$$l_{sf}^{\uparrow(\downarrow)} = \sqrt{D^{\uparrow(\downarrow)}\tau_{sf}^{\uparrow(\downarrow)}}$$

Distinct densities of current at the interface between materials of different types (e.g. F and NM) creates a spin imbalance.

This effect is called spin accumulation.

Relaxation towards equilibrium conditions causes spins to diffuse near the interface. The *average* spin-diffusion length ($l^*_{sf,F(N)}$) is the characteritic length for this effect.

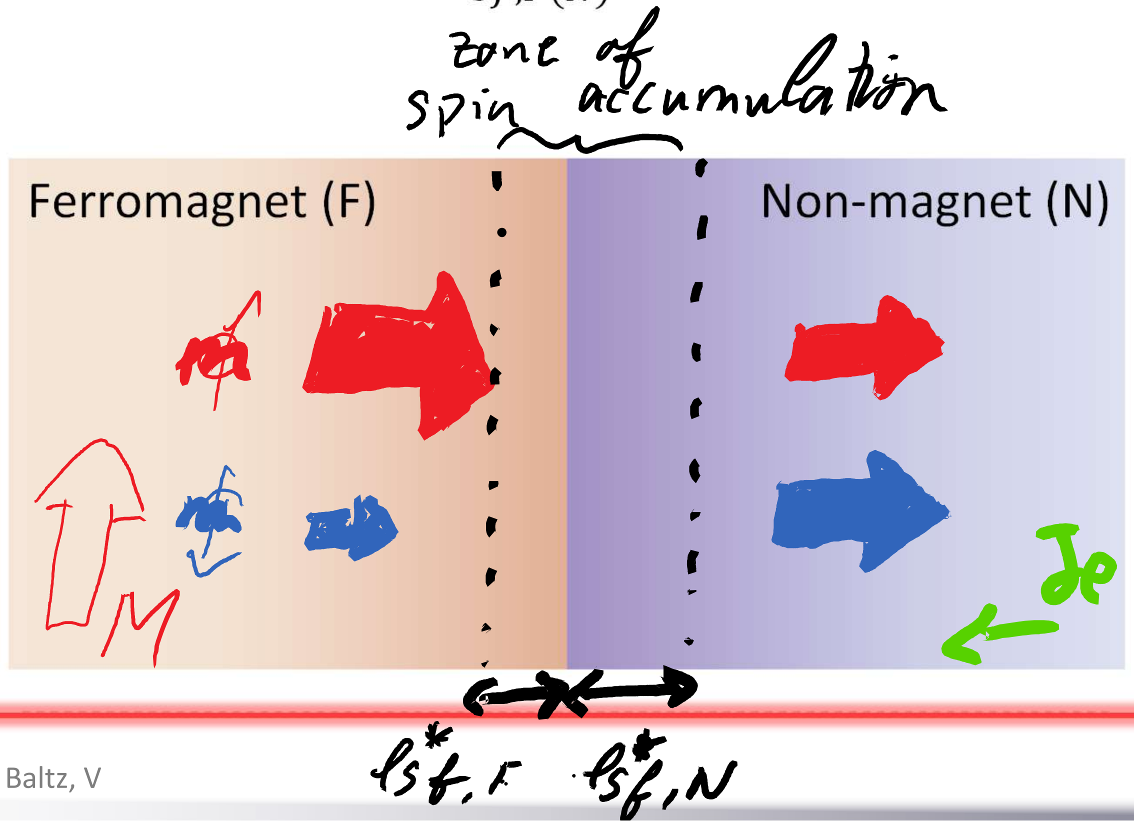

Drude model of electronic transport

$\boldsymbol{j} = \sigma \boldsymbol{E}$ with $\sigma = \frac{N(\varepsilon_F) e^2 \tau_e}{m_e} = N(\varepsilon_F) e^2 D$

$\boldsymbol{j} = \sigma \frac{\boldsymbol{\nabla} \mu_e}{e}$ with $\boldsymbol{E} = -\boldsymbol{\nabla} V$ electric potential

and $\mu_e = -eV$ electrostatic potential

Drift-diffusion and generalized Ohm's law

$\boldsymbol{j} = \sigma \frac{\boldsymbol{\nabla} \mu}{e}$ where $\mu = \mu_e + \mu_n$ is the electro chemical potential

and $\mu_n = \mu_{n_0} + \frac{e^2 D}{\sigma} \delta n$ is the chemical potential

at equilibrium $= \frac{\delta n}{N(\varepsilon_F)}$ ← excess particle density

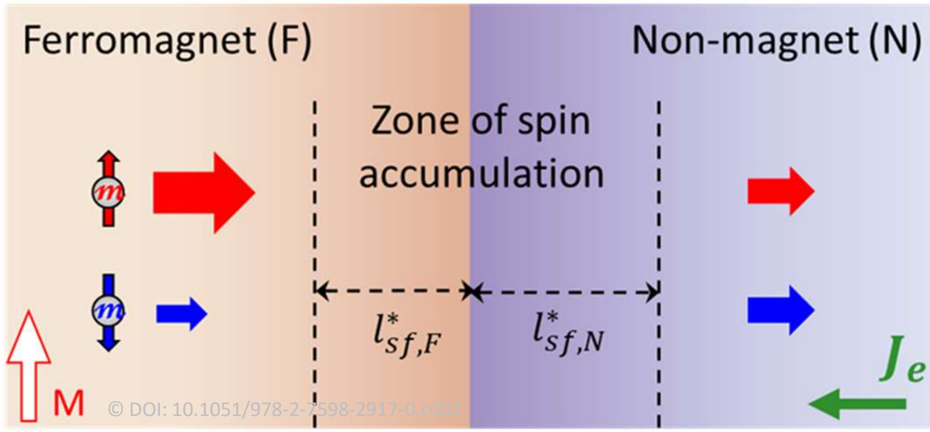

In the next slides, we will explain how to determine:

- the spin imbalance: $\mu_s = -(\mu^{\uparrow} - \mu^{\downarrow})$
- the spin current: $\boldsymbol{J_s} = -(\boldsymbol{j}^{\uparrow} - \boldsymbol{j}^{\downarrow})$

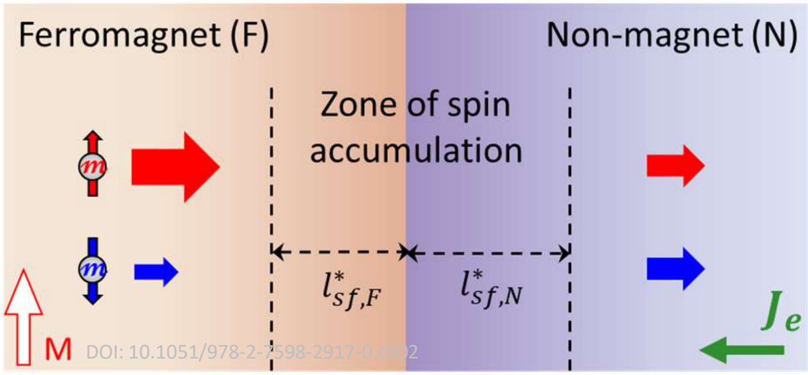

(1) Reminder: Ohm's law

$$j^{\uparrow(\downarrow)}_{F,N} = \sigma^{\uparrow(\downarrow)}_{F,N} \frac{\nabla \mu^{\uparrow(\downarrow)}_{F,N}}{e}$$

4 equations

$$\text{with } \mu^{\uparrow(\downarrow)}_{F,N} = \frac{e^2 D^{\uparrow(\downarrow)}_{F,N}}{\sigma^{\uparrow(\downarrow)}_{F,N}} \delta n^{\uparrow(\downarrow)}_{F,N}$$

(drift is omitted to facilitate reading)

(2) Charge (e) and spin (s) current

(F,N subscripts omitted here and in the next slide, to facilitate reading)

$$J_e = j^{\uparrow} + j^{\downarrow}$$
$$J_s = -(j^{\uparrow} - j^{\downarrow})$$

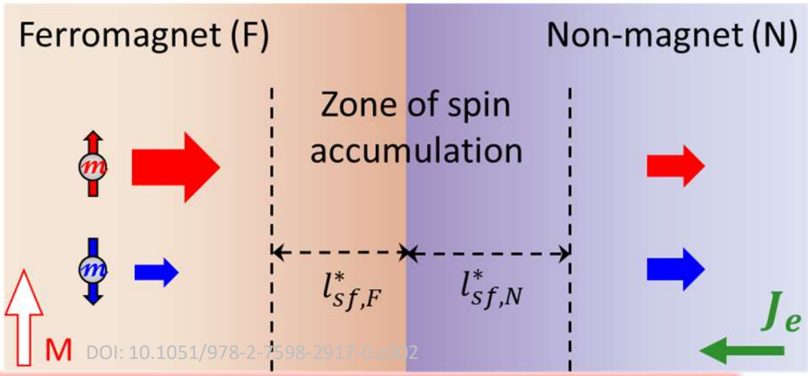

(3) Charge conservation:

$$\vec{\nabla}\cdot \vec{J}_e = 0 \qquad \vec{\nabla}\cdot \equiv \mathrm{div}$$

(4) Total angular momentum conservation:

'Nothing is lost, nothing is created, everything is transformed' (Antoine Lavoisier)

any loss in spin current must be due to spin-flips

$$\vec{\nabla}\cdot \vec{J}_s = -e\left(\frac{\delta n^{\uparrow}}{\tau_{sf}^{\uparrow}} - \frac{\delta n^{\downarrow}}{\tau_{sf}^{\downarrow}}\right)$$

Note: the flux of angular momentum current is not conservative, however total angular momentum is conserved.

(5) Using Eqs. (1) to (4), it is possible to show that CPP transport at an heterogeneous interface is governed by a simple diffusion equation describing spin accumulation or chemical potential imbalance $\mu_s = -(\mu^{\uparrow} - \mu^{\downarrow})$

$$\nabla^2 \mu_s - \frac{\mu_s}{l_{sf}^{*2}} = 0$$

where l_{sf}^* can be viewed as an average spin-diffusion length: $\frac{1}{l_{sf}^{*2}} = \frac{1}{l_{sf}^{\uparrow 2}} + \frac{1}{l_{sf}^{\downarrow 2}}$

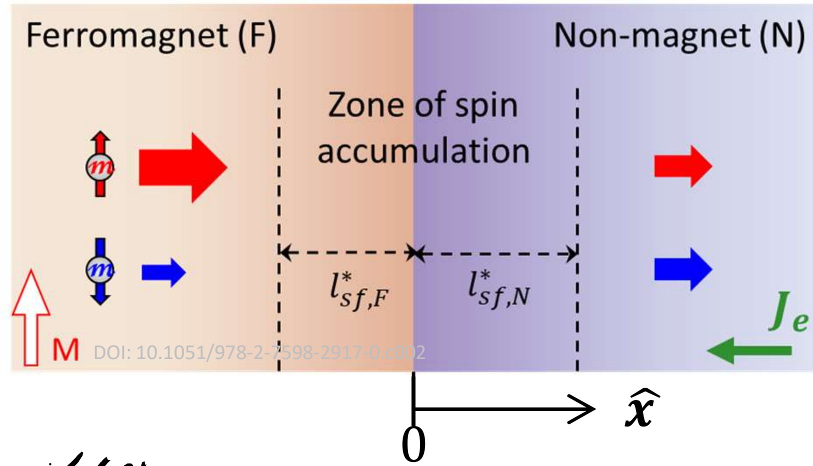

(6) In a 1D problem, the solutions of Eq. (5) take the following form:

$$\mu_{s,F(N)}(x) = A_{F(N)} e^{x/l^*_{sf,F(N)}} + B_{F(N)} e^{-x/l^*_{sf,F(N)}}$$

2 équations

(7) Boundary conditions for infinite layers:

$$\lim_{x \to -(+)\infty} \left(\mu_{s,F(N)} \right) = 0$$

(8) Continuity of μ_s and J_s across the interface:

$$\mu_{s,F}(0) = \mu_{s,N}(0) \quad \text{and} \quad J_{s,F}(0) = J_{s,N}(0)$$

(9) Using Eqs. (6) to (8), it is possible to calculate the spin accumulation and the charge current in the F/N bilayer.

Example and detailed calculations, cf. Exercice 2

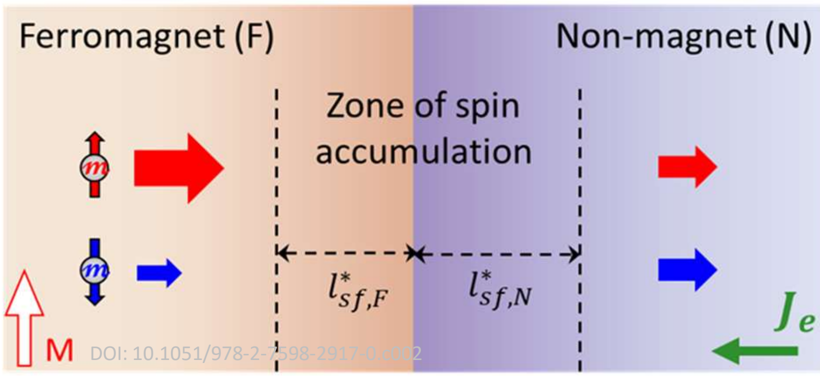

As the result of spin accumulation, a spin polarization diffuses in the N layer

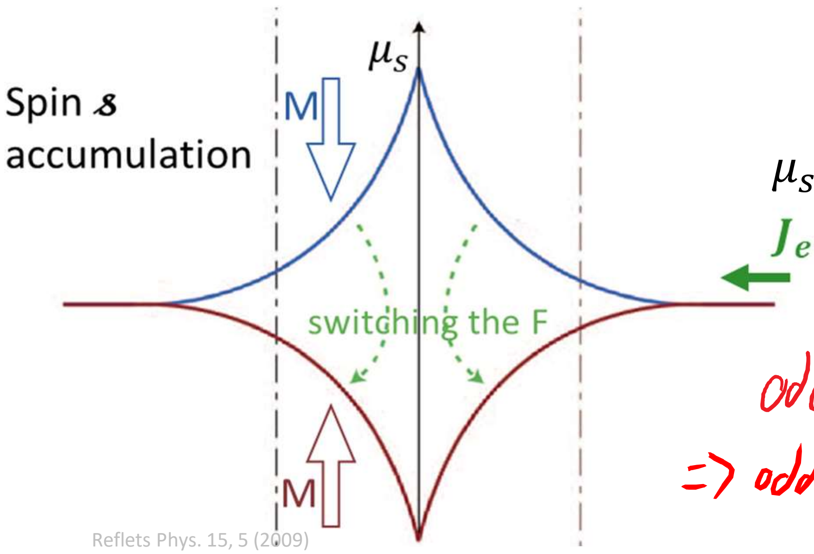

$$\mu_{s,F(N)}(x) = 2e\beta J_e l^*_{sf,N}\rho_N \left(1+\frac{l^*_{sf,N}\rho_N}{l^*_{sf,F}\rho^*_F}\right)^{-1} e^{+(-)\frac{x}{l^*_{sf,F(N)}}}$$

material dependent

with $\beta = \frac{\alpha-1}{1+\alpha}$ *and* $\alpha = \frac{\rho_F^{\downarrow}}{\rho_F^{\uparrow}}$

(polarization of the F layer)

and $\rho_F^* = \rho_F/(1-\beta^2)$

odd in β

=> odd in M : $\mu_s(-M) = -\mu_s(M)$

odd in J_e

=> $\mu_s(F/N) = -\mu_s(N/F)$

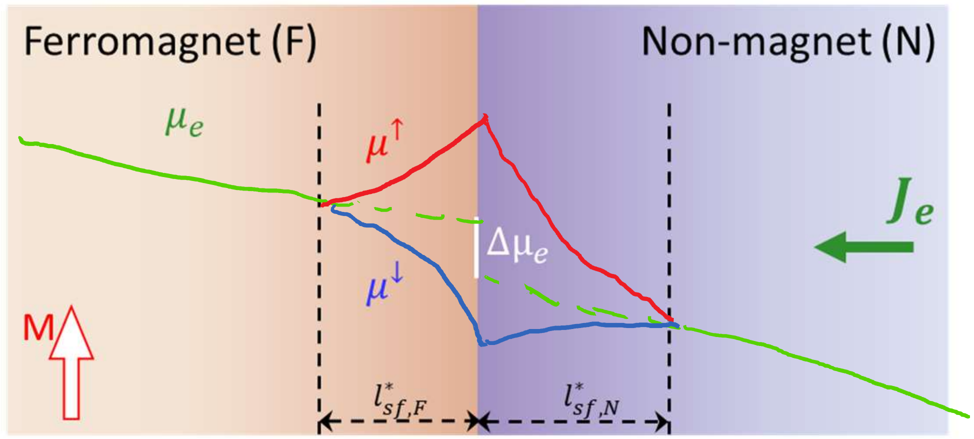

Spin-coupled interface resistance:

$$r_s = -\frac{\Delta\mu_e}{e J_e} = \frac{\mu_{s,F}(0)}{e J_e} = \frac{\mu_{s,N}(0)}{e J_e}$$

spin accumulation over finite length is related to a discontinuity of electrostatic potential: $\Delta\mu_e$

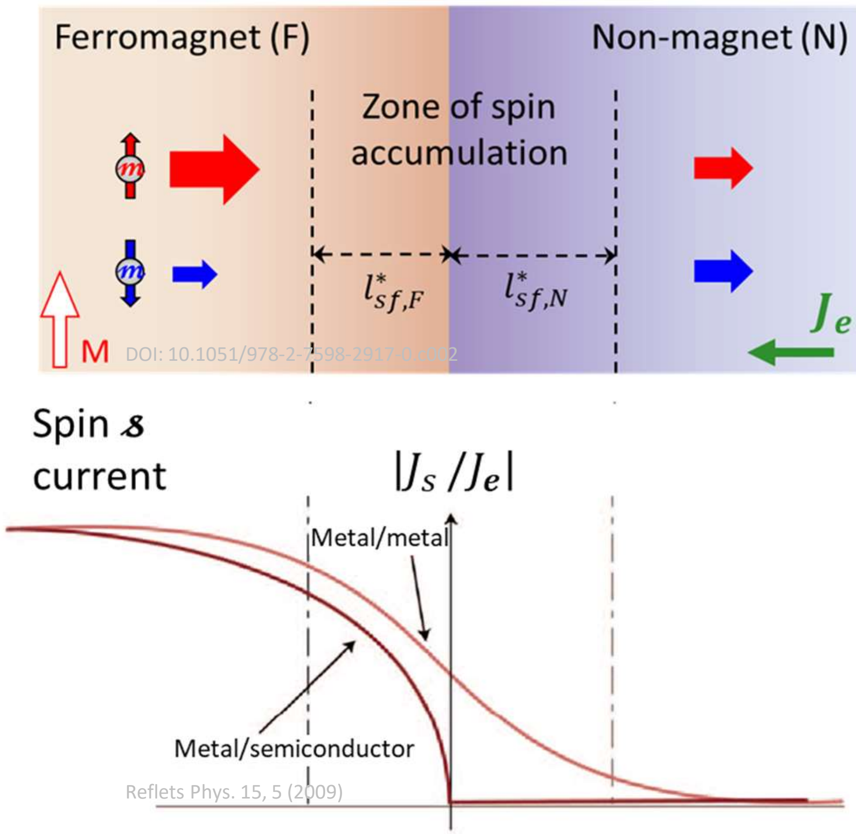

As the result of spin accumulation,
a spin polarization diffuses in the N layer

$$\begin{cases} J_{s,F}(x) = -\beta J_e\left[1-\left(1+\dfrac{l^*_{sf,F}\rho^*_F}{l^*_{sf,N}\rho_N}\right)^{-1} e^{\frac{x}{l^*_{sf,F}}}\right] \\ J_{s,N}(x) = -\beta J_e\left(1+\dfrac{l^*_{sf,N}\rho_N}{l^*_{sf,F}\rho^*_F}\right)^{-1} e^{-\frac{x}{l^*_{sf,N}}} \end{cases}$$

Note: when $l^*_{sf,N}\rho_N \gg l^*_{sf,F}\rho^*_F$ (F-Metal/N-semiconductor), $J_{s,N}(x) \to 0$

⇒ No spin polarization diffuses the N layer
a.k.a. spin impedance mismatch issue

Reminder:
$\mu_s(-M) = -\mu_s(M)$
and
$\mu_s(F/N) = -\mu_s(N/F)$

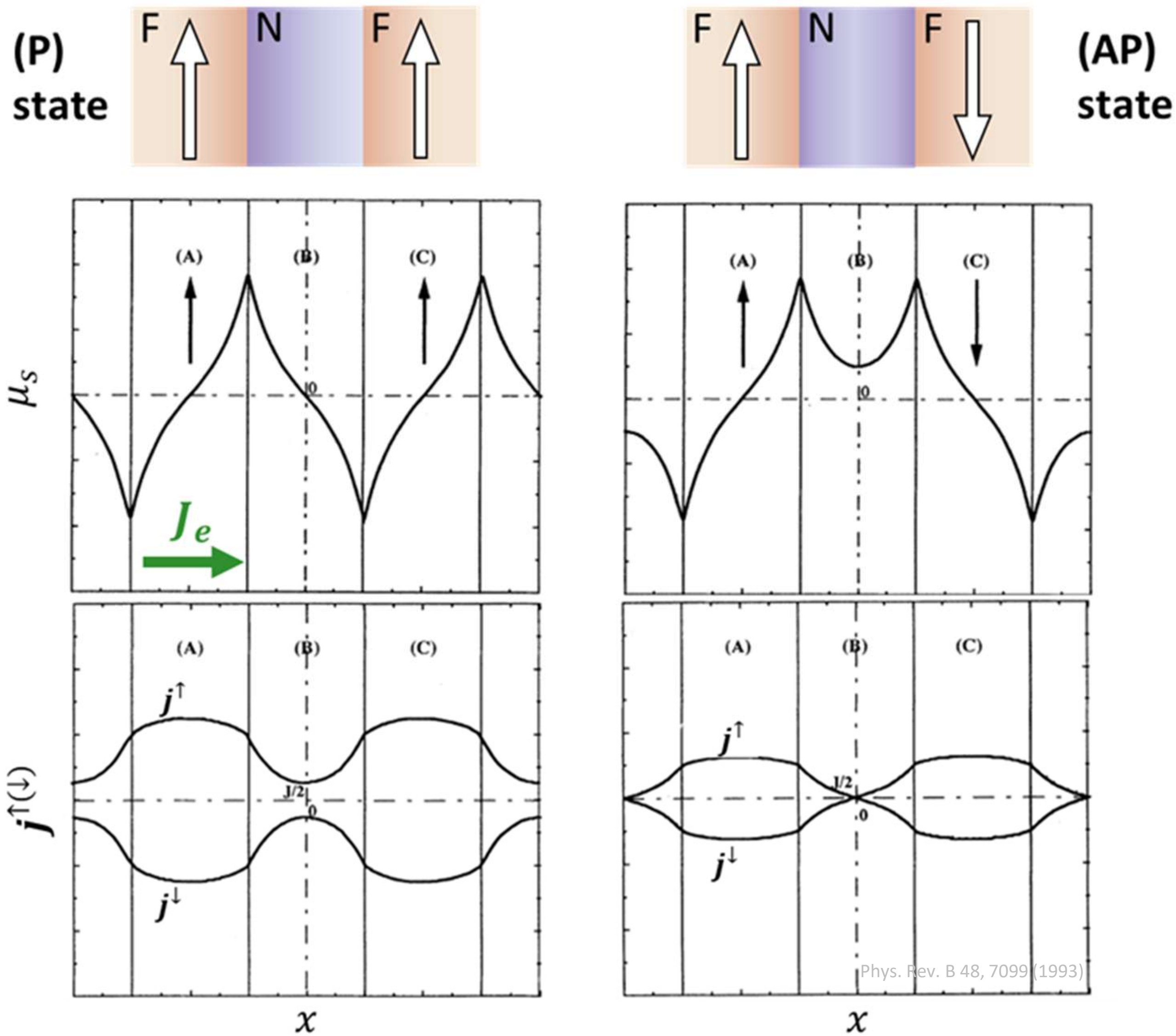

Phys. Rev. B 48, 7099 (1993)

Equivalent circuits (for $d_{N(F)} \ll l^*_{sf,N(F)}$)

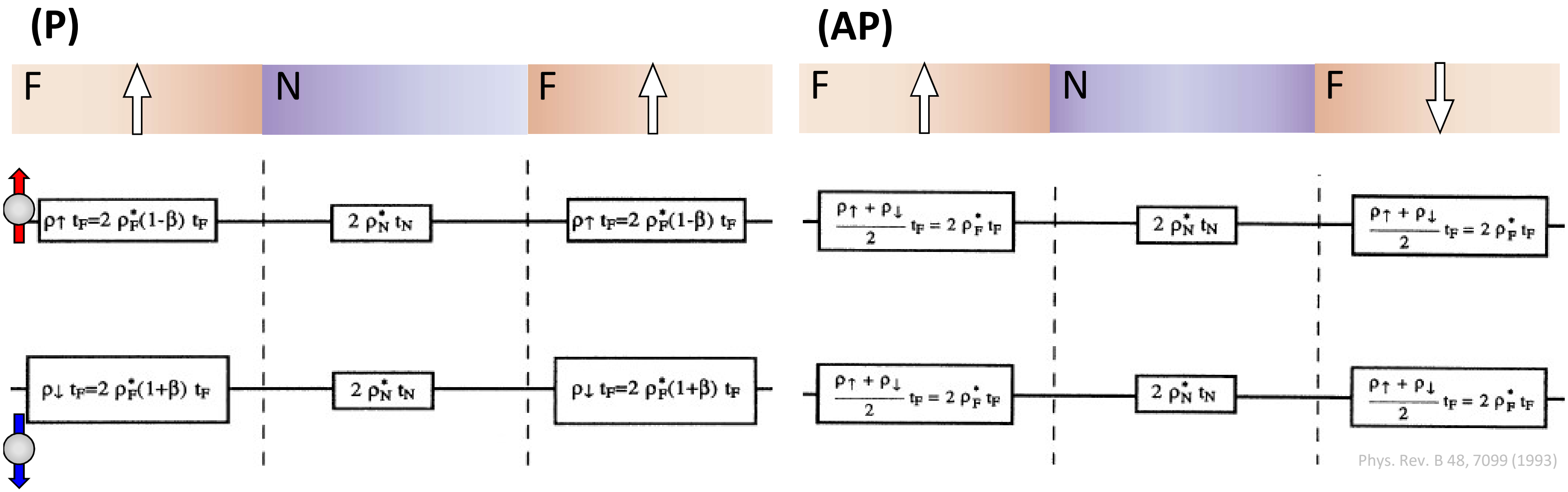

$$\text{CPP-GMR} = \frac{\rho^{AP}-\rho^{P}}{\rho^{AP}} = \beta^2 \frac{(2\rho_F^* d_F)^2}{(\rho_N^* d_N + 2\rho_F^* d_F)^2}$$

- In the previous slides on CPP-GMR, only bulk spin-dependent scattering was considered.

- Refined models must consider interfaces, because e. g. decoherent roughness-induced stray fields and changes in the local DOS creates:

1) interfacial spin-dependent electronic scattering ($\tau^{\uparrow}_{e,interface} \neq \tau^{\downarrow}_{e,interface}$).

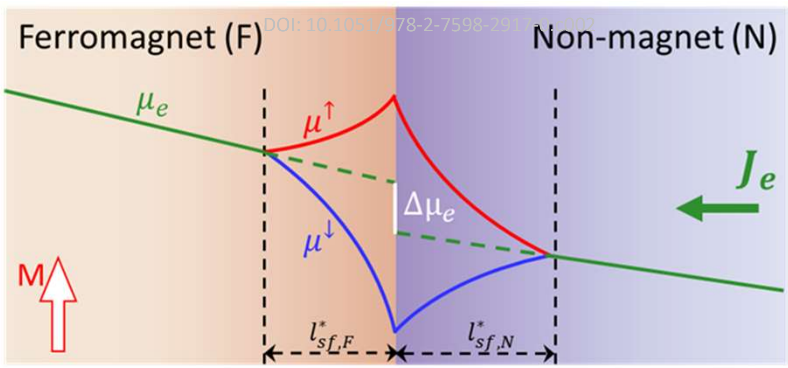

Bulk $\rho_F^{\uparrow(\downarrow)} = 2\rho_F^*(1 \mp \beta)$

with $\beta = \frac{\alpha-1}{1+\alpha}$ and $\alpha = \frac{\rho_F^{\downarrow}}{\rho_F^{\uparrow}}$

Interface $r_{interface}^{\uparrow(\downarrow)} = 2r_b^*(1 \mp \gamma)$

The interface is considered as an infinitesimally thin extra layer, and the electrochemical potential is no more continuous, giving rise to extra resistances in series in each spin-channel. An interfacial spin asymmetry parameter (γ) is introduced.

2) interfacial spin-dependent spin-flip scattering ($\tau_{interface}^{\uparrow\downarrow(\downarrow\uparrow)}$) to account for the fact that only a fraction of the spin current coming from the F layer effectively reaches the N layer. This effect is called the spin memory loss (SML). It is modelled by the following ratio:

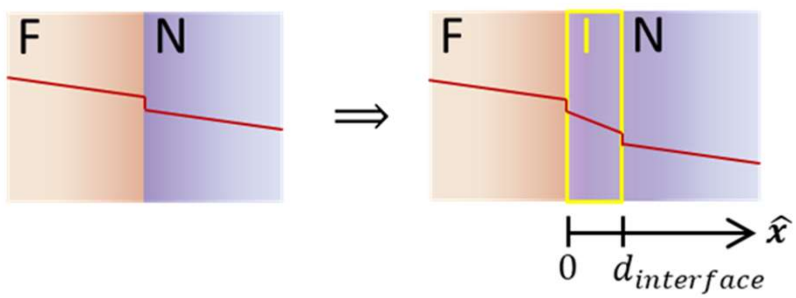

$$R_{SML} = \frac{J_s(x = d_{interface})}{J_s(x = 0)}$$

The interface is considered as thin extra layer with finite dimensions, $t_{interface}$ and possessing a finite spin-flip length, $l_{sf,interface}^{*}$. Spin-flipping by the interface is modelled by the interfacial spin-flip parameter, $\delta = d_{interface}/l_{sf,interace}^{*}$

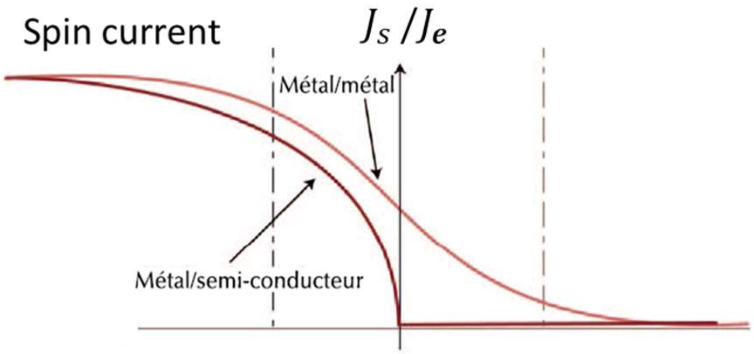

$$\begin{cases} J_{s,F}(x) = \beta J_e \left[1 - \left(1 + \frac{l^*_{sf,F}\rho^*_F}{l^*_{sf,N}\rho_N}\right)^{-1} e^{\frac{x}{l^*_{sf,F}}}\right] \\ J_{s,N}(x) = \beta J_e \left(1 + \frac{l^*_{sf,N}\rho_N}{l^*_{sf,F}\rho^*_F}\right)^{-1} e^{-\frac{x}{l^*_{sf,N}}} \end{cases}$$

$+ \ f(r^*_b, \gamma)$
$+ \ f(\rho_{inter} l^*_{sf,inter}, \delta)$

Bulk

Material	Measured resistivity 4K/ 300K	β Bulk scattering asymmetry	l^*_{SF}
Cu	0.5-0.7μΩ.cm 3-5	0 0	500nm 50-200nm
Au	2μΩ.cm 8	0 0	35nm 25nm
$Ni_{80}Fe_{20}$	10-15 22-25	0.73-0.76 0.70	5.5 4.5
$Ni_{66}Fe_{13}Co_{21}$	9-13 20-23	0.82 0.75	5.5 4.5
Co	4.1-6.45 12-16	0.27 – 0.38 0.22-0.35	60 25
$Co_{90}Fe_{10}$	6-9 13-18	0.6 0.55	55 20
$Co_{50}Fe_{50}$	7-10 15-20	0.6 0.62	50 15
$Pt_{50}Mn_{50}$	160 180	0 0	1 1
Ru	9.5-11 14-20	0 0	14 12

Interface

Material	Measured R.A interfacial resistance	γ Interfacial scattering assymetry
Co/Cu	0.21mΩ.μm² 0.21-0.6	0.77 0.7
$Co_{90}Fe_{10}$/Cu	0.25-0.7 0.25-0.7	0.77 0.7
$Co_{50}Fe_{50}$/Cu	0.45-1 0.45-1	0.77 0.7
NiFe/Cu	0.255 0.25	0.7 0.63
NiFe/Co	0.04 0.04	0.7 0.7
Co/Ru	0.48 0.4	-0.2 -0.2
Co/Ag	0.16 0.16	0.85 0.80

Material	$\rho_I l^*_{sf,inter}$ Interfacial spin resistance	δ Interfacial spin-flip parameter
Co/Cu	2 fΩ.m²	0.25
Cu/Pt	1.7	0.9
Co/Pt	0.83	0.9
Co/Cu/Pt	0.85	1.2

Phys. Rev. B 73, 184418 (2006)
Handbook of Spintronics, Springer, Dordrecht (2016)

$\mu_s \sim 10 - 100\ \mu eV$

$J_e \sim 10^5 - 10^6\ A.cm^{-2}$

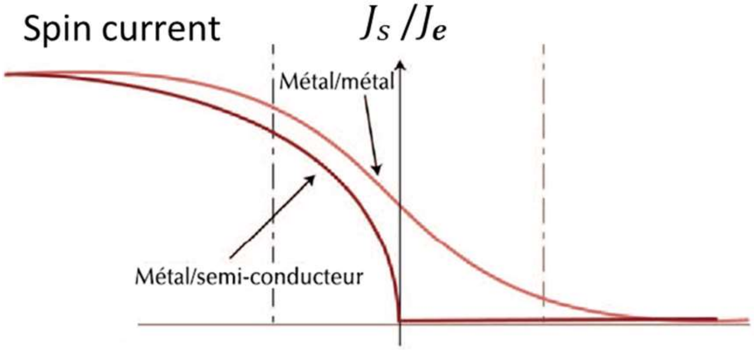

$$
\begin{cases}
J_{s,F}(x) = \beta J_e \left[1 - \left(1 + \dfrac{l^*_{sf,F}\rho^*_F}{l^*_{sf,N}\rho_N}\right)^{-1} e^{\frac{x}{l^*_{sf,F}}}\right] \\
J_{s,N}(x) = \beta J_e \left(1 + \dfrac{l^*_{sf,N}\rho_N}{l^*_{sf,F}\rho^*_F}\right)^{-1} e^{-\frac{x}{l^*_{sf,N}}}
\end{cases}
$$

$+ f(r_b^*, \gamma)$

$+ f(\rho_{inter} l^*_{sf,inter}, \delta)$

Name	ρ	β	r	γ	l_{SF}
$Ni_{80}Cr_{20}$	140 $\mu\Omega$ cm	0	0.5 mΩ μm^2	0.5	20 nm
$Ni_{80}Fe_{20}$	25	0.7	0.3	0.7	4.5
$Co_{50}Fe_{50}$	16	0.7	0.3	0.7	15
Cu	5	0	0.3	0.7	50
$Co_{50}Fe_{50}$	16	0.7	0.5	0.1	15
$Pt_{50}Mn_{50}$	180	0	0.8	0	2
$Ni_{80}Cr_{20}$	140	0	0.5	0	20
IrMn	150	0	0.5	0.1	1

J. App. Phys. 94, 3278 (2003)

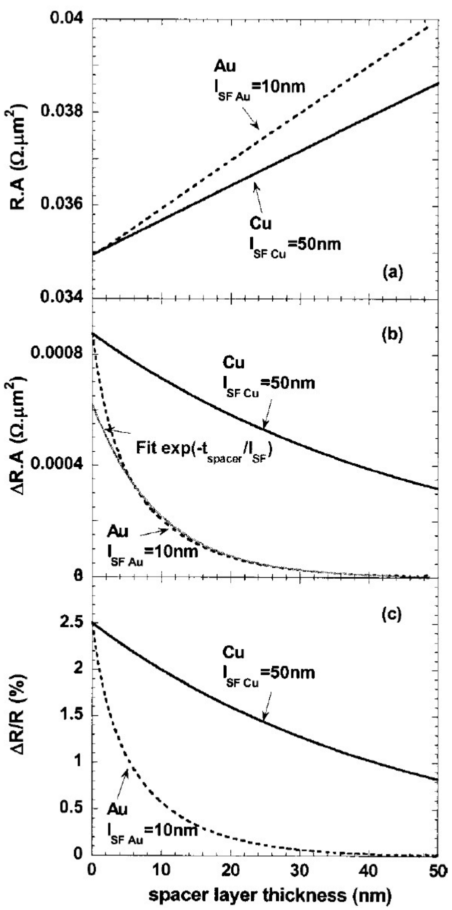

CoFe(1) / Cu (t_N) /CoFe(3)
vs CoFe(1) / Au (t_N) /CoFe(3)

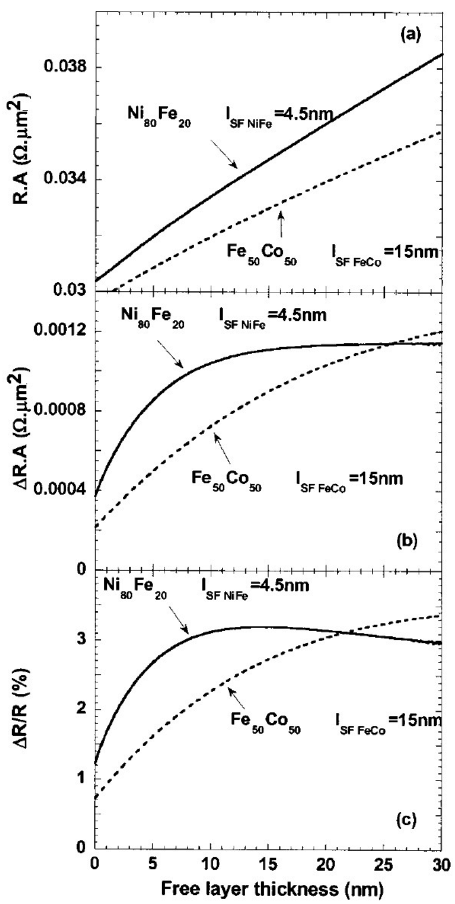

NiFe(t_F) / CoFe(1) / Cu(4) / CoFe (3)
vs CoFe(t_F) / Cu(4) / CoFe (3) (nm)

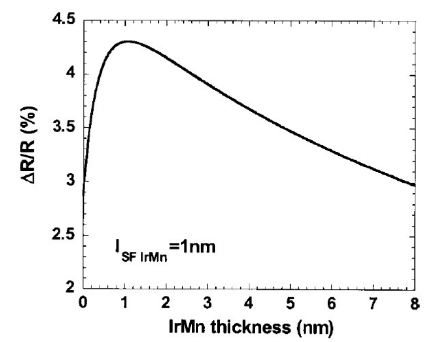

NiFe(4) / CoFe(1) / Cu(4) / CoFe (3)
/ IrMn(t_{IrMn}) / NiCr(5)

- In the uniform 1D GMR formalism, it is convenient to describe spin accumulation with electrochemical potentials, μ_s, to match theory with electrical measurements.

- A spin accumulation can also be described by a net magnetization $\boldsymbol{m}$. Using this latter formalism is for example convenient when considering interactions between spin accumulation and the layer's magnetization $\boldsymbol{M}$, e.g. for spin transfer torque (see lecture 3).

$$\boldsymbol{m} \approx -\mu_B \boldsymbol{n}$$

$$\boldsymbol{m} \approx -\mu_B N \boldsymbol{\mu}$$

$A.m^2$ (μ_B), $eV^{-1}atom^{-1}$ (N), eV ($\boldsymbol{\mu}$)

$\boldsymbol{m}$~0.0001μ_B per atom
versus
$\boldsymbol{m_{ferro}}$~1μ_B per atom

The use of $\boldsymbol{m}$ also implicitly recalls that spin accumulation is described by a vector. This is especially needed to deal with 3D, non-uniformity (e. g. of $\boldsymbol{J_e}$) and non-collinearity (e. g. between $\boldsymbol{M}$ of several layers).

Finally, note that because spin accumulation is described by a vector in the general case (3 components of $\boldsymbol{m}$), spin current is described by a 3x3 tensor (3 components of $\boldsymbol{J_s}$ flowing along 3 directions in space).

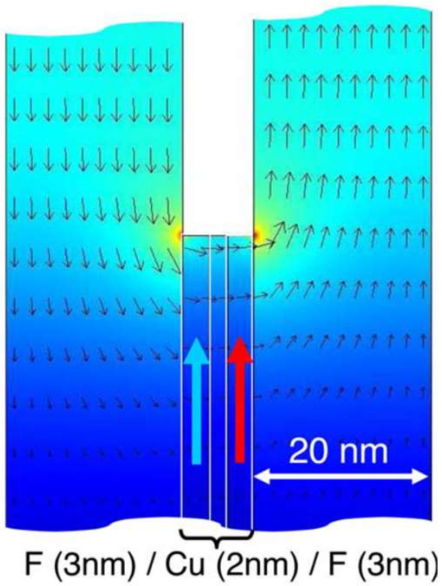

IEEE Magn. Lett. 1, 3000304 (2010)

The color map indicates the amplitude of the charge current, J_e(scalar). The arrows indicate the flow of charges, $\boldsymbol{J_e}$ (vector).

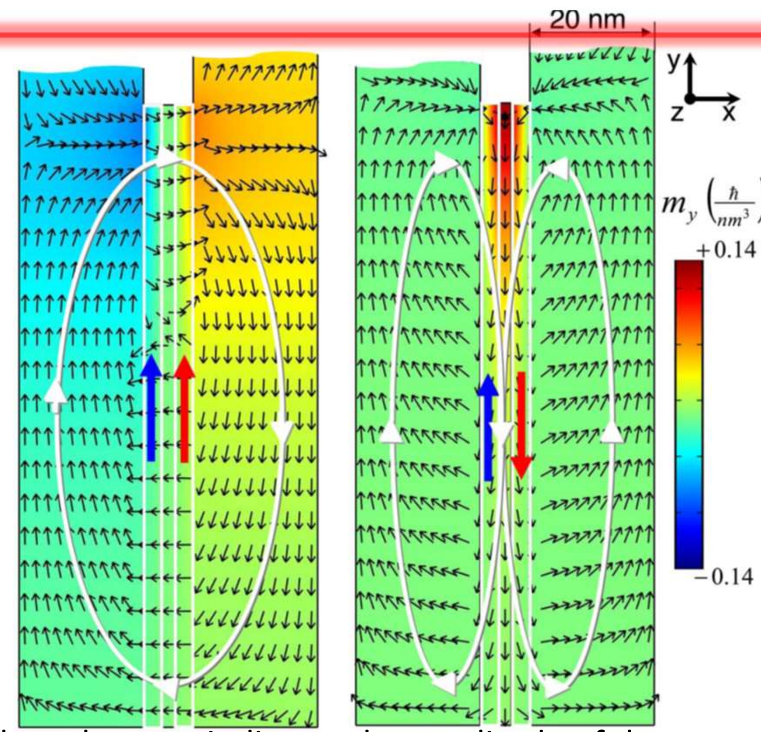

The color map indicates the amplitude of the y-component of spin accumulation, m_y (scalar). The arrows indicate the corresponding flow of y-spins, $\boldsymbol{J_s^y}$ (vector).

IEEE Magn. Lett. 1, 3000304 (2010)

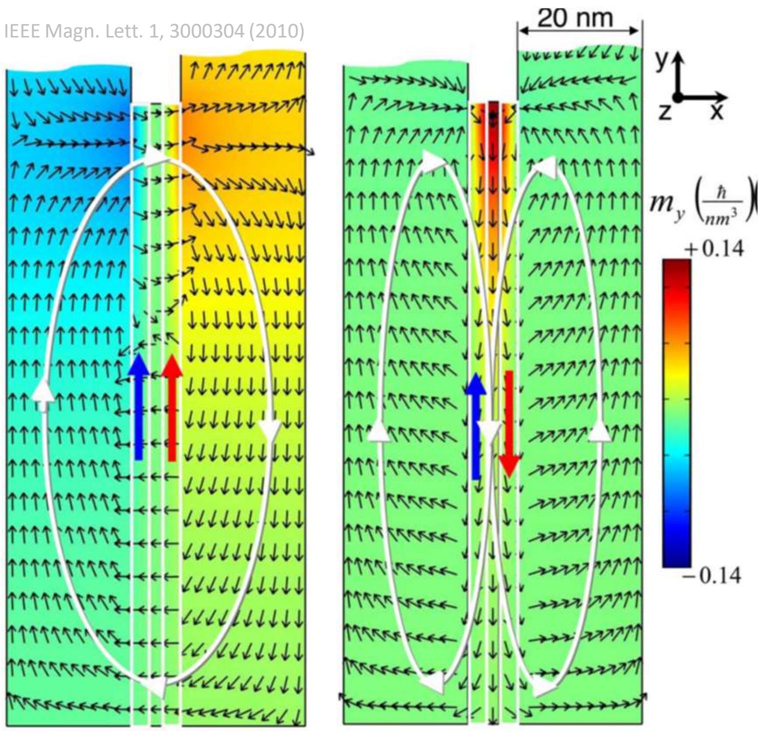

The color map indicates the amplitude of the y-component of spin accumulation, m_y (scalar). The arrows indicate the corresponding flow of y-spins (vector), $J_s^y = J_s^{yx}\hat{x} + J_s^{yy}\hat{y}$

spin

$$J_s = \bar{\bar{J}}_s = \left[J_s^{(x)} \quad J_s^{(y)} \quad J_s^{(z)} \right]$$

$$\bar{\bar{J}}_s = \begin{bmatrix} J_s^{xx} & yx & zx \\ xy & yy & zy \\ xz & yz & zz \end{bmatrix}$$

spin ↘ ↙ space

2^nd odr tensor $= \bar{\bar{J}}_s$

- Spin accumulation ($\boldsymbol{m}$) also exists in magnetic textures like domain walls (DWs), when the spins of the itinerant *s*-electrons are unable to follow magnetization ($\boldsymbol{M}$) (spin-mistracking). However, spin accumulation in DW most often gives rise to negligible resistance in the diffusive regime. This DW effect coexists with other contributions: one is called 'intrinsic' domain wall magnetoresistance (DWMR) and arises from spin-dependent scattering subsequent to spin-mistracking; another relates to AMR (DWAMR) due to SO-interactions.

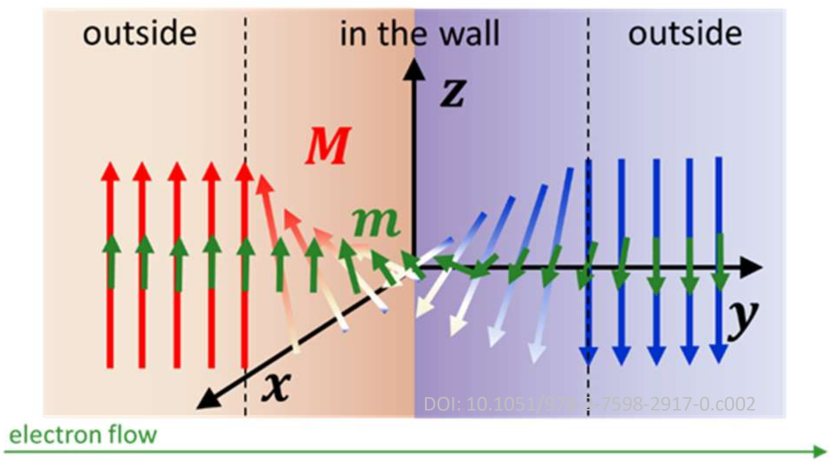

Bloch wall

$$\frac{\Delta\rho}{\rho} = \frac{\rho_{withDW} - \rho_{withoutDW}}{\rho_{withoutDW}} = \frac{\rho_{DW} - \rho_0}{\rho_0}$$

Here:

$$\Delta\rho_{AMR} = 0$$

$$\Delta\rho_{\boldsymbol{m}} = \frac{8\sqrt{3}}{9}\beta^2\rho_F^*\xi^2\lambda_e \sim 0$$

$$\Delta\rho_{DWMR} = \frac{12}{5}\beta^2\rho_F^*\xi^2 w_{DW}\left(1 + \frac{5}{3}\sqrt{1-\beta^2}\right) \sim few\ \%$$

$$\xi = \left(\frac{l_{sd}}{l_{sf}^*}\right)^2$$

spin mistracking parameter (ability of $\boldsymbol{m}$ to follow $\boldsymbol{M}$)

See also lecture 3 for spin transfer torque in DWs.

- **Electronic transport**
  - Electron mean free path vs. Spin diffusion length
  - Electrochemical potential
- **Spin accumulation at a single interface (the Valet/Fert ½classical model)**
  - Drift-diffusion equations to describe spin currents + Boundary conditions
  - Impedance matching
  - Interface (spin-dependent scattering, spin-flip scattering)
- **Spin accumulation in heterostructures**
  - The example of the CPP-GMR effect
- **References:**
  - A. Fert, Reflets Phys. **15**, 5 (2009) and references therein
  - P. S. Bechthtold **B7**, in S. Blügel *et al* (eds) Spintronics - from GMR to quantum information (2009)
  - G. Zahnd, PhD thesis manuscript (2017), https://tel.archives-ouvertes.fr/tel-01791039v2/document
  - Theory of CPP-GMR: T. Valet and A. Fert, Phys. Rev. B **48**, 7099 (1993)
  - 1st exp: W. P. Pratt *et al*, Phys. Rev. Lett. **66**, 3060 (1991)
  - Numbers: J. Bass and W. P. Pratt, J. Phys. Cond. Mat. **19**,183201 (2007);
    N. Strelkov *et al*, J. App. Phys. **94**, 3278 (2003)
  - Non-uniformity: N. Strelkov *et al*, Phys. Rev. B **84**, 024416 (2011)
  - Impedance mismatch: A. Fert and H. Jaffrès, Phys. Rev. B **64**, 184420 (2001)
  - Spin memory loss: J.-C. Rojas-Sánchez *et al*, Phys. Rev. Lett. **112**, 106602 (2014).

Lectures on spintronics

Master 2 Univ. Grenoble Alpes

Vincent Baltz
CNRS Researcher at SPINTEC

Lecture 1	–	04 Dec.
Lecture 2	–	07 Dec.
Lecture 3	–	11 Dec.
Lecture 4	–	14 Dec.
Exercises 1 & 2	–	21 Dec.

vincent.baltz@cea.fr
https://fr.linkedin.com/in/vincentbaltz
www.spintec.fr/af-spintronics/

1h30

I. Brief overview of the field of spintronics and its applications

II. First notions to describe electron and spin transport – AMR, CIP-GMR

1h30

III. Spin accumulation – CPP-GMR

1h30

IV. Transfer of angular momentum – STT

1h30

V. Berry curvature, parity and time symmetries – AHE

VI. Brief non-exhaustive introduction to current topics

1h30

Exercise 1 - Anisotropic magnetoresistance (AMR)

Exercise 2 – The spin pumping (SP) and inverse spin Hall effects (ISHE)

IV. Transfer of angular momentum – STT

Spin transfer torque (STT) and giant magnetoresistance (GMR) are reciprocal effects.

GMR
$\boldsymbol{M}$ influences $\boldsymbol{J}$

STT
$\boldsymbol{J}$ influences $\boldsymbol{M}$

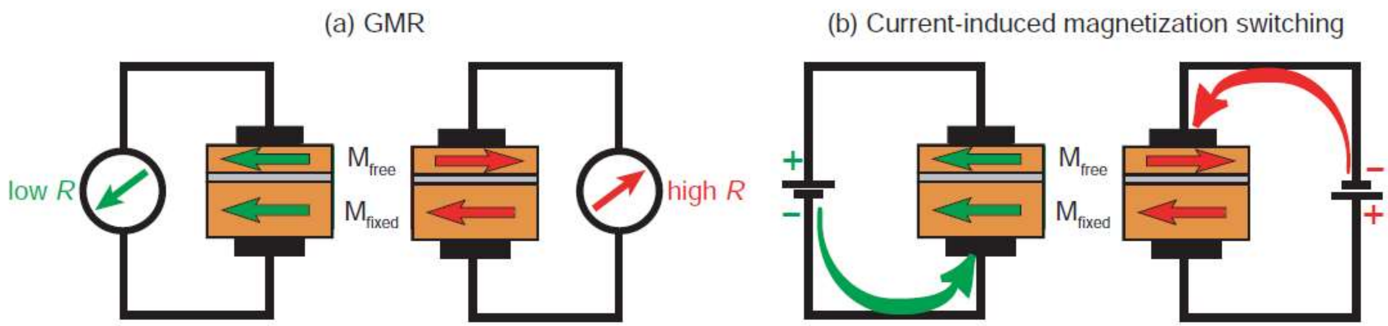

Spintronics - from GMR to quantum information, Jülich (2009)

Fig. 1: *Phenomenology of (a) GMR and (b) current-induced magnetization switching. (a) The electric resistance of a trilayer structure consisting of two ferromagnets separated by a non-magnetic, metallic interlayer depends on the alignment of the layer magnetizations. (b) The stable alignment of the magnetizations depends on the polarity, i.e. the direction, of the current flowing perpendicularly through the trilayer.*

In a F_{pinned}/N/F_{free} trilayer, electrons flowing from the pinned layer to the free layer acquire a spin-polarization in the F_{pinned} layer and accumulate ($\boldsymbol{m} \parallel \boldsymbol{M_{pinned}}$) at the interfaces with the F_{free} layer.

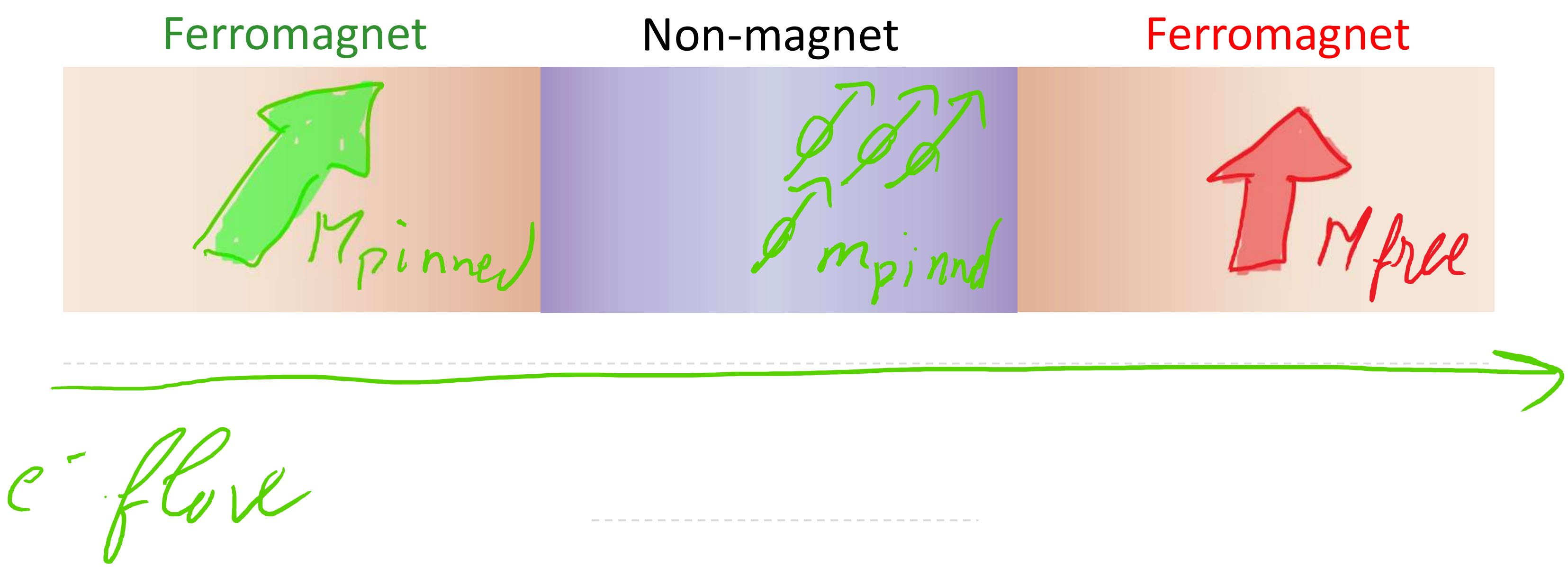

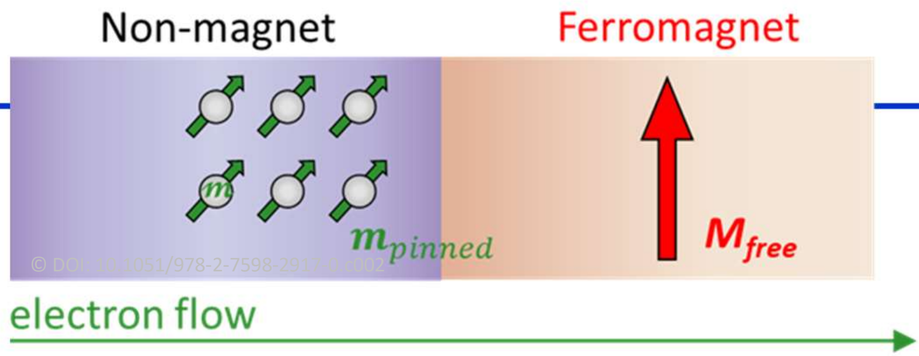

Spin accumulation $\boldsymbol{m}$ and magnetization $\boldsymbol{M}_{free}$ are coupled via the *sd* exchange interactions:

$$\mathcal{H}_{sd} = -J_{sd}\, \hat{m}_{pinned} \cdot \hat{M}_{free}$$

In the reference frame of the s-electrons, $\boldsymbol{m}$ experiences an effective field and a subsequent torque created by $\boldsymbol{M}_{free}$:

$$H \propto J_{sd} M_{free}$$

Conversely, in the reference frame of the layer's magnetization, $\boldsymbol{M}_{free}$ also experiences an effective field and a torque (called the spin tranfer torque, STT) due to $\boldsymbol{m}$:

$$H \propto J_{sd} m_{pinned} \quad \text{and} \quad T \propto -\frac{1}{|\gamma|}\frac{dM_{free}}{dt}$$

Conservation of total angular momentum gives (if all other relaxation channels are closed):

$$\frac{d\boldsymbol{m}}{dt} = -\frac{d\boldsymbol{M}_{free}}{dt}$$

Only projections of $\boldsymbol{m}$ perpendicular to $\boldsymbol{M}_{\boldsymbol{free}}$ give rise to an actual torque.
Therefore, STT is often written and discussed as follows:

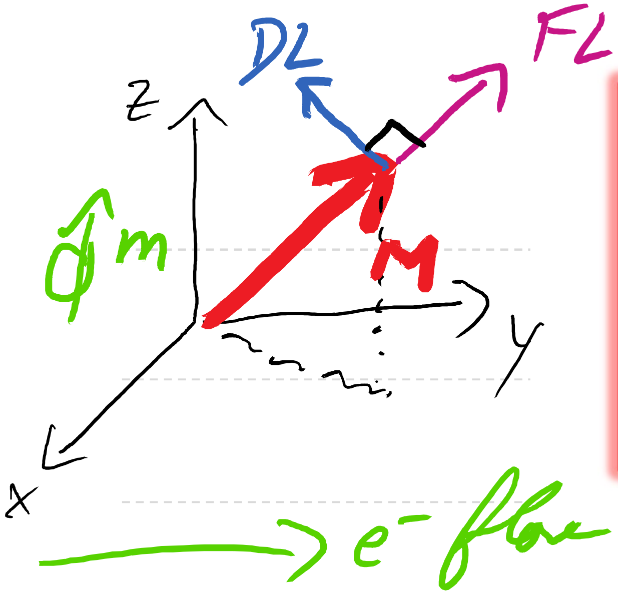

$$-T = \frac{\tau_{DL}}{M_s^2} M \times (m \times M) + \frac{\tau_{FL}}{M_s^2} m \times M$$

a_j	b_j
In-plane	Perpendicular
Slonczewski	Transverse
(anti)Damping-like (DL)	Field-like (FL)

Notes: - τ_{DL} and τ_{FL} depend on material (e.g. M_s), geometry, current ($\boldsymbol{J}$)

- $\boldsymbol{m}$ depends on the effect that gave rise to spin accumulation.
Directions of FL and DL torques may be inverted depending on the direction of $\boldsymbol{m}$.
For STT, $\boldsymbol{m} \parallel \boldsymbol{M}_{\boldsymbol{pinned}}$. In some other structures for spintronics, effects arising from spin-orbit coupling, like spin-Hall and Rashba, can give rise to different spin accumulation and torques. These torques are called spin-orbit torques, SOT (see lecture V).

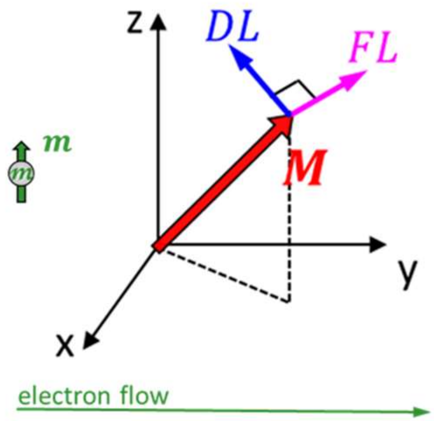

$$-\boldsymbol{T} = \frac{\tau_{DL}}{M_S^2}\boldsymbol{M} \times (\boldsymbol{M} \times \boldsymbol{m}) + \frac{\tau_{FL}}{M_S^2}\boldsymbol{m} \times \boldsymbol{M}$$

Damping-like (DL) Field-like (FL)

In the next slides, we will discuss toy models to:

- determine $\boldsymbol{T}$
- see how magnetization is influenced by $\boldsymbol{T}$

Reminder about the quantum mechanical treatment of charge and spin:

Charge

density of charge

$\rho = -e\langle\psi|\psi\rangle$

density of charge current

$$\boldsymbol{J_e} = -e\mathcal{R}e(\langle\psi|\mathbf{v}|\psi\rangle)$$
$$= \frac{e\hbar}{m}\Im m(\langle\psi|\boldsymbol{\nabla}|\psi\rangle)$$

Spin

density of spin

$s = \langle\psi|\mathbf{S}|\psi\rangle = \frac{\hbar}{2}\langle\psi|\boldsymbol{\sigma}|\psi\rangle$

density of spin current

$$\boldsymbol{Q} = \boldsymbol{J_s} = \mathcal{R}e(\langle\psi|\mathbf{S}\otimes\mathbf{v}|\psi\rangle)$$
$$= -\frac{\hbar^2}{2m}\Im m(\langle\psi|\boldsymbol{\sigma}\otimes\boldsymbol{\nabla}|\psi\rangle)$$

ψ is the spinor, here spin-half electron wave function
$\mathbf{v}$ is the velocity operator
$\mathbf{S}$ is the spin operator, linked to the Pauli operator, $\boldsymbol{\sigma}$
with $\sigma^x = \begin{pmatrix}0 & 1\\1 & 0\end{pmatrix}$, $\sigma^y = \begin{pmatrix}0 & -i\\i & 0\end{pmatrix}$, and $\sigma^z = \begin{pmatrix}1 & 0\\0 & -1\end{pmatrix}$*; z= quantification axis*

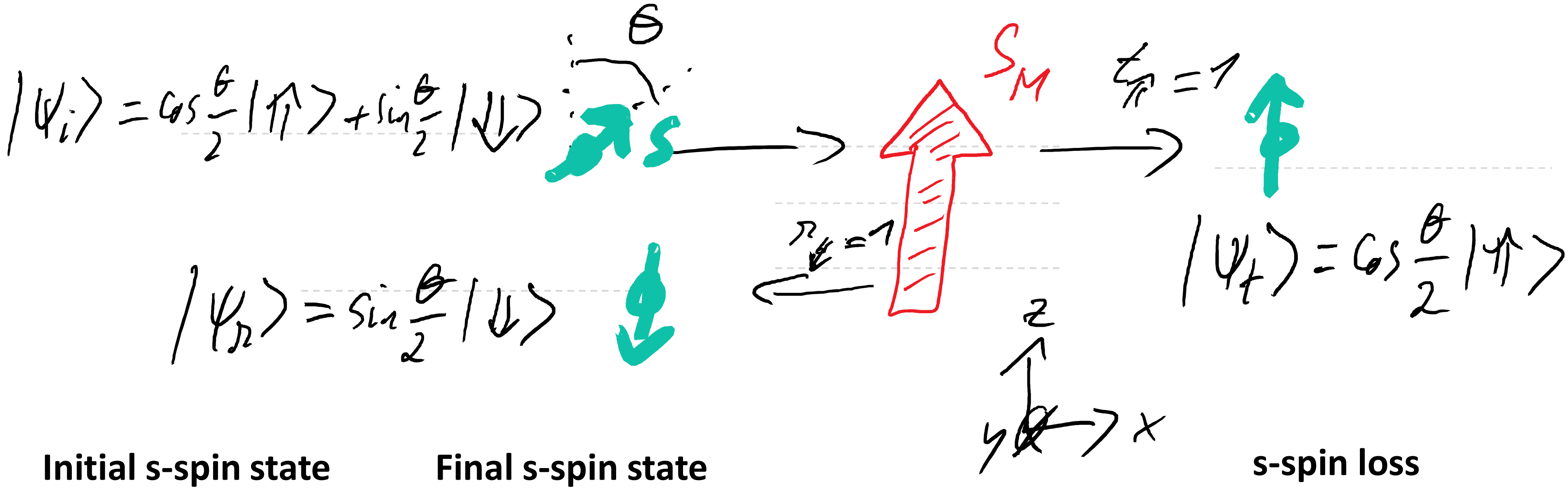

Initial s-spin state

$s_i^x = \frac{\hbar}{2}\sin\theta$

$s_i^z = \frac{\hbar}{2}\cos\theta$

Final s-spin state

$s_f^x = s_t^x + s_r^x = \dots = 0$

$s_f^z = s_t^z + s_r^z = \dots = \frac{\hbar}{2}\cos\theta$

s-spin loss

$\Delta s^x = -\frac{\hbar}{2}\sin\theta$

$\Delta s^z = 0$

Conservation of total angular momentum **'Nothing is lost, nothing is created, everything is transformed'**

$$\Delta s + \Delta S_M = 0 \Rightarrow \Delta S_M = \Delta S_M^x = \frac{\hbar}{2}\sin\theta$$

Note: the propagation terms (e^{ikx} and e^{-ikx} in $\psi_{i(t)}$ and ψ_r) were ommited here to facilitate the message delivery.

Calculation of the spin components (Homework)

$$\mathbf{s} = \langle\psi|\mathbf{S}|\psi\rangle \quad \text{with } \mathbf{S} = \frac{\hbar}{2}\boldsymbol{\sigma}$$

$$\langle\Uparrow| = (1 \quad 0), and\ |\Uparrow\rangle = \begin{pmatrix}1\\0\end{pmatrix}$$

$$\langle\Downarrow| = (0 \quad 1), and\ |\Downarrow\rangle = \begin{pmatrix}0\\1\end{pmatrix}$$

Initial state

$$s_i^x = \langle\psi_i|\mathbf{S}^x|\psi_i\rangle = \left(\cos\frac{\theta}{2} \quad \sin\frac{\theta}{2}\right)\frac{\hbar}{2}\begin{pmatrix}0 & 1\\ 0 & 1\end{pmatrix}\begin{pmatrix}\cos\frac{\theta}{2}\\ \sin\frac{\theta}{2}\end{pmatrix} = \frac{\hbar}{2}2\cos\frac{\theta}{2}\sin\frac{\theta}{2}$$

$$= \frac{\hbar}{2}\sin\theta$$

$$s_i^z = \langle\psi_i|\mathbf{S}^z|\psi_i\rangle = \_\_\_\_\_\_\_\_$$

Final state

$$s_t^x = \langle\psi_t|\mathbf{S}^x|\psi_t\rangle = \_\_\_\_\_\_\_\_$$

$$s_t^z = \langle\psi_t|\mathbf{S}^z|\psi_t\rangle = \_\_\_\_\_\_\_\_$$

$$s_r^x = \langle\psi_r|\mathbf{S}^x|\psi_r\rangle = \_\_\_\_\_\_\_\_$$

$$s_r^z = \langle\psi_r|\mathbf{S}^z|\psi_r\rangle = \_\_\_\_\_\_\_\_$$

Loss

$\Delta s^x = (s_t^x + s_r^x) - s_i^x =$ ________ and $\Delta s^z = (s_t^z + s_r^z) - s_i^x =$ ________

$$|\psi_i\rangle \propto \cos\frac{\theta}{2}|\Uparrow\rangle + \sin\frac{\theta}{2}|\Downarrow\rangle$$

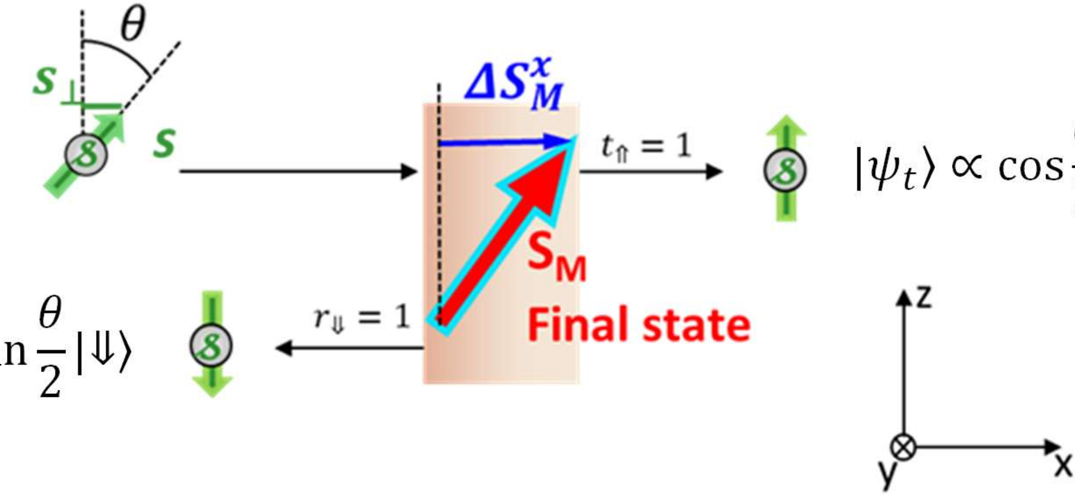

$$|\psi_t\rangle \propto \cos\frac{\theta}{2}|\Uparrow\rangle$$

$$|\psi_r\rangle \propto \sin\frac{\theta}{2}|\Downarrow\rangle$$

$$\boldsymbol{\Delta S_M} = \Delta S_M^x\,\hat{\boldsymbol{x}} = \frac{\hbar}{2}\sin\theta\,\hat{\boldsymbol{x}} = \boldsymbol{s}_\perp$$

It is said that the transverse component of spin angular momentum is absorbed.

This absorption was actually the result of a torque, $\boldsymbol{T}$, acting on $\boldsymbol{S_M}$.

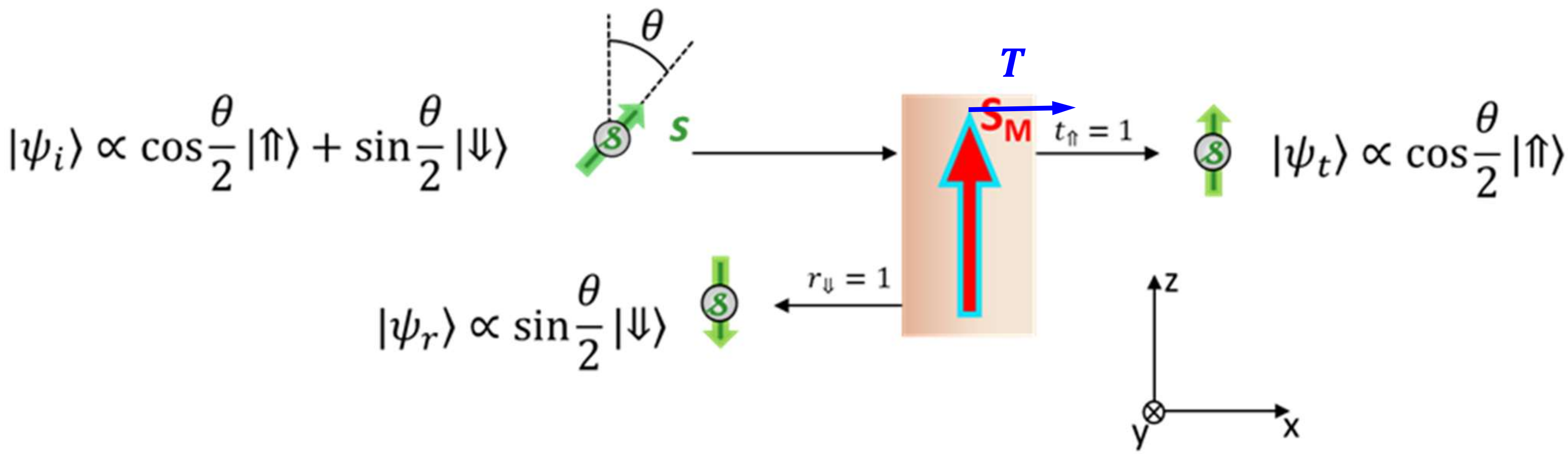

The spin transfer torque, $\boldsymbol{T}$, can directly be calculated from the flux of spin current entering and leaving the effective volume impacted:

$$\boldsymbol{T} = -\iint \hat{\boldsymbol{x}} \cdot \boldsymbol{Q} dA = A\hat{\boldsymbol{x}} \cdot (\boldsymbol{Q}_i + \boldsymbol{Q}_r - \boldsymbol{Q}_t)$$

$$\boldsymbol{T} = \frac{A}{V_{eff}} \frac{\hbar^2 k}{2m} \sin\theta\, \hat{\boldsymbol{x}} = \frac{A}{V_{eff}} \frac{\hbar^2 k}{2m} \widehat{\boldsymbol{S}_{\boldsymbol{M}}} \times \left(\hat{\boldsymbol{s}} \times \widehat{\boldsymbol{S}_{\boldsymbol{M}}}\right)$$

Here, we see that $\boldsymbol{T}$ is damping-like.

Calculation of the torque (Homework)

spin → space → Q^{ab} = flow of a-spins along b

Density of spin current:

$$\boldsymbol{Q} = -\frac{\hbar}{m}\Im m(\langle\psi|\boldsymbol{S}\cdot\boldsymbol{\nabla}|\psi\rangle) \quad \text{with } Q^{ab} = -\frac{\hbar}{m}\Im m(\langle\psi|\boldsymbol{S}^a\cdot\boldsymbol{\nabla}_{\boldsymbol{b}}|\psi\rangle)$$

$$= -\frac{\hbar k_b}{m}\langle\psi|\boldsymbol{S}^a|\psi\rangle$$

$$= -\frac{\hbar k_b}{m}s^a$$

$$\boldsymbol{Q} = \bar{\bar{Q}} = -\frac{\hbar k_x}{m}\begin{bmatrix} s^x & s^y & s^z \\ 0 & 0 & 0 \\ 0 & 0 & 0 \end{bmatrix} \quad \text{and} \quad \hat{\boldsymbol{x}}\cdot\boldsymbol{Q} = \frac{\hbar k_x}{m}(s^x + s^y + s^z)\hat{\boldsymbol{x}}$$

Torque:

$$\boldsymbol{T} = \hat{\boldsymbol{x}}\cdot(\boldsymbol{Q}_i + \boldsymbol{Q}_r - \boldsymbol{Q}_t)$$

$$\boldsymbol{T} = -\frac{\hbar k_x}{m}(\Delta s^x + \Delta s^y + \Delta s^z)\hat{\boldsymbol{x}}$$

$$\boldsymbol{T} = \frac{\hbar^2 k_x}{2m}\sin\theta\,\hat{\boldsymbol{x}}$$

For calculations of $\Delta s^x, \Delta s^y, \Delta s^z$, cf. slide 10.

Other ingredients can be introduced to explain the physical origin of STT more accurately:

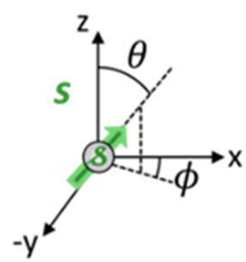

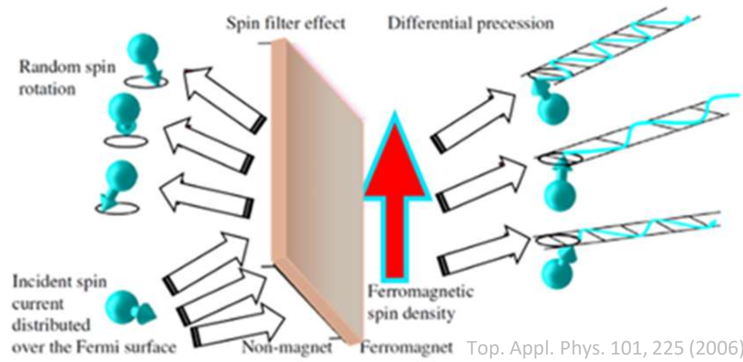

Top. Appl. Phys. 101, 225 (2006)

- Spin filtering : spin dep. $t_{\uparrow(\downarrow)}$ and $r_{\uparrow(\downarrow)}$
- spin rotation ϕ and dephasing $\delta\phi$ upon reflection : $e^{i(\phi+\delta\phi)}$
- spin precession upon transmission in the F : $e^{i(k_\uparrow - k_\downarrow)x}$

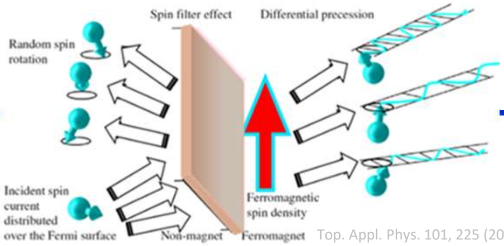

Top. Appl. Phys. 101, 225 (2006)

These ingredients are taken into account by considering complex number transmission ($t_\downarrow, t_\uparrow$) and reflection ($r_\downarrow, r_\uparrow$) coefficients. Below is the example with spin dephasing upon reflection:

$$Q_r^{xx} = -\frac{\hbar k_x}{m}\sin\theta\,\mathcal{R}e\left(r_\Uparrow^* r_\Downarrow e^{i\phi}\right)$$

$$Q_r^{yx} = -\frac{\hbar k_x}{m}\sin\theta\,\mathfrak{I}m\left(r_\Uparrow^* r_\Downarrow e^{i\phi}\right)$$

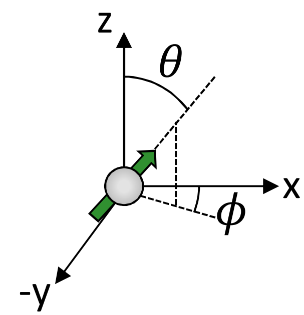

with, by definition, $r_\Uparrow^* r_\Downarrow = |r_\Uparrow^* r_\Downarrow| e^{i\delta\phi}$

Describes reflection along axes transverse to $\boldsymbol{S_M} \parallel \hat{\boldsymbol{z}}$. This term relates to the transverse reflection coefficient or the spin-mixing coefficient (mixing stands for mixing of the eigen states no spin-flip is involved).
(Advanced) It is the spin-mixing conductance in the magnetoelectronic circuit theory.

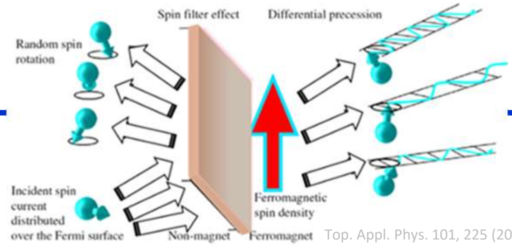

Top. Appl. Phys. 101, 225 (2006)

$$|\psi_i\rangle \propto \cos\frac{\theta}{2}|\Uparrow\rangle + \sin\frac{\theta}{2}|\Downarrow\rangle$$

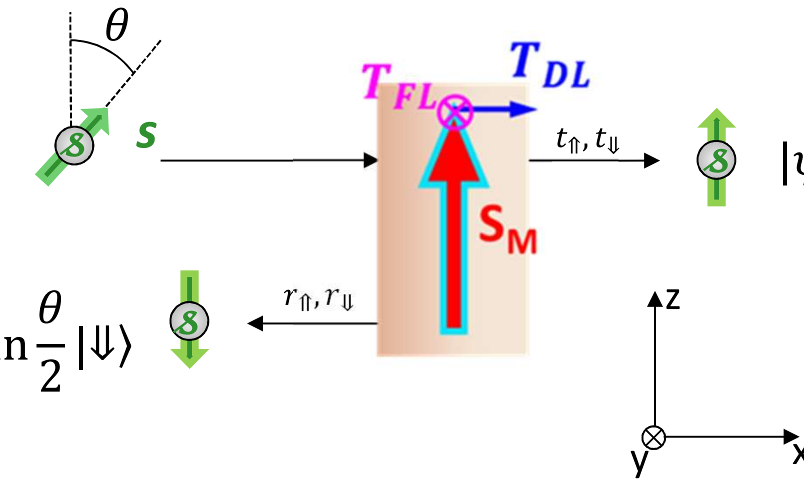

$$|\psi_t\rangle \propto \cos\frac{\theta}{2}|\Uparrow\rangle$$

$$|\psi_r\rangle \propto \sin\frac{\theta}{2}|\Downarrow\rangle$$

When dephasing is introduced by considering complex transmission ($t_\Uparrow, t_\Downarrow$) and reflection ($r_\Uparrow, r_\Downarrow$) coefficients, both DL and FL terms contribute to the torque:

$$\boldsymbol{T} = \frac{A}{V_{eff}}\frac{\hbar^2 k}{2m}\sin\theta\left[\left(1 - \mathcal{Re}(t_\Uparrow t_\Downarrow^* + r_\Uparrow r_\Downarrow^*)\right)\hat{\boldsymbol{x}} - \Im m(t_\Uparrow t_\Downarrow^* + r_\Uparrow r_\Downarrow^*)\hat{\boldsymbol{y}}\right]$$

$$\boldsymbol{T} = \frac{A}{V_{eff}}\frac{\hbar^2 k}{2m}\left[g_r^{\uparrow\downarrow}\hat{\boldsymbol{S}}_M \times \left(\hat{\boldsymbol{s}} \times \hat{\boldsymbol{S}}_M\right) + g_i^{\uparrow\downarrow}\hat{\boldsymbol{S}}_M \times \hat{\boldsymbol{s}}\right]$$

with $g^{\uparrow\downarrow} = 1 - (t_\Uparrow t_\Downarrow^* + r_\Uparrow r_\Downarrow^*)$, the spin mixing coefficient

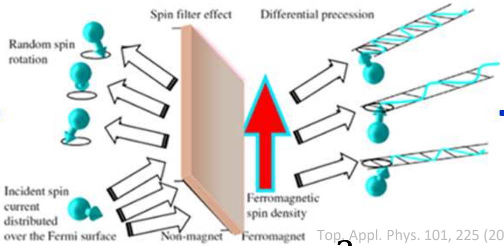

$$\boldsymbol{T} = \frac{A}{V_{eff}}\frac{\hbar^2 k}{2m}\left[\left(1 - \mathcal{Re}(t_\Uparrow t_\Downarrow^* + r_\Uparrow r_\Downarrow^*)\right)\widehat{\boldsymbol{S_M}} \times \left(\widehat{\boldsymbol{S_M}} \times \hat{\boldsymbol{s}}\right) + \mathfrak{Im}(t_\Uparrow t_\Downarrow^* + r_\Uparrow r_\Downarrow^*)\widehat{\boldsymbol{S_M}} \times \hat{\boldsymbol{s}}\right]$$

Notes:

$T = 0$ if $t_\Uparrow = t_\Downarrow$ and $r_\Uparrow = r_\Downarrow$ (no spin filtering) (Note: $|t^2_{\Uparrow(\Downarrow)}| + |r^2_{\Uparrow(\Downarrow)}| = 1$)
$T = 0$ if $\theta = 0$ or $\theta = \pi$ (collinearity)

The above formula considered $\boldsymbol{T}$ created by one type of electron wave only. $\boldsymbol{T_{total}}$ can be obtained by summation over the Fermi surface of the N layer corresponding to all possible incident wave vectors.

Reflected (dephased) spins affect spin accumulation, e. g. resulting in a non-trivial θ-dependence of STT).

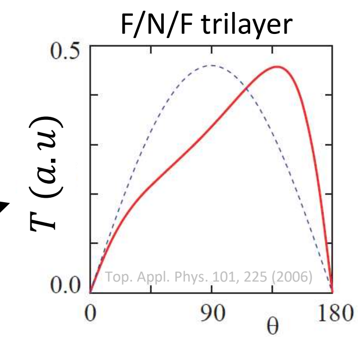

In metallic structures, some transverse components average out: $\mathcal{Re}(t_\Uparrow t_\Downarrow^*) = \mathfrak{Im}(t_\Uparrow t_\Downarrow^*) \approx 0$ and $\mathfrak{Im}(r_\Uparrow r_\Downarrow^*) \ll \mathcal{Re}(t_\Uparrow t_\Downarrow^* + r_\Uparrow r_\Downarrow^*)$. The FL term is small (less than 5% of the DL). This contrasts with tunnel junctions, where the *k*-selection upon tunnelling reduces the effect of averaging (FL ~ 30% of DL).

$R_\perp = \mathcal{Re}(r_\Uparrow r_\Downarrow^*)$ and $R_\times = \mathfrak{Im}(r_\Uparrow r_\Downarrow^*)$ describe reflection along axes transverse to $\boldsymbol{S_M}$. They are called the transverse reflection coefficients or spin-mixing coefficients.

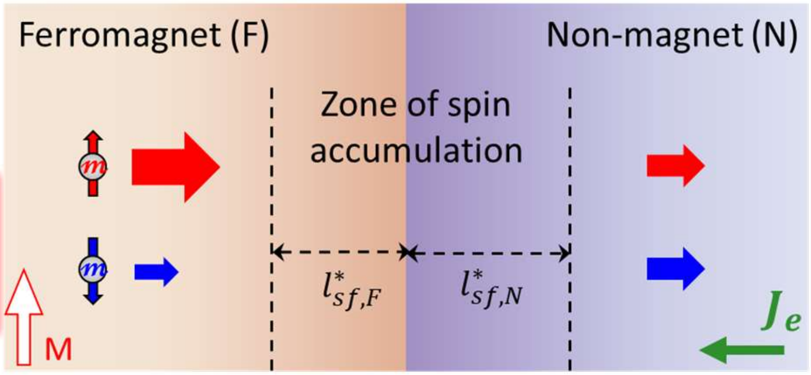

Transfer of angular momentum must be introduced in the diffusion equations of transport.

Charge conservation:

$$\nabla \cdot J_e = 0$$

Total angular momentum conservation:
any loss in spin current must be due to spin-flips (1st term) or to spin transfer torque i. e. precession of the spin accumulation around the local magnetization due to *s–d* exchange interaction (2nd term).

$$\nabla \cdot \boldsymbol{J_s} = \frac{\sigma^*(1-\beta^2)}{4el^{*\,2}_{sf}}\boldsymbol{\mu}_s + \frac{\sigma^*}{4eM_s l_{sd}^2}(\boldsymbol{M}\times\boldsymbol{\mu}_s)$$

l^*_{sf} is the average spin-diffusion length defined in lecture 2
$l_{sd} = \sqrt{2D\hbar/J_{sd}}$ is the 'exchange' spin-reorientation length, i. e. the distance over which the spin polarization is reoriented along $\boldsymbol{M}$ (typically, $l_{sd}\sim 1\ nm$ in metals)

Typical critical current densities for switching magnetization by STT are $J_{e,crit} \sim 10^{7}\ A.cm^{-2}$, hence the need for nm lateral dimensions (in addition to nm-thick layers due to l^{*}_{sf} and l_{sd})

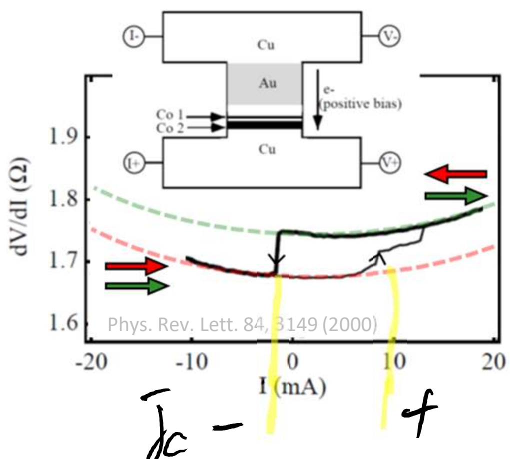

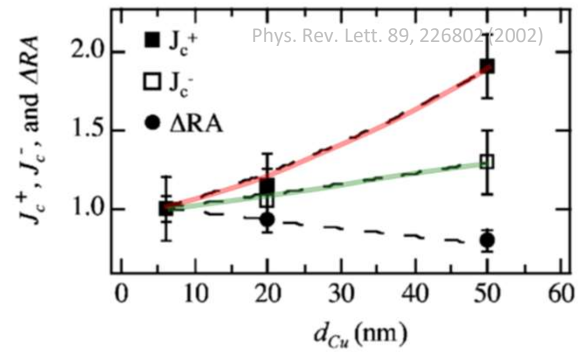

Note that the switching is polarity dependent:

$J_c^{+} > J_c^{-}$

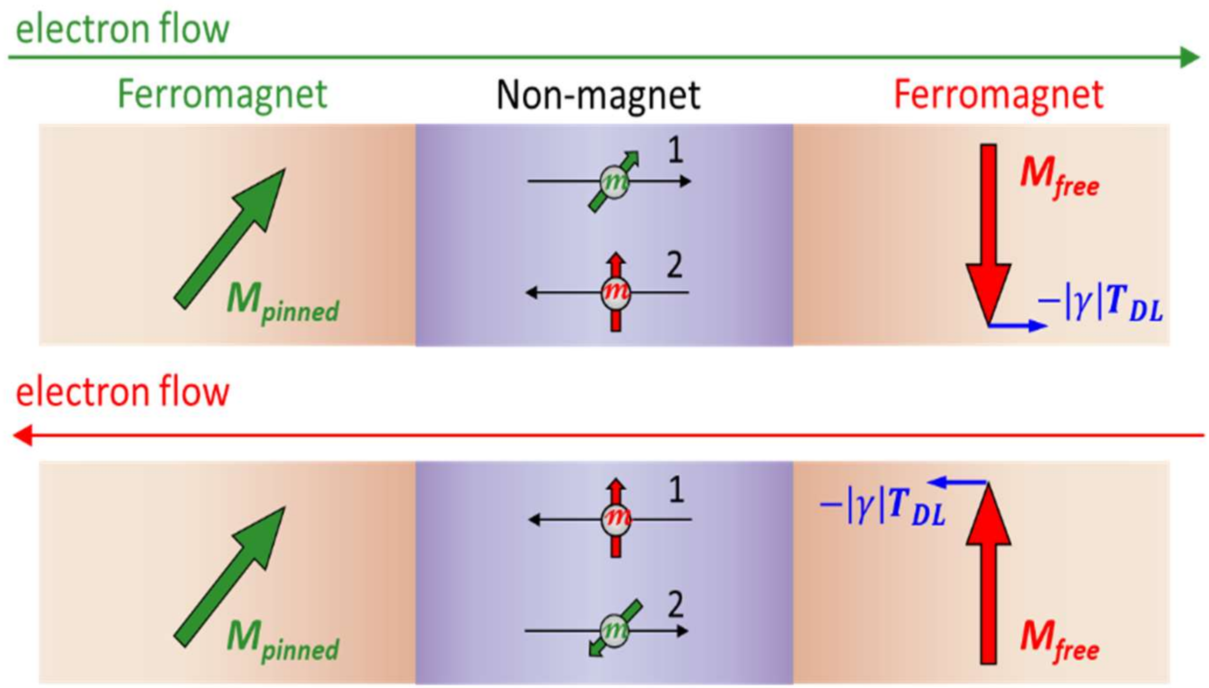

For a positive electron flux ($J^{-}_{e,crit}$), spins travel only once across the N (Cu) layer.

For a negative electron flux ($J^{+}_{e,crit}$), spins travel twice across the N (Cu) layer.

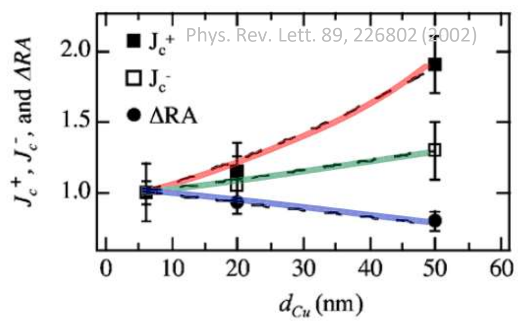

$\Delta RA \propto \exp(\frac{-d_{Cu}}{\lambda}) \Rightarrow \lambda = (190 \pm 20)$ nm

$J_c^- \propto \exp(\frac{d_{Cu}}{\lambda}) \Rightarrow \lambda = (170 \pm 40)$ nm

$J_c^+ \propto \exp(\frac{2d_{Cu}}{\lambda}) \Rightarrow \lambda = (140 \pm 30)$ nm

Introducing the STT DL term in the LLG equation:

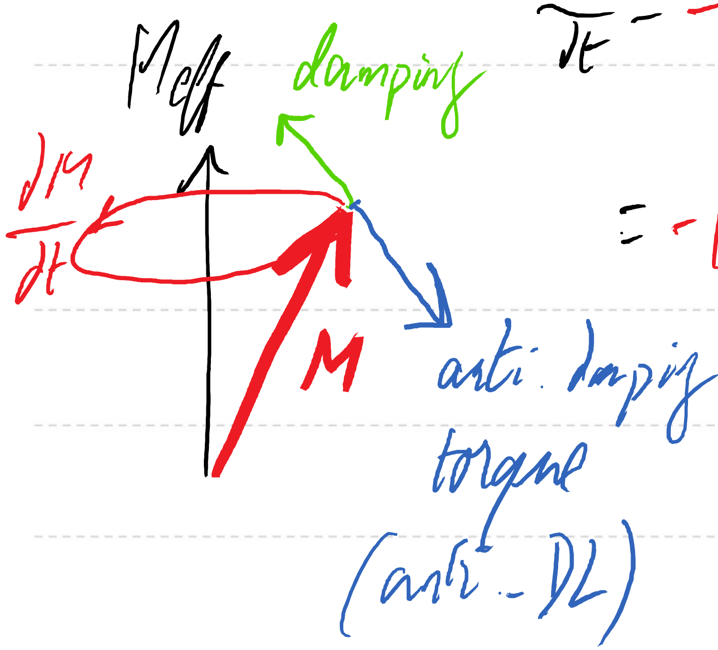

$$\frac{d\mathbf{M}}{dt} = -|\gamma|\mathbf{T}_{Larmor} - |\gamma|\mathbf{T}_{Damping} - |\gamma|\mathbf{T}_{DL} - |\gamma|\mathbf{T}_{FL}$$

$$= -|\gamma|\mathbf{M}\times\mu_0\mathbf{H}_{eff} + \mathbf{M}\times\frac{d\mathbf{M}}{dt}$$

$$+|\gamma|\frac{\tau_{DL}}{M_s^2}\mathbf{M}\times(\mathbf{m}\times\mathbf{M})$$

$$+|\gamma|\frac{\tau_{FL}}{M_s}(\mathbf{m}\times\mathbf{M})$$

4. The STT term in magnetization dynamics equations

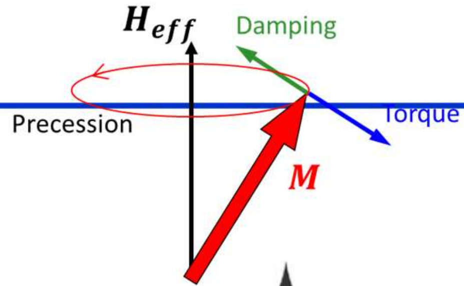

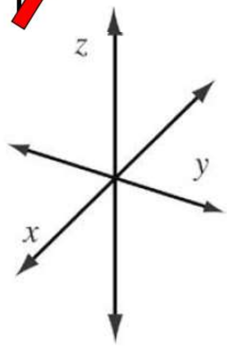

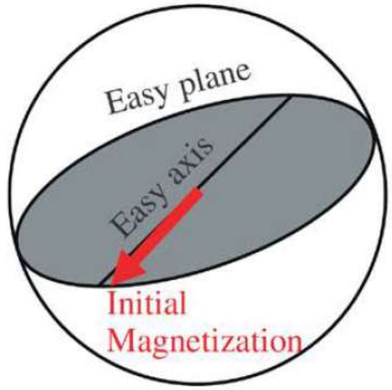

Stable precession
STT = damping

Switching
STT > damping

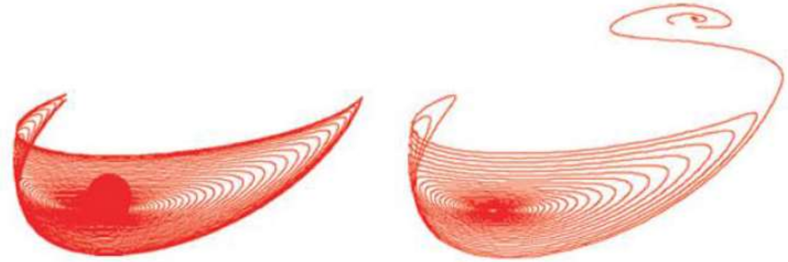

J. Mag. Magn. Mat. 320, 1190 (2008)

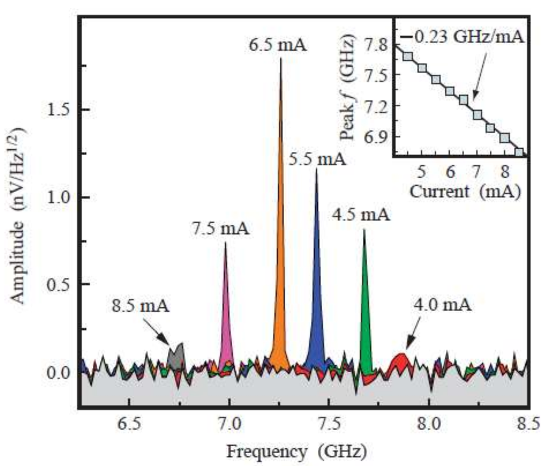

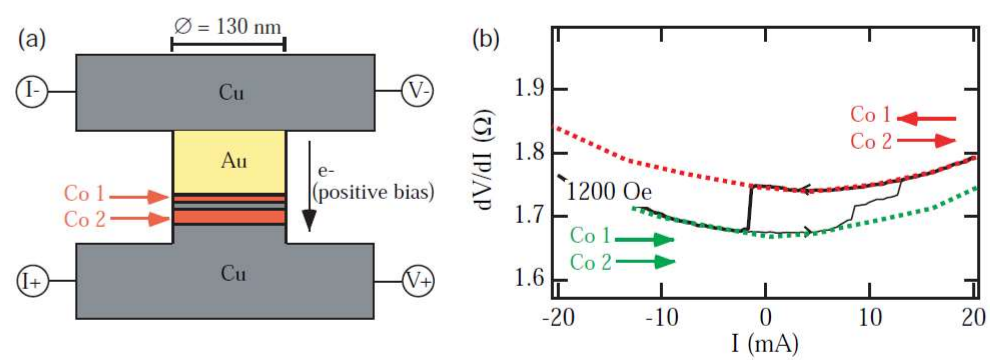

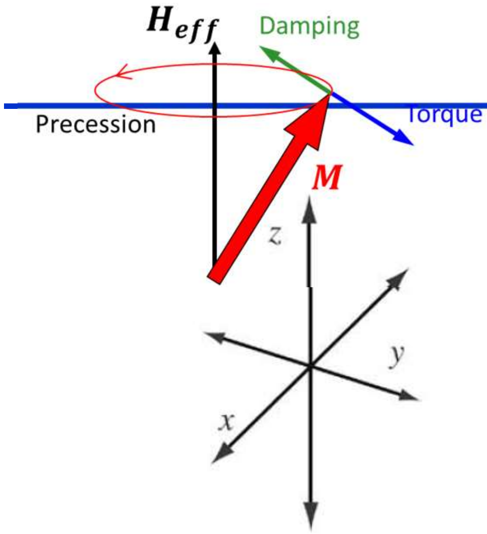

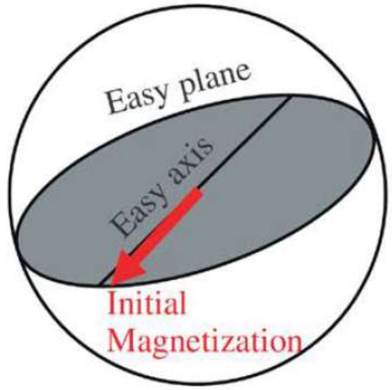

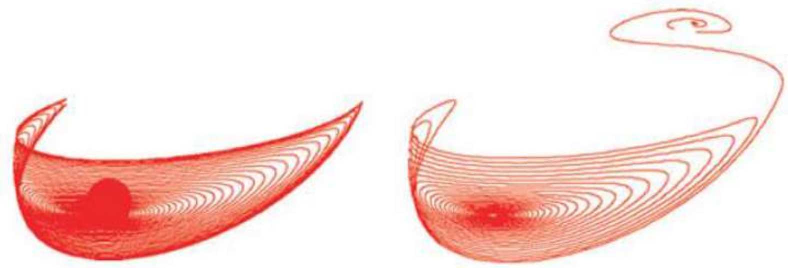

J. Mag. Magn. Mat. 320, 1190 (2008)

$$\frac{d\boldsymbol{M}}{dt} = -|\gamma|\boldsymbol{M} \times (\mu_0 \boldsymbol{H_{eff}}) + \frac{\alpha}{M_S}\boldsymbol{M} \times \frac{d\boldsymbol{M}}{dt} + |\gamma|\frac{\tau_{DL}}{M_S^2}\boldsymbol{M} \times (\boldsymbol{m} \times \boldsymbol{M}) + \simeq 0 \quad \text{with } \tau_{DL} = \frac{J_e\hbar\beta}{2eM_S d_F}$$

Estimating the critical current density, stability criterion (with H=0, H_k~0):

$$|\gamma|\tau_{DL,crit} = 2\pi\frac{\alpha}{dt} = 2\pi\alpha f \Rightarrow |\gamma|\frac{J_e\hbar\beta}{2eM_S d_F} = 2\pi\frac{|\gamma|\mu_0 M_S}{2}$$

$$J_{e,crit} = \frac{e\mu_0 M_S^2 d_F \alpha}{\hbar\beta}$$

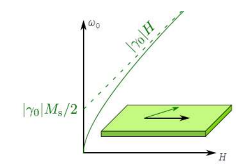

For permalloy ($Ni_{80}Fe_{20}$): $\alpha = 0.008$, $M_S = 0.8\ \mathrm{MA.m^{-1}}$, g=2.1, P=0.3.
Let's consider: $d_F = 3\ \mathrm{nm}$, $\Rightarrow J_{e,crit} \sim 1 \times 10^7\ \mathrm{A.cm^{-2}}$

STT has another reciprocal effect called spin pumping

Spin transfer torque
$\boldsymbol{J_s}$ puts $\boldsymbol{M}$ into motion

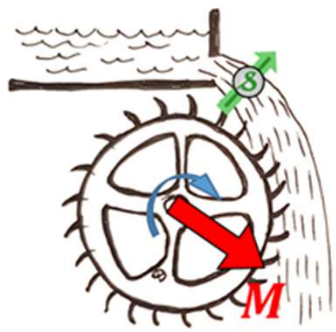

Spin pumping
The motion of $\boldsymbol{M}$ induces $\boldsymbol{J_s}$

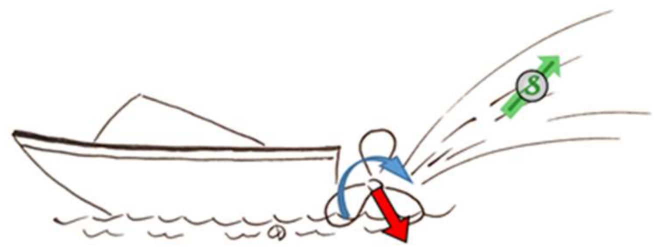

DOI: 10.1051/978-2-7598-2917-0.c002

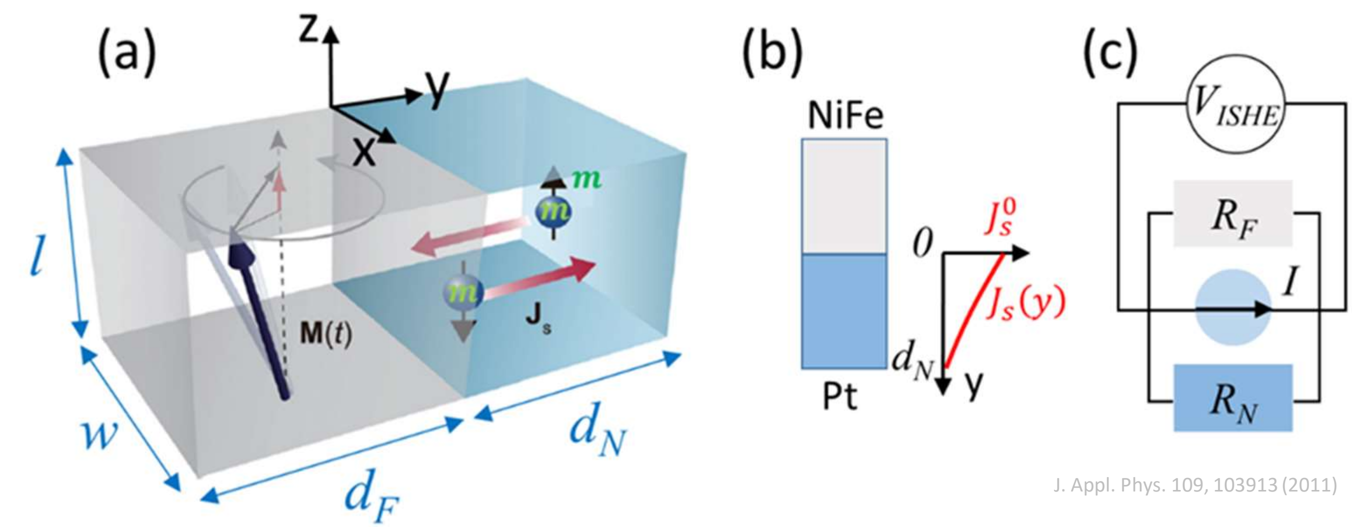

J. Appl. Phys. 109, 103913 (2011)

$$J_s^0 = J_s^{pump} - J_s^{back} = \frac{e}{2\pi M_S^2}\mathcal{Re}\left(g_{eff}^{\uparrow\downarrow}\right)\boldsymbol{M}\times\frac{d\boldsymbol{M}}{dt} + \frac{e}{2\pi M_S}\Im m\left(g_{eff}^{\uparrow\downarrow}\right)\frac{d\boldsymbol{M}}{dt}$$

cf. Exercice 2

Spin transfer torque also exists in magnetic textures like domain walls (DWs):

- when the moments of the itinerant *s*-electrons ($\boldsymbol{m}$ in the sketch below) follow adiabatically the magnetization ($\boldsymbol{M}$), then $\boldsymbol{\nabla} \cdot \boldsymbol{J_s} \propto \boldsymbol{\nabla} \cdot \boldsymbol{M}$ builds ups. This gives rise to an 'adiabatic' contribution to STT.
- when the spins are unable to follow $\boldsymbol{M}$ (spin-mistracking), then spin accumulation builds up, giving rise to a 'non-adiabatic' contribution.

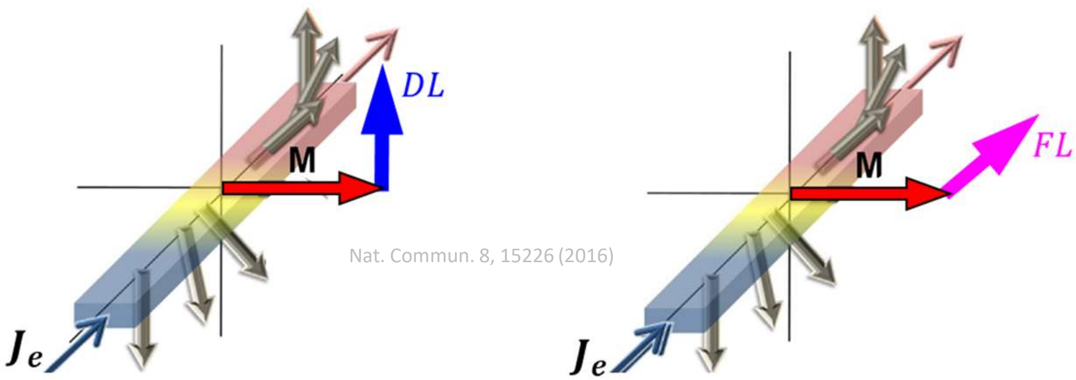

Nat. Commun. 8, 15226 (2016)

$$-\boldsymbol{T} = \frac{\hbar\beta}{2eM_S^3(1+\xi^2)}\boldsymbol{M} \times [\boldsymbol{M} \times (\boldsymbol{J_e} \cdot \boldsymbol{\nabla})\boldsymbol{M}] + \frac{\hbar\beta\xi}{2eM_S^2(1+\xi^2)}\boldsymbol{M} \times (\boldsymbol{J_e} \cdot \boldsymbol{\nabla})\boldsymbol{M}$$

DL
Adiabatic

FL
Non-adiabatic

- Spin transfer torque can also be efficient to move magnetic textures.

$$-\boldsymbol{T} = \frac{\hbar\beta}{2eM_S^3(1+\xi^2)}\boldsymbol{M}\times[\boldsymbol{M}\times(\boldsymbol{J_e}\cdot\boldsymbol{\nabla})\boldsymbol{M}] + \frac{\hbar\beta\xi}{2eM_S^2(1+\xi^2)}\boldsymbol{M}\times(\boldsymbol{J_e}\cdot\boldsymbol{\nabla})\boldsymbol{M}$$

$$\xi = \frac{\tau_{sd}}{\tau_{sf}^*}$$

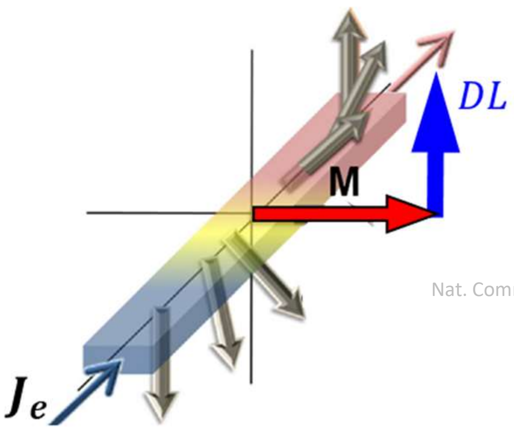

Nat. Commun. 8, 15226 (2016)

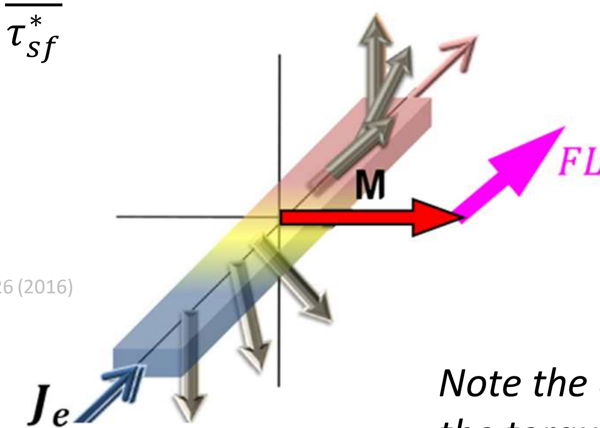

Example for a Bloch wall

Note the distortion effect of the torque, redistributing the initial conditions for the calculation of ***T***

$\xi \ll 1$ in weakly SO-coupled dense-moment F metals, e. g. (Co) => DL $\gg$ FL

$\xi \gg 1$ in strongly SO-coupled dilute-moment F semiconductors, e. g. (Ga,Mn)As => FL $\gg$ DL

- Possible application of STT in magnetic textures: the racetrack memory.

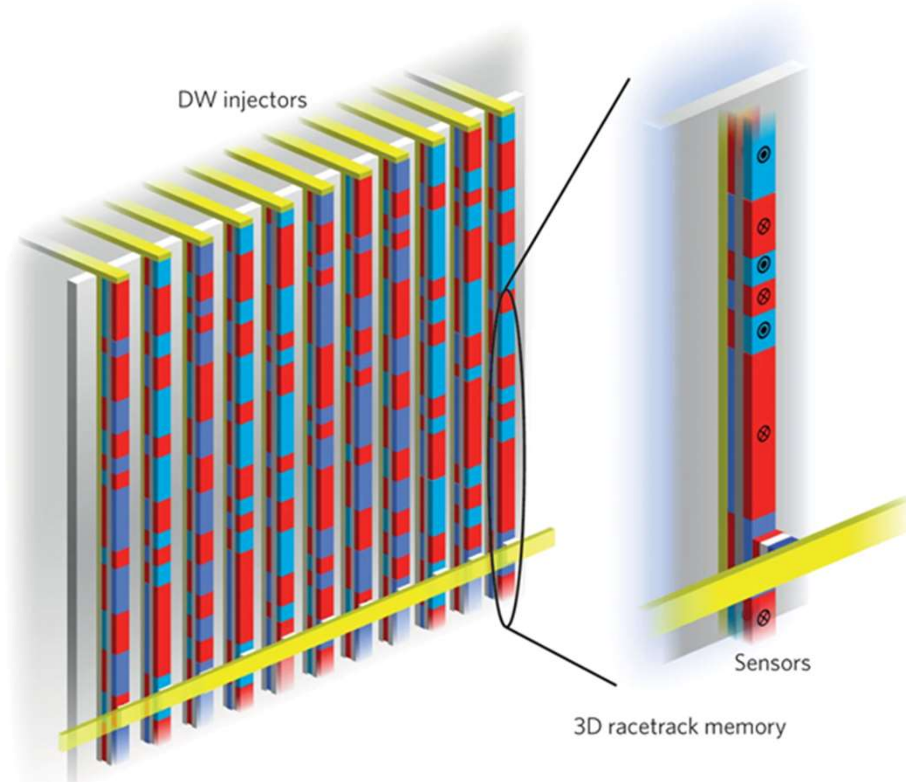

Nat. Nanotech. 10, 195 (2015)

- **Spin transfer torque - STT**
  - sd coupling between spin accumulation and magnetization
  - Damping-like vs field-like contributions
  - Quantum mechanical model
- **STT in diffusion equation of transport**
  - Loss of spin current = spin-flips + STT
  - Critical currents for switching: $J_e^{P \to AP} > J_e^{AP \to P}$
- **STT in magnetization dynamics equations**
  - Precession vs switching
  - Magnetic textures
- **References:**

  - D. E. Bürgler **D3**, in S. Blügel *et al* (eds) Spintronics - from GMR to quantum information (2009)
  - Tutorial articles: D. C. Ralph & M. D. Stiles, JMMM **320**, 1190 (2008); M. D. Stiles & J. Miltat, Topics in Appl. Phys. **101**, 225 (2006); and references therein
  - Models: J. C. Slonczewski, JMMM **159**, L1 (1996); L. Berger, Phys. Rev. B **54**, 9353 (1996)
  - Experiments: J. Katine *et al*, Phys. Rev. Lett. 84, 3149 (2000); W. H. Rippard *et al*, *ibid* **92**, 027201 (2004)
  - STT in transport: N. Strelkov *et al*, Phys. Rev. B **84**, 024416 (2011)
  - Spin pumping: Y. Tserkovnyak *et al*, Rev. Mod. Phys. **77**, 1375 (2005)
  - STT in DWs: S. Zhang & Z. Li , Phys. Rev. Lett. **93**, 127204 (2004)
  - Racetrack memory: S. S. P. Parkin *et al*, Science **320**, 190 (2008)

Lectures on spintronics

Master 2 Univ. Grenoble Alpes

Vincent Baltz

CNRS Researcher at SPINTEC

Lecture 1	–	04 Dec.
Lecture 2	–	07 Dec.
Lecture 3	–	11 Dec.
Lecture 4	–	14 Dec.
Exercises 1 & 2	–	21 Dec.

vincent.baltz@cea.fr

https://fr.linkedin.com/in/vincentbaltz

www.spintec.fr/af-spintronics/

1h30

I. Brief overview of the field of spintronics and its applications

II. First notions to describe electron and spin transport – AMR, CIP-GMR

1h30

III. Spin accumulation – CPP-GMR

1h30

IV. Transfer of angular momentum – STT

1h30

V. Berry curvature, parity and time symmetries – AHE

VI. Brief non-exhaustive introduction to current topics

1h30

Exercise 1 - Anisotropic magnetoresistance (AMR)

Exercise 2 – The spin pumping (SP) and inverse spin Hall effects (ISHE)

V. Berry curvature, parity and time symmetries – AHE

(Ordinary) Hall effect - 1879

Anomalous Hall effect - 1881

Spin Hall effect - 2004

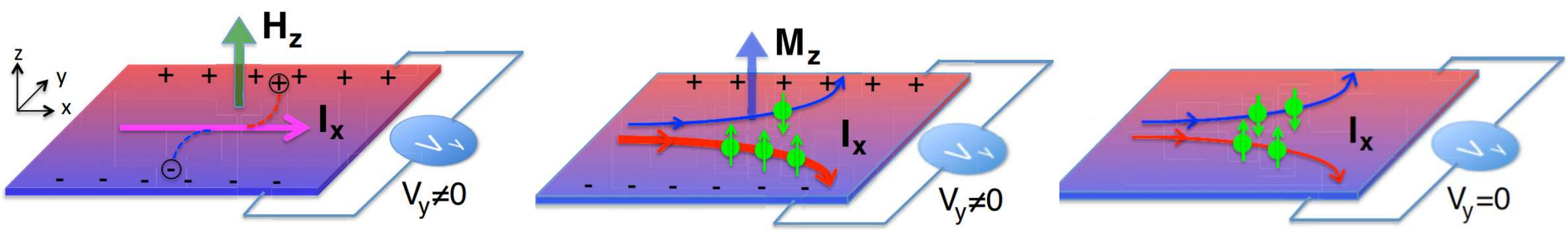

arXiv:1509.05507

Crude link: AHE = SHE for a spin polarized material
AHE = SHE x Polarization

$$J_e = \bar{\bar{\sigma}} . E = \begin{pmatrix} \sigma_{xx} & \sigma_{xy} & 0 \\ -\sigma_{xy} & \sigma_{yy} & 0 \\ 0 & 0 & 0 \end{pmatrix} E$$

(Ordinary) Hall effect

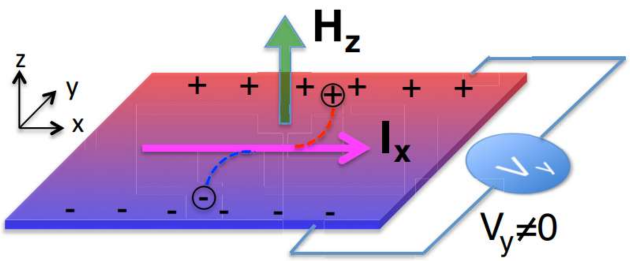

arXiv:1509.05507

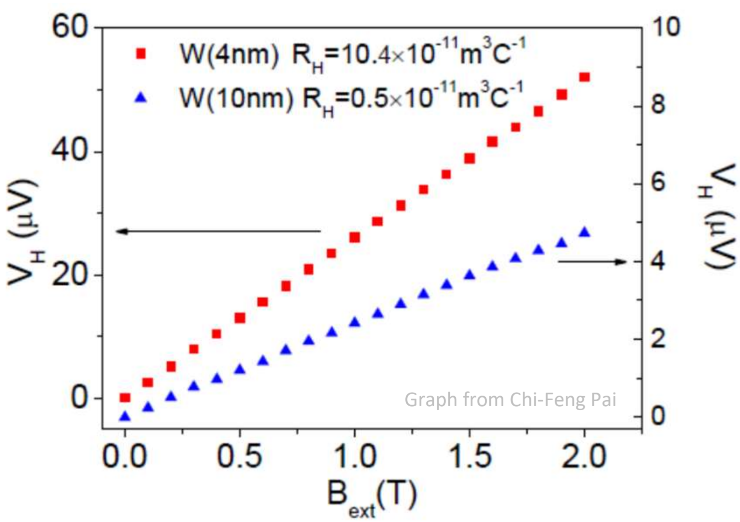

Change of momentum

$$\hbar \dot{\boldsymbol{k}} = -e\boldsymbol{E} - e\dot{\boldsymbol{r}} \times B(\boldsymbol{r})$$

$$\rho_{xy} = \mathrm{R_0 H_Z} = -\frac{1}{\mathrm{ne}}\mathrm{H_Z}$$

In symmetry words:

1. *B* breaks the time reversal ($\mathcal{T}$)-symmetry of the system
2. the Lorentz force connects electrons to $\mathcal{T}$-breaking

$$\rho_{xy}(\boldsymbol{r}) = -\rho_{xy}(-\boldsymbol{r})$$

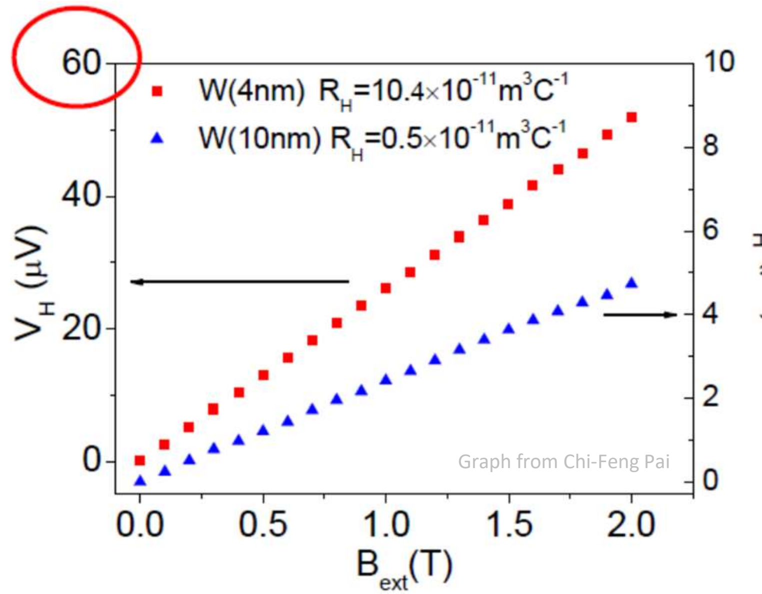

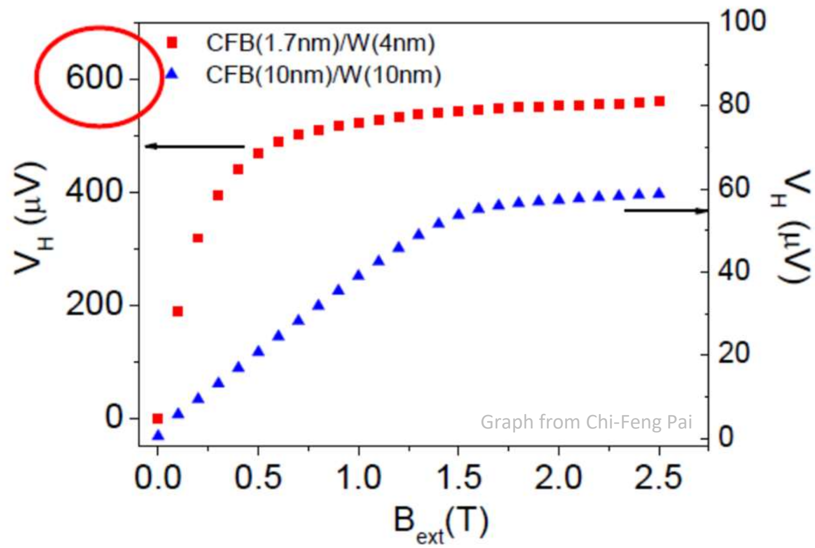

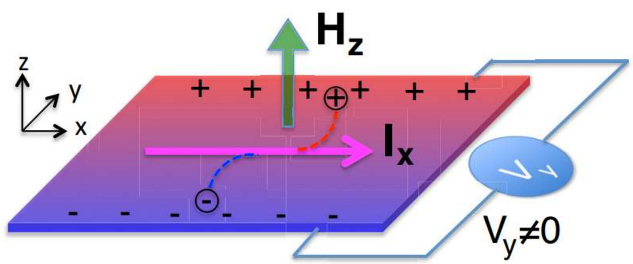

arXiv:1509.05507

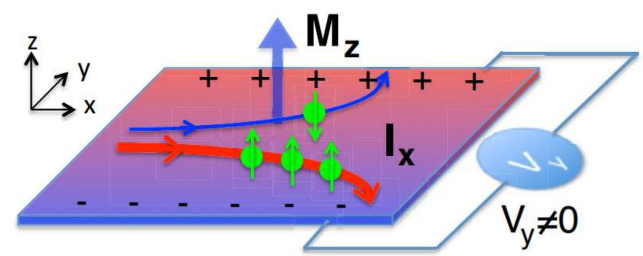

arXiv:1509.05507

$\rho_{xy} = R^N \mu_0 H_z$

Ordinary Hall effect

$\rho_{xy} = R^N \mu_0 H_z + R^A \mu_0 M_z$

+ Anomalous Hall effect

Extrinsic + intrinsic origin

Anomalous Hall effect

Intrinsic origin

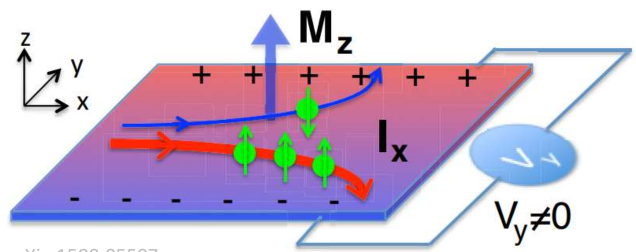

arXiv:1509.05507

$$\rho_{xy} = R^A \mu_0 M_z$$

In symmetry words:

1. M_z breaks the time reversal ($\mathcal{T}$)-symmetry of the system
2. the spin-orbit coupling connects electrons to $\mathcal{T}$-breaking

$$\rho_{xy}(\boldsymbol{r}) = -\rho_{xy}(-\boldsymbol{r})$$

More generally,
Change of position

$$v_n(\boldsymbol{k}) = \frac{\partial \varepsilon_n(\boldsymbol{k})}{\hbar \partial \boldsymbol{k}} - \dot{\boldsymbol{k}} \times \Omega_n(\boldsymbol{k})$$

transversal velocity due to the Berry curvature Ω

$$\boldsymbol{v}_n(\boldsymbol{k}) = \frac{\partial \varepsilon_n(\boldsymbol{k})}{\hbar \partial \boldsymbol{k}} - \dot{\boldsymbol{k}} \times \underbrace{\boldsymbol{\Omega}_n(\boldsymbol{k})}$$

Transversal velocity
Berry curvature

Electonic transport in a material under an external potential gradient is calculated from the Schrödinger equation:

Energy band dispersion
energy eigenvalues

$\varepsilon_n(\boldsymbol{k}(t))$

Berry curvature dispersion
from Bloch wavefunction eigenstates

$|\psi_n(\boldsymbol{k}(t))\rangle$

$\boldsymbol{k(t)}$ gauge invariant crystal momentum, includes the time varying external potential in the electron frame

'A uniform ***E*** means that V(***r***) varies linearly in space and breaks the translational symmetry of the crystal so that Bloch's theorem cannot be applied. To avoid this difficulty, one can let the electric field enter through a uniform vector potential ***A****(t)* that changes in time.'

The Berry formalism stems from the adiabatic theorem in quantum mechanics: a physical system remains in its instantaneous eigenstate, up to a phase throughout the process of a cyclic evolution, if a given perturbation is acting on it slowly enough.

Water

$|\psi_n(k)\rangle$

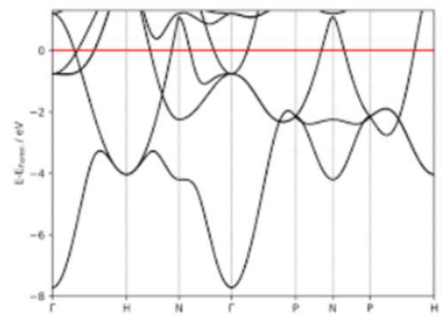

$\varepsilon_n(\boldsymbol{k})$

Vodka

$e^{i\varphi}|\psi_n(k)\rangle$

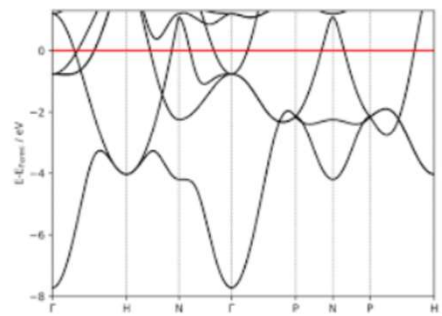

$\varepsilon_n(\boldsymbol{k})$

Picture from www.uzh.ch

$$\mathcal{H}|\psi_n(\boldsymbol{k})\rangle = \varepsilon_n(\boldsymbol{k})|\psi_n(\boldsymbol{k})\rangle$$

$$e^{i\varphi}|\psi_n(\boldsymbol{k})\rangle \; ; \; \varepsilon_n(\boldsymbol{k})$$

$$\varphi = \varphi^{geo.}(\boldsymbol{k}) + \varphi^{dyn.}(\varepsilon_n)$$

$\varphi^{dyn.}(\varepsilon_n)$

Dynamic phase:
Usual phase that appears even for a time independent Hamiltonian.
It addresses the following question: how long did the journey last ?

$\varphi^{geo}(\boldsymbol{k}) = \gamma_n(\boldsymbol{k})$

Geometric (Berry) phase:
Phase related to variations of $\boldsymbol{k}$ and only dependent on the trajectory of this parameter. It addresses the following question:
what trajectory did the system follow ?

Geometric (Berry) phase:
only dependent on the trajectory of this parameter.
It addresses the following question:
which way did the system go during the journey ?

$$\varphi^{geo.}(\boldsymbol{k}) = \gamma_n(\boldsymbol{k})$$

<u>Simple example of parallel transport on a closed contour $\mathcal{C}$</u>

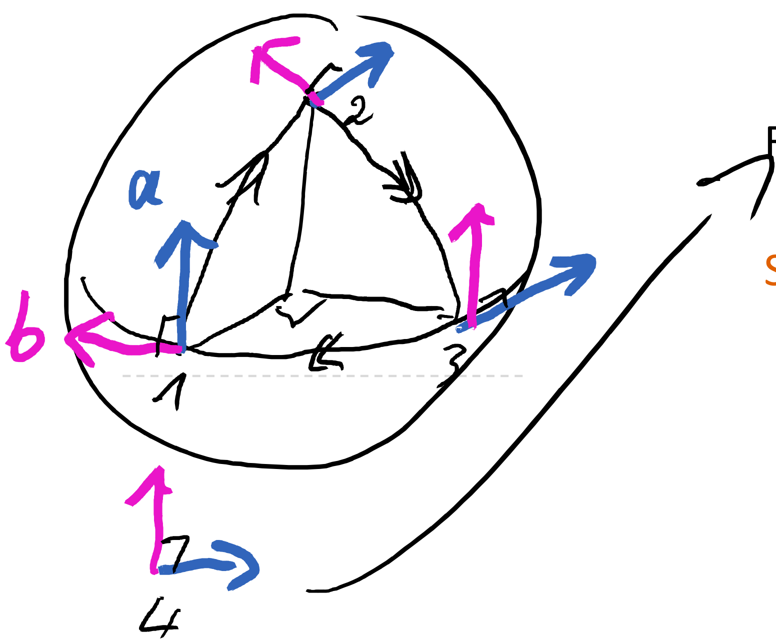

Rotation of $\boldsymbol{a}$, $\boldsymbol{b}$ by: $\varphi^{geo} = \frac{\pi}{2}$

Solid angle subtended by the contour: $\frac{1}{8} 4\pi = \frac{\pi}{2}$

Adapted from Jean Dalibard's lecture
www.college-de-france.fr

Geometric (Berry) phase:
only dependent on the trajectory of this parameter.
It addresses the following question:
which way did the system go during the journey ?

$$\varphi^{geo.}(\boldsymbol{k}) = \gamma_n(\boldsymbol{k})$$

<u>General formalism for parallel transport on a closed contour $\mathcal{C}$</u>

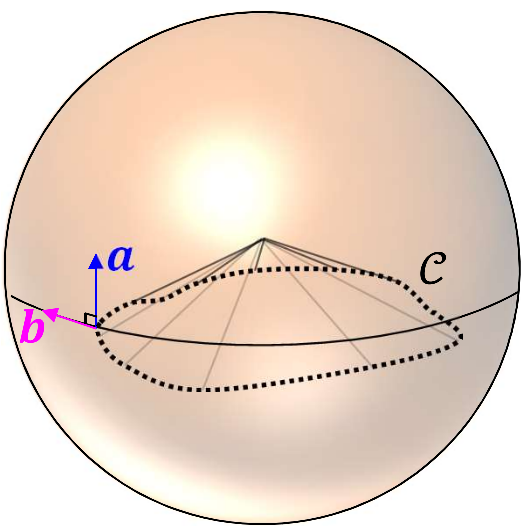

Rotation of $\boldsymbol{a}$, $\boldsymbol{b}$ by: $\varphi^{geo.}$

$$a_f = a_i \cos\varphi^{geo} - b_i \sin\varphi^{geo}$$

$$b_f = a_i \sin\varphi^{geo} + b_i \cos\varphi^{geo}$$

Consider $\psi_i = a_i + i b_i$

One obtains $\psi_f = a_f + i b_f = e^{i\varphi^{geo}} \psi_i$

$\varphi^{geo.}(\mathcal{C})$ is the solid angle subtended by $\mathcal{C}$

Adapted from Jean Dalibard's lecture
www.college-de-france.fr

'It is now well recognized that information on the Berry curvature is essential in a proper description of the dynamics of Bloch electrons, which has various effects on transport and thermodynamic properties of crystals.'

$$\mathcal{H}|\psi_n(\boldsymbol{k})\rangle = \varepsilon_n(\boldsymbol{k})|\psi_n(\boldsymbol{k})\rangle$$

$$e^{i\gamma_n(\boldsymbol{k})}|\psi_n(\boldsymbol{k})\rangle$$

Berry phase	$\gamma_n(\boldsymbol{k}) = \oint \mathcal{A}_n(k)\, d\boldsymbol{k} = \iint \Omega_n(\boldsymbol{k})\, d^2\boldsymbol{k}$	Global
Berry connection	$\mathcal{A}_n(\boldsymbol{k}) = \langle\psi_n(\boldsymbol{k})\|i\boldsymbol{\nabla}_{\boldsymbol{k}}\|\psi_n(\boldsymbol{k})\rangle$	
Berry curvature	$\Omega_n(\boldsymbol{k}) = \boldsymbol{\nabla}_{\boldsymbol{k}} \times \langle\psi_n(\boldsymbol{k})\|i\boldsymbol{\nabla}_{\boldsymbol{k}}\|\psi_n(\boldsymbol{k})\rangle$	Local

Analogies

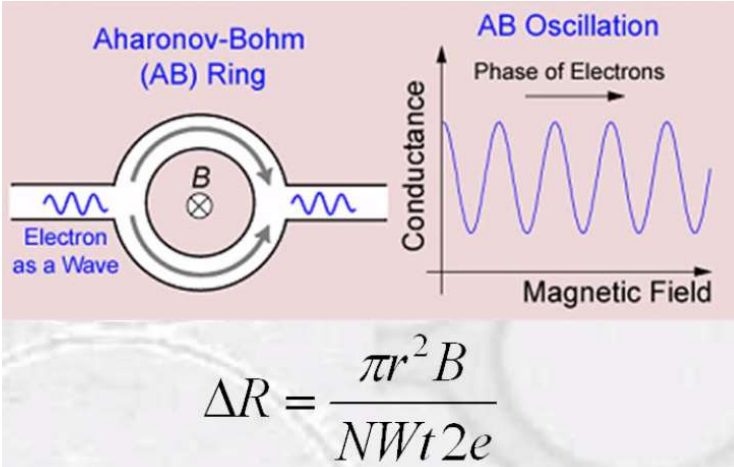

Berry curvature
$\Omega_n(\boldsymbol{k})$

Magnetic field
$B(\boldsymbol{r})$

Berry connection
$\mathcal{A}_n(\boldsymbol{k})$

Vector potential
$A(\boldsymbol{r})$

Berry phase
$\gamma_n(\boldsymbol{k})$
$= \oint \mathcal{A}_n(\boldsymbol{k})\, d\boldsymbol{k} = \iint \Omega_n(\boldsymbol{k})\, d^2\boldsymbol{k}$

Bohm-Ahronov phase
$\varphi(\boldsymbol{r})$
$= \oint A(\boldsymbol{r})\, d\boldsymbol{r} = \iint B(\boldsymbol{r})\, d^2\boldsymbol{r}$

Chern number
$\nu = \frac{1}{2\pi} \oiint \Omega_n(\boldsymbol{k})\, d^2\boldsymbol{k} = integer$

Dirac monopole
$q_m = \oiint B(\boldsymbol{r})\, d^2\boldsymbol{r} = integer\, \frac{h}{e}$

Semiclassical transport theory

System dimension

$$J_e = -e\sum_n \int_{BZ} v_n(k)\, g(\varepsilon_n(k))\, \frac{d^d k}{(2\pi)^d}$$

$$J_e = \bar{\bar{\sigma}}.E = \begin{pmatrix} \sigma_{xx} & \sigma_{xy} & 0 \\ -\sigma_{xy} & \sigma_{yy} & 0 \\ 0 & 0 & 0 \end{pmatrix}$$

$$v_n(\mathbf{k}) = \frac{\partial \varepsilon_n(\mathbf{k})}{\hbar \partial \mathbf{k}} - \dot{\mathbf{k}} \times \boldsymbol{\Omega}_n(\mathbf{k})$$

$$g(\varepsilon_n) = f(\varepsilon_n) + \delta g(\varepsilon_n)$$

$$\dot{\mathbf{k}} = -\frac{e}{\hbar}\mathbf{E}$$

$$\sigma_{xy} = \frac{e^2}{h}\sum_n \frac{1}{(2\pi)^{d-1}} \int_{BZ} \Omega_n(k)\, f(\varepsilon_n(k))\, d^d k$$

σ_{xy} $(S.cm^{-1})$	bcc Fe	fcc Ni	hcp Co
Fermi loop	750	−2275	478
Fermi loop (first term)	7	0	−4
Berry curvature	753	−2203	477
Previous theory	751[a]	−2073[b]	492[b]
Expt.	1032[c]	−646[d]	480[e]

Phys. Rev. B 76, 195109 (2007)

Ab initio calculations

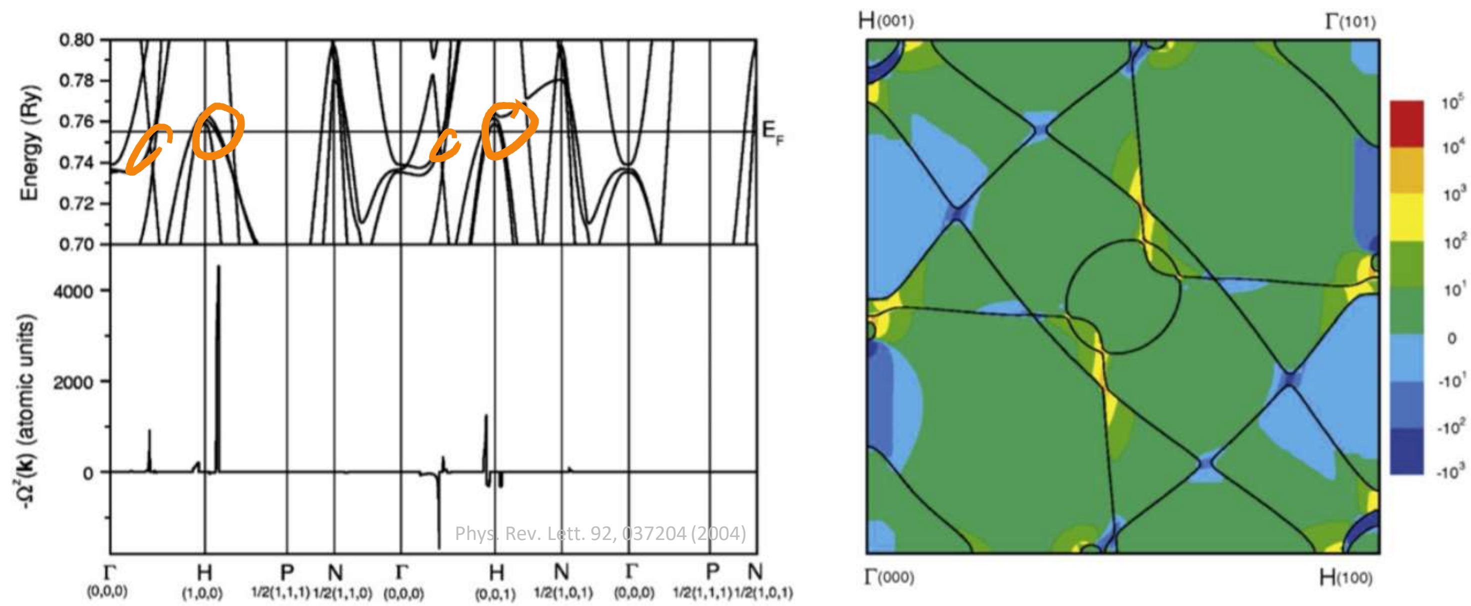

Figure 15. Left: band structure of bulk Fe near Fermi energy (upper panel) and Berry curvature $\Omega^z(\mathbf{k})$ (lower panel) along symmetry lines. Right: Fermi surface in (010) plane (solid lines) and Berry curvature $-\Omega^z(\mathbf{k})$ in atomic units (color map). Reproduced with permission from [41]. Copyright 2004 American Physical Society.

Ab initio calculations

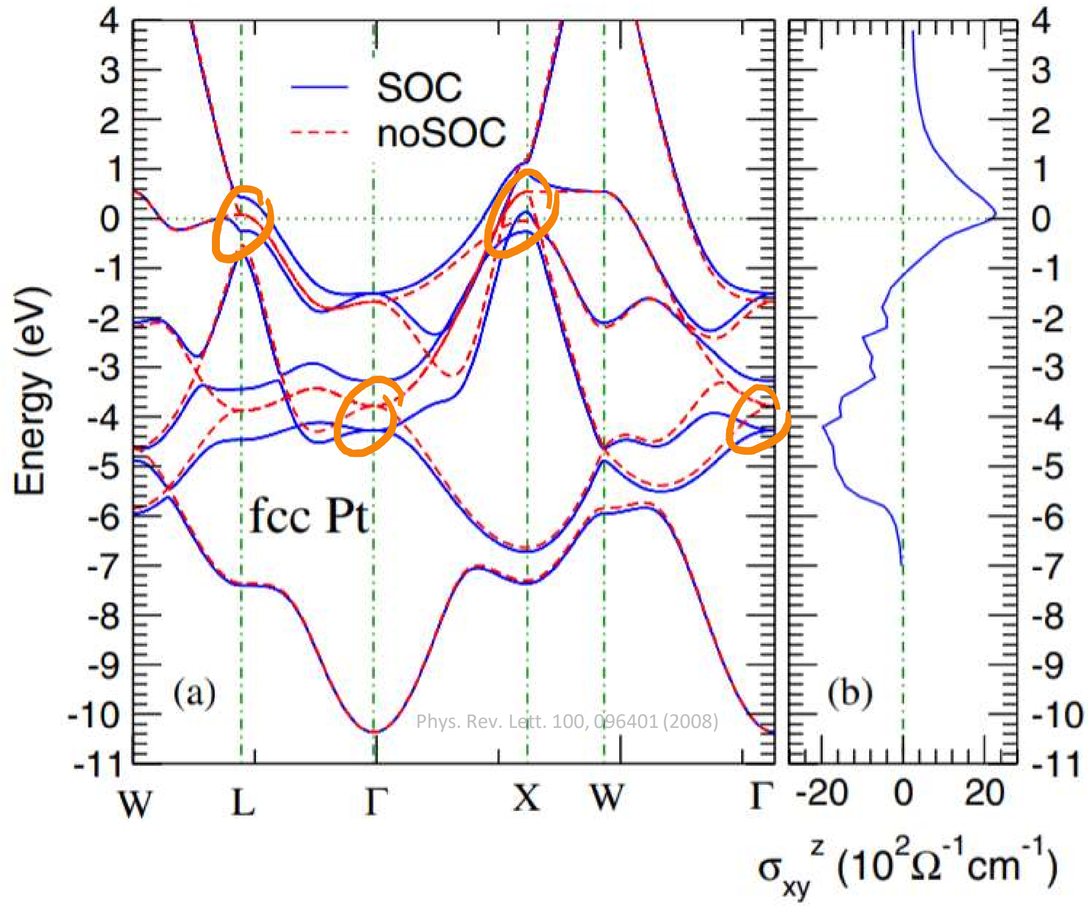

The intrinsic spin Hall conductivity of 4d and 5d metals

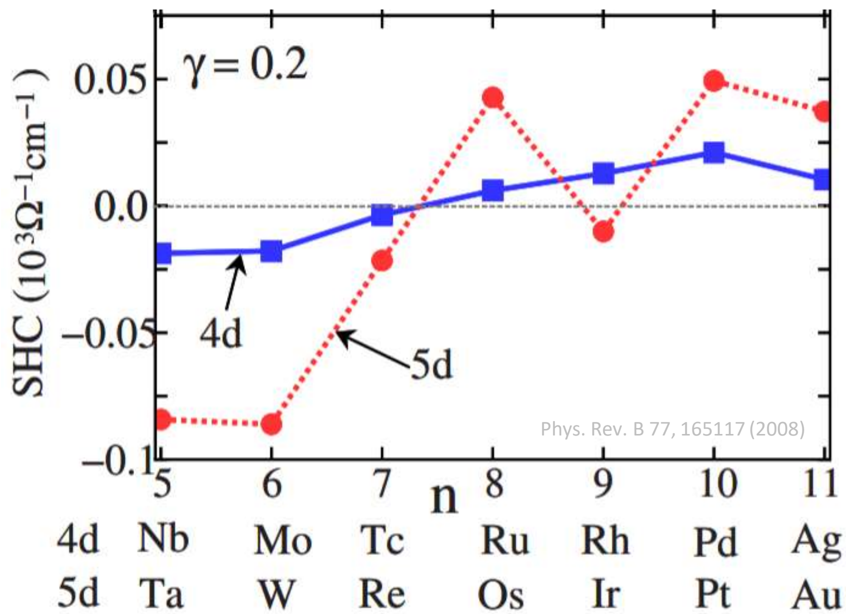

Metals	Structure	Electron number	SOI (Ry)
Nb	bcc	5 $(4d^4 5s^1)$	0.006
Mo	bcc	6 $(4d^5 5s^1)$	0.007
Tc	hcp	7 $(4d^6 5s^1)$	0.009
Ru	hcp	8 $(4d^7 5s^1)$	0.01
Rh	fcc	9 $(4d^8 5s^1)$	0.011
Pd	fcc	10 $(4d^{10} 5s^0)$	0.013
Ag	fcc	11 $(4d^{10} 5s^1)$	0.019
Ta	bcc	5 $(5d^3 6s^2)$	0.023
W	bcc	6 $(5d^4 6s^2)$	0.027
Re	hcp	7 $(5d^5 6s^2)$	0.025
Os	hcp	8 $(5d^6 6s^2)$	0.025
Ir	fcc	9 $(5d^9 6s^0)$	0.025
Pt	fcc	10 $(5d^9 6s^1)$	0.03
Au	fcc	11 $(5d^{10} 6s^1)$	0.03

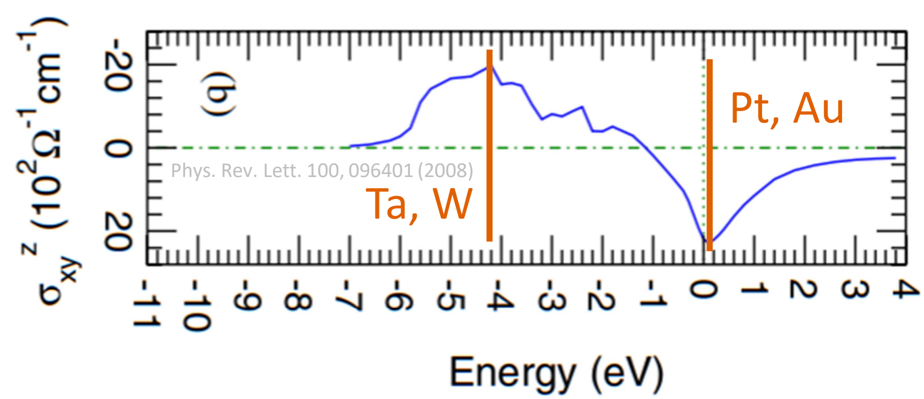

$$\sigma_{xy} = \frac{e^2}{\hbar} \sum_n \frac{d^d \boldsymbol{k}}{(2\pi)^{d-1}} \int \boldsymbol{\Omega}_n(\boldsymbol{k}) f(\varepsilon_n(\boldsymbol{k})) d^d \boldsymbol{k}$$

This is the 'unquantized' version of the Hall effect for a system in *d* dimension.

The quantum Hall effect:

Under a strong magnetic field, 2D electron gas is quantized into a discrete Landau level:

$$\sigma_{xy} = \frac{e^2}{h} \sum_n \frac{1}{2\pi} \oint_{BZ} \Omega_n(k)\, d^2k$$

integer Chern number C_n

$$\sigma_{xy} = \frac{e^2}{h} \sum_n C_n$$

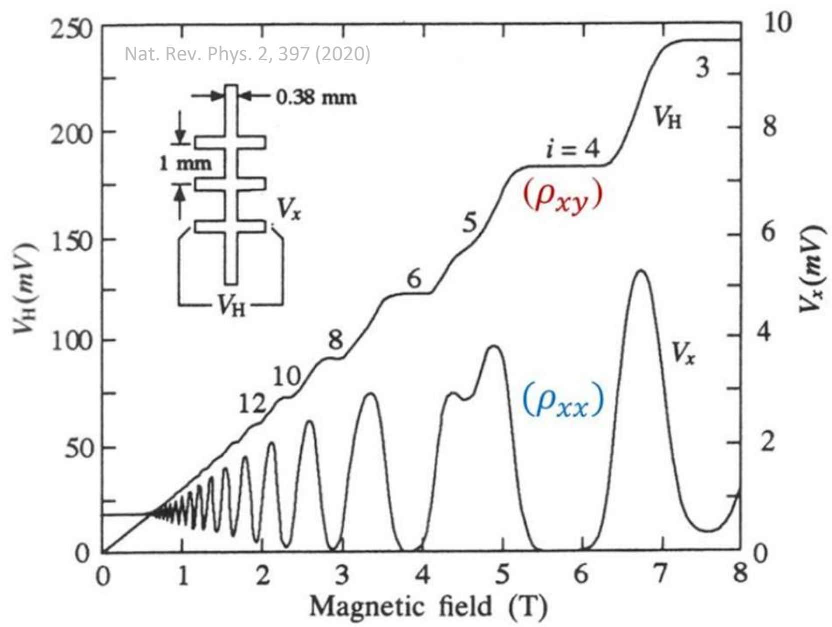

Von Klitzing constant : $\mathbf{R_K = h/e^2}$

A whole family of Hall effects, beyond the Hall trio:

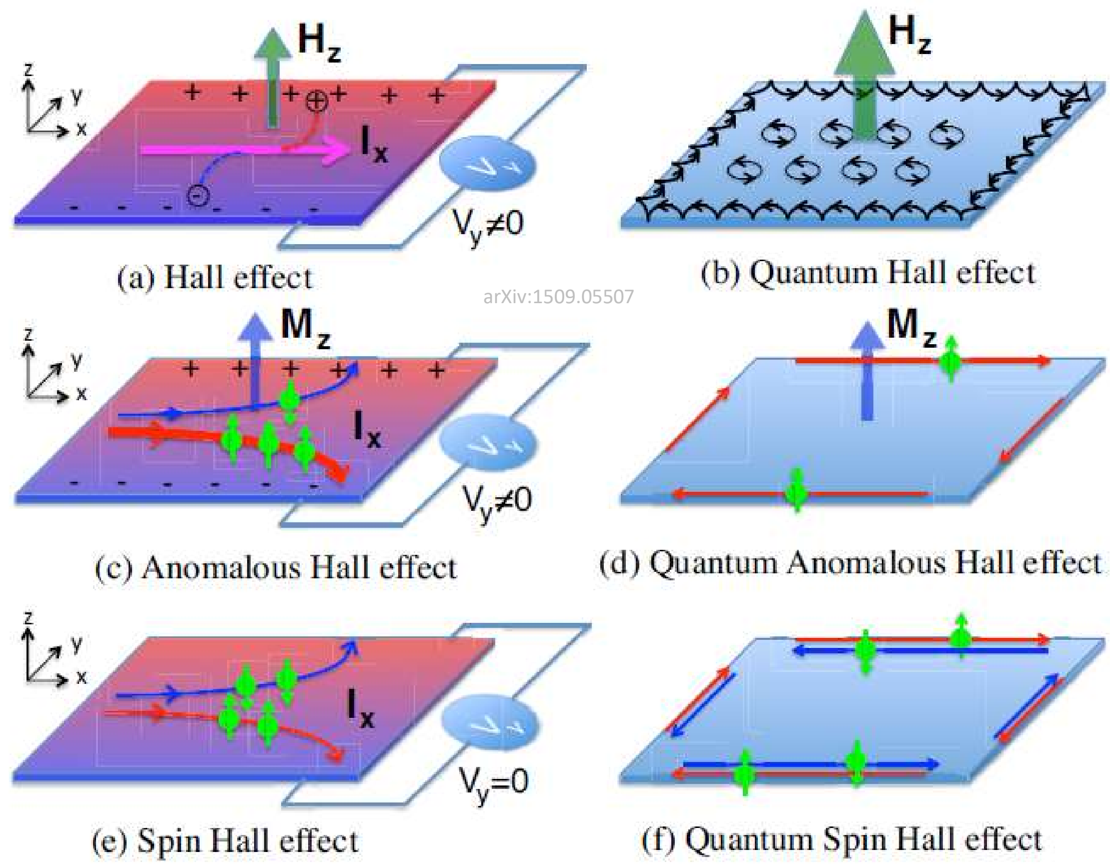

Nobel Prizes related to QHE:

1980	K. Von Klitzing	QHE
1998	H. Störmer, D. Tsui, R. Laughlin	Fractional QHE
2010	A. Geim, K. Novoselov	Graphene
2016	D. J. Thouless, F. D. M. Haldane, J. M. Kosterlitz	Topological insulator

Von Klitzing constant : $\mathbf{R_K = h/e^2}$ depends only on physical constants

More stable and reproducible than any other resistance (25812.807 Ohm)

SiCsubstrate/Graphene = QHE new standard

QHE key to the new definition of units in 2018

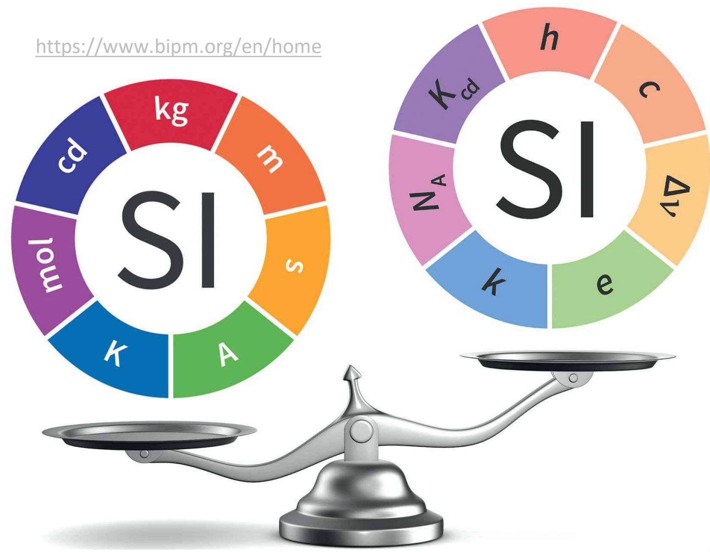

Intrinsic origin relates to the Bloch states – **Berry curvature**

$$\boldsymbol{v}_n(\boldsymbol{k}) = \frac{\partial \varepsilon_n(\boldsymbol{k})}{\hbar \partial \boldsymbol{k}} - \dot{\boldsymbol{k}} \times \underbrace{\boldsymbol{\Omega}_n(\boldsymbol{k})}$$

Transversal velocity

$$\sigma_{xy} = \frac{e^2}{\hbar} \sum_n \frac{d^d\boldsymbol{k}}{(2\pi)^{d-1}} \int \boldsymbol{\Omega}_n(\boldsymbol{k}) f(\varepsilon_n(\boldsymbol{k})) d^d\boldsymbol{k}$$

Non-zero $\boldsymbol{\Omega}_n$ requires breaking of time-reversal ($\mathcal{T}$) or spatial inversion ($\mathcal{P}$) symmetry

P: $\Omega(-k) = \Omega(k)$

T: $\Omega(-k) = -\Omega(k)$

PT: $\Omega(k) = -\Omega(k) = 0$

Demonstration:

P $k \to -k$; $\dot{k} \to -\dot{k}$

T $k \to -k$; $\dot{k} \to \dot{k}$

and $v_n(-k) = -v_n(k)$; $\varepsilon_n(-k) = \varepsilon_n(k)$; $\frac{\partial \varepsilon_n(k)}{\hbar \partial k} \to -\frac{\partial \varepsilon_n(k)}{\hbar \partial k}$

Intrinsic origin relates to the Bloch states – **Berry curvature**

$$\boldsymbol{v}_n(\boldsymbol{k}) = \frac{\partial \varepsilon_n(\boldsymbol{k})}{\hbar \partial \boldsymbol{k}} - \underbrace{\dot{\boldsymbol{k}} \times \boldsymbol{\Omega}_n(\boldsymbol{k})}_{\text{Transversal velocity}}$$

$$\sigma_{xy} = \frac{e^2}{\hbar} \sum_n \frac{d^d\boldsymbol{k}}{(2\pi)^{d-1}} \int \boldsymbol{\Omega}_n(\boldsymbol{k}) f(\varepsilon_n(\boldsymbol{k})) d^d\boldsymbol{k}$$

Non-zero $\boldsymbol{\Omega}_n$ requires breaking of time-reversal ($\mathcal{T}$) or spatial inversion ($\mathcal{P}$) symmetry

$\boldsymbol{\mathcal{P}}$		$\boldsymbol{\mathcal{T}}$		$\boldsymbol{\mathcal{PT}}$
$\Omega(-k) = \Omega(k)$	+	$\Omega(-k) = -\Omega(k)$	→	$\Omega(k) = -\Omega(k) = 0$

Such type of Hall effect therefore exists even if $M_z = 0$
- spin Hall effect in general, ρ_{xy}^{z}
- see also anomalous Hall in antiferromagnets, $\rho_{xy} = \mathrm{R_0 H_Z} + \mathrm{R_S M_Z} + \rho_{xy}^{AF}$

Spontaneous Hall effect in antiferromagnets even if $M_z = 0$?

→ **Yes**! The key is breaking of $\mathcal{T}$-symmetry

Breaking $\mathcal{T}$-symmetry ➡ Non-zero Berry curvature ➡ Intrinsic Hall effect

$$\rho_{xy} = \mathrm{R_0 H_Z} + \mathrm{R_S M_Z} + \rho_{xy}^{AF}$$

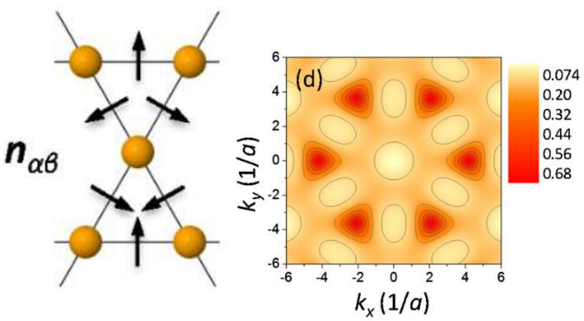

Chirality + spin-orbit coupling
Non-collinear and non-coplanar γ-$IrMn_3$

Phys. Rev. Lett. 112, 017205 (2014)

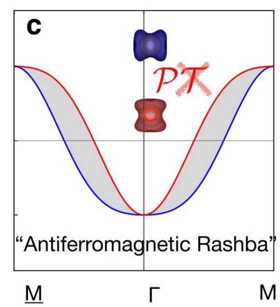

Anisotropic AF densities
+ weak spin-orbit coupling
Collinear and coplanar RuO_2

Science Advances, 6, eaaz8809 (2020)
arXiv:2002.08712

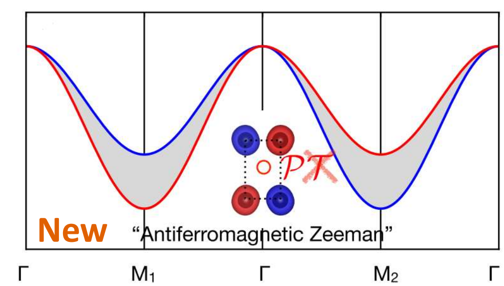

Multisublattice AF densities
No need for spin-orbit coupling
Collinear and coplanar Mn_5Si_3

arXiv:2012.15651

Typical examples of dispersion spectra

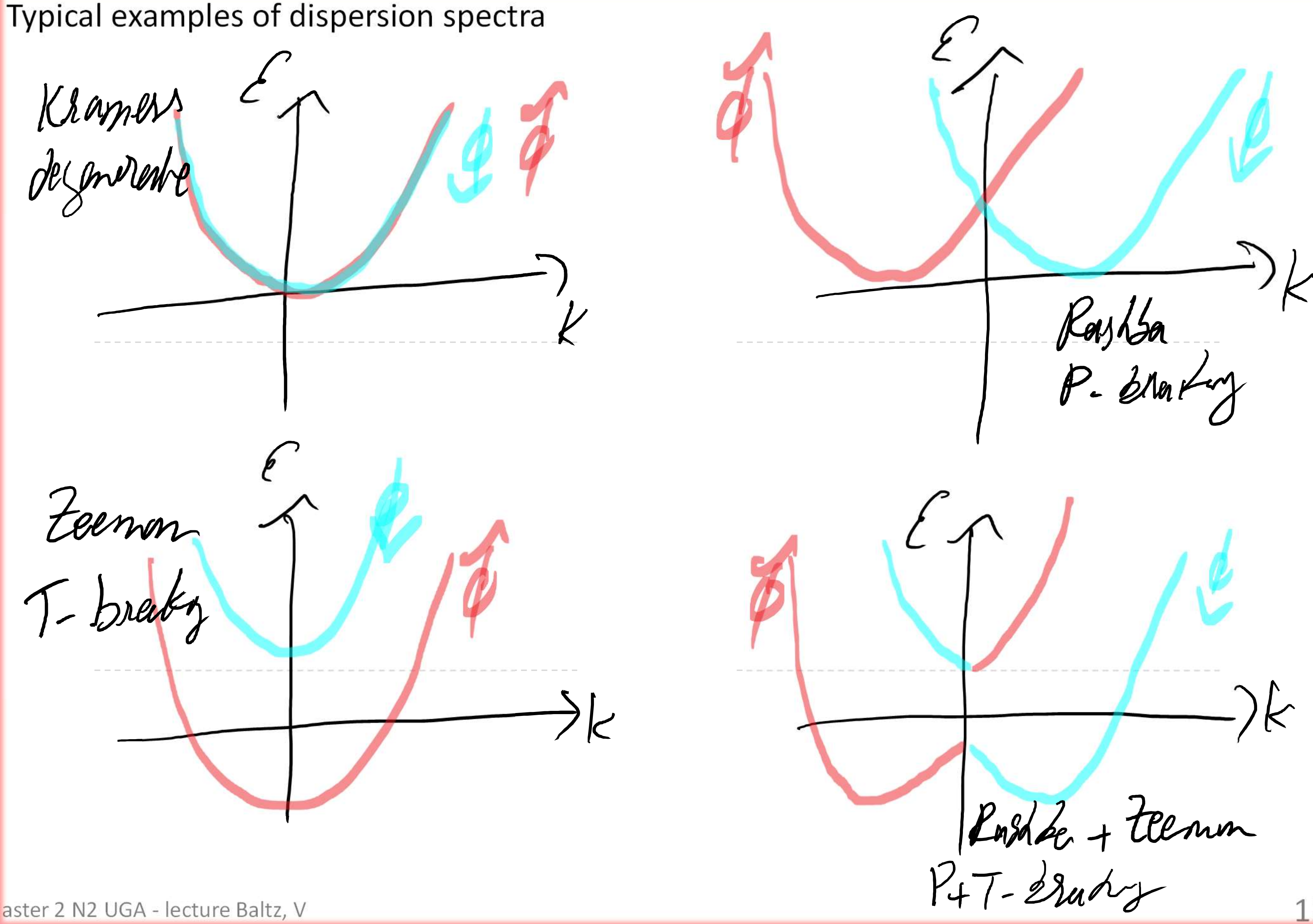

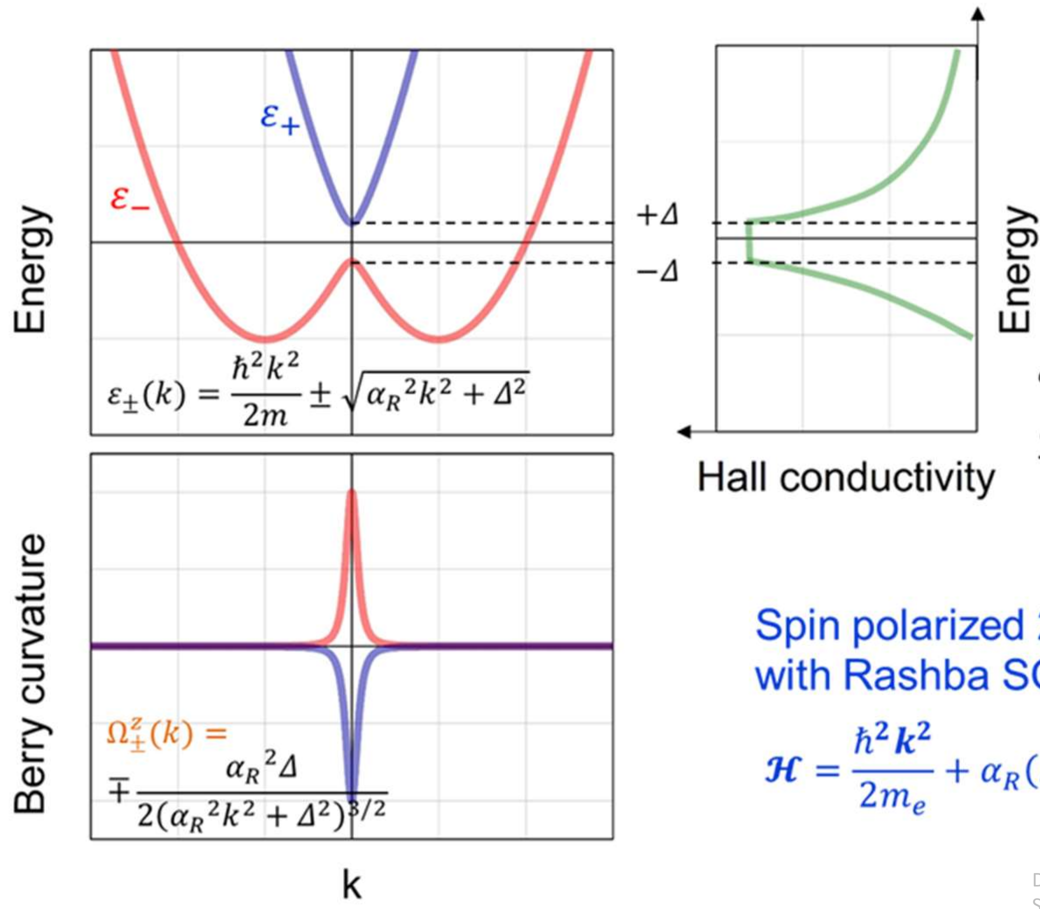

$$\sigma_{xy} = \frac{e^2}{\hbar} \int \sum_{\pm} \Omega^z_\pm(k)\, f(\varepsilon(k)) \frac{d^2 k}{(2\pi)^2}$$

Spin polarized 2D electron gas with Rashba SO coupling

$$\mathcal{H} = \frac{\hbar^2 \boldsymbol{k}^2}{2m_e} + \alpha_R(\boldsymbol{k} \times \boldsymbol{\sigma}) \cdot \boldsymbol{e}_z - \Delta \boldsymbol{\sigma}_z$$

DOI: 10.1051/978-2-7598-2917-0.c002
See also Rev. Mod. Phys. 82, 1959 (2010)

Note: beware the color code, when blue/red is commonly used to distinguish majority and minority-spin bands (see slide 123), it is also commonly used to distinguish the upper/lower band, no matter spin (see slide 124).

Slide 124:

Ω_z : the Berry curvature is non-zero around the gap and non-zero curvatures required combining Rashba (λ) and Zeeman (Δ) contributions. It has the same form as the Berry curvature in one valley of graphene.

σ_{xy} : for $\varepsilon_F < -\Delta$ the Hall conductivity first increases when increasing the Fermi energy, as one integrates the contribution to the Berry curvature of the lower band. In the gap (for $-\Delta < \varepsilon_F < \Delta$), the Hall conductivity saturates as the lower band fully contributed. Above the gap (for $\varepsilon_F > \Delta$), the Hall conductivity reduces as one integrates the contribution to the Berry curvature of the upper band which opposes that of the lower band.

Thermal (Nernst) counterparts to electrical Hall effects

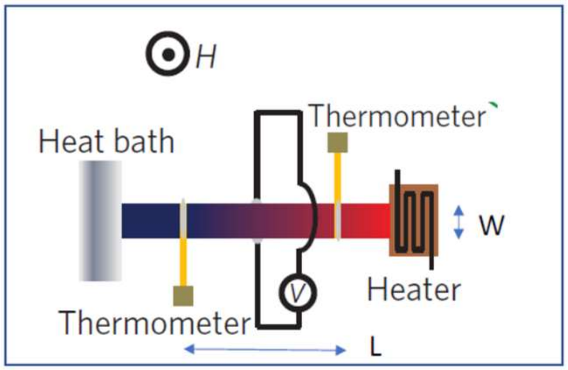

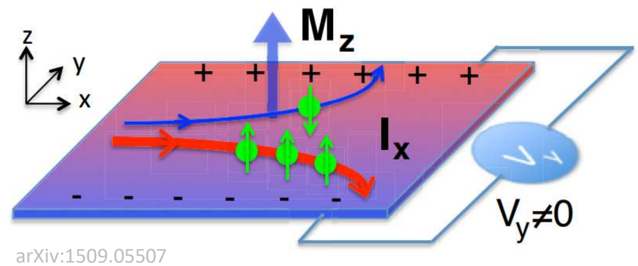

thermopower

$J_e = \sigma S \cdot \nabla T$

resistivity

$J_e = \sigma \cdot \nabla V$

Link via the Mott relation

$$S_{metal} = -\frac{\pi^2 k_B T}{3e}\frac{c'(\mu)}{c(\mu)} \quad \text{with} \quad c(\mu) = 1/\rho = N(\varepsilon_F)e^2 D$$

Extrinsic contributions to the Hall effects

Anomalous Hall effect | Spin Hall effect

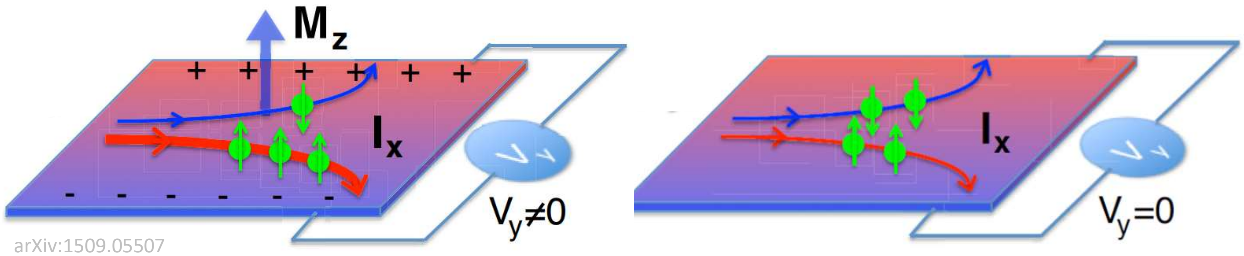

arXiv:1509.05507

$$J_e = \begin{pmatrix} \sigma_{xx} & \sigma_{xy} & 0 \\ -\sigma_{xy} & \sigma_{yy} & 0 \\ 0 & 0 & \sigma_{zz} \end{pmatrix} E$$

Extrinsic + Intrinsic origins

$$\sigma_{xy} = \sigma_{xy}^{i} + \sigma_{xy}^{sj} + \sigma_{xy}^{sk}$$

Side jump

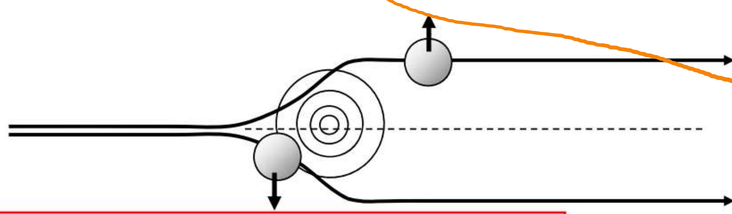

The electron velocity is deflected in opposite directions by the opposite electric fields experienced upon approaching and leaving an impurity. The time-integrated velocity deflection is the side jump.

Skew scattering

Asymmetric scattering due to the effective spin-orbit coupling of the electron or the impurity.

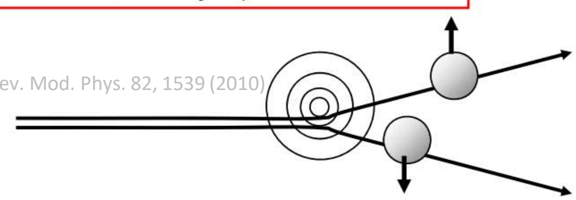

Rev. Mod. Phys. 82, 1539 (2010)

- **Berry curvature**
  - cyclic adiabatic evolution
  - describes the dynamics of Bloch electrons (in a periodic crystal structure)
  - has various effects on transport and thermodynamic properties of crystals
- **Anomalous Hall effect**
  - Intrinsic contribution: requires breaking of the $\mathcal{PT}$ combination – example of spin polarized 2D electron gas with Rashba SO coupling
  - Extrinsic contribution: due to spin-dependent scattering (skew and side jump)
- **$\mathcal{P}$ and $\mathcal{T}$ symmetries**
  - Bulk contribution: relates to group theory
  - Structure contribution: example of the Rashba interface effect
- **References:**
  - Berry curvature: D. Xiao *et al*, Rev. Mod. Phys. **82**, 1959 (2010)
    Jean Dalibard's lecture, www.college-de-france.fr
  - Hall effects family: N. Nagaosa *et al*, Rev. Mod. Phys. **82**, 1539 (2010)
    H. Weng *et al*, A-APPS Bulletin **23**, 3 (2013)
    K. von Klitzing *et al*, Nat. Rev. Phys. **2**, 397 (2020)
  - Rashba effect: A. Manchon *et al*, Nat. Mater. **14**, 871 (2015)

VI. Brief non-exhaustive introduction to current topics

Intended applications:

- Information technology-IT (e.g. memory, processors, data security)
- Biomedical (e.g. sensors)
- Telecommunication-T (e.g. transceiver)
- Artificial intelligence-AI (e.g. neuromorphic computing)

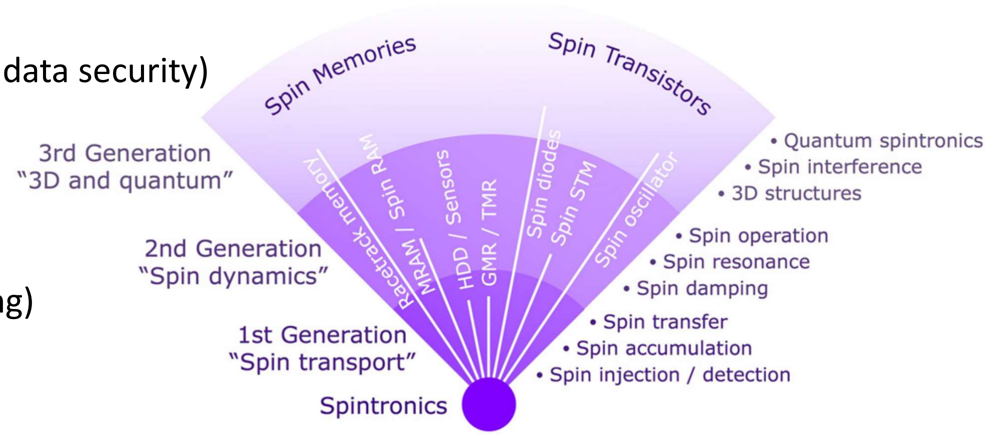

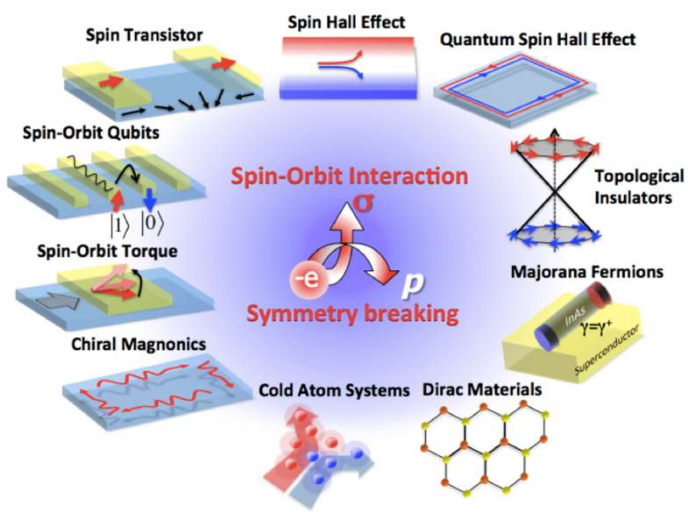

Among current research topics:

- Symmetry, topology [1,2]
- Transfer of angular momentum: electron, phonon, photon [2-6]
- Ultimate time scales [3,4,6]
- 'New' materials / structures / instrumentation [6-9]
- Quantum spintronics
- Mature fields: MRAM/Design (IT), Sensors (IT, Bio), Oscillators (T, AI) [7]

For further reading:

- Symmetry/Topology (DMI, Skyrmions, TI etc)
  [1] A. Soumyanarayanan *et al*, Nature **539**, 509 (2016)

- Spin orbit torques
  [2] A. Manchon *et al*, Rev. Mod. Phys. **91**, 035004 (2019)

- Magnonics/THz
  [3] A. V. Chumak *et al*, Nat. Phys. **11**, 453 (2015); JPDAP **50**, 300201 (2017)
  J. Walowski *et al*, J. Appl. Phys. **120**, 140901 (2016)

- Opto-magnetism
  [4] A. Kirilyuk *et al*, Rev. Mod. Phys. **82**, 2731 (2010)

- Spin currents
  [5] S. Maekawa et al (Eds), Spin currents, Oxford Uni. Press (2012)

- Antiferromagnetic spintronics
  [6] V. Baltz *et al*, Rev. Mod. Phys. **90**, 015005 (2018);
  T. Jungwirth *et al*, Nature Nano. **11**, 231 (2016)

- Future perspectives for spintronic devices
  [7] A. Hirohata *et al*, J. Phys. D: Appl. Phys. **47**, 193001 (2014);
  B. Dieny *et al* (Eds), Intro to MRAM, IEEE Press, Wiley (2017)

- 3D nanomagnetism
  [8] A. Fernández-Pacheco, Nat. Commun. **8**, 15756 (2017)

- Thoughts about data handling and material criticality
  [9] O. Fruchart, http://fruchart.eu/olivier/slides/magn/magn-fruchart-cnano2018.pdf

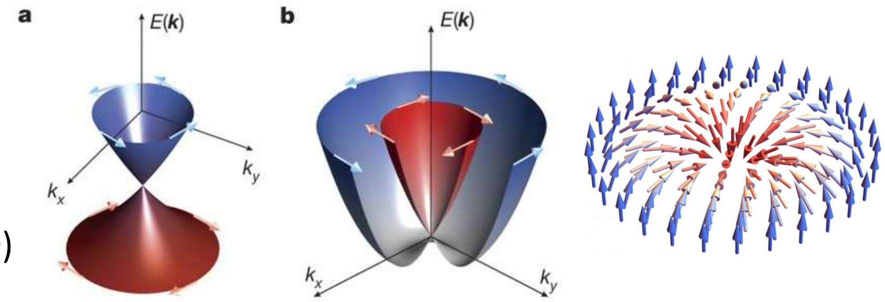

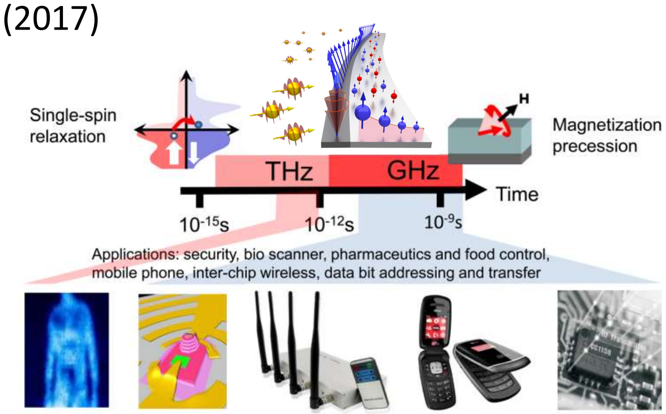

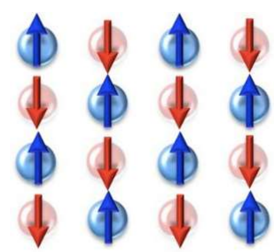

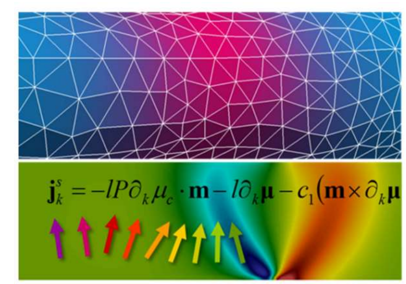

Complete slides posted online on the UGA Moodle platform

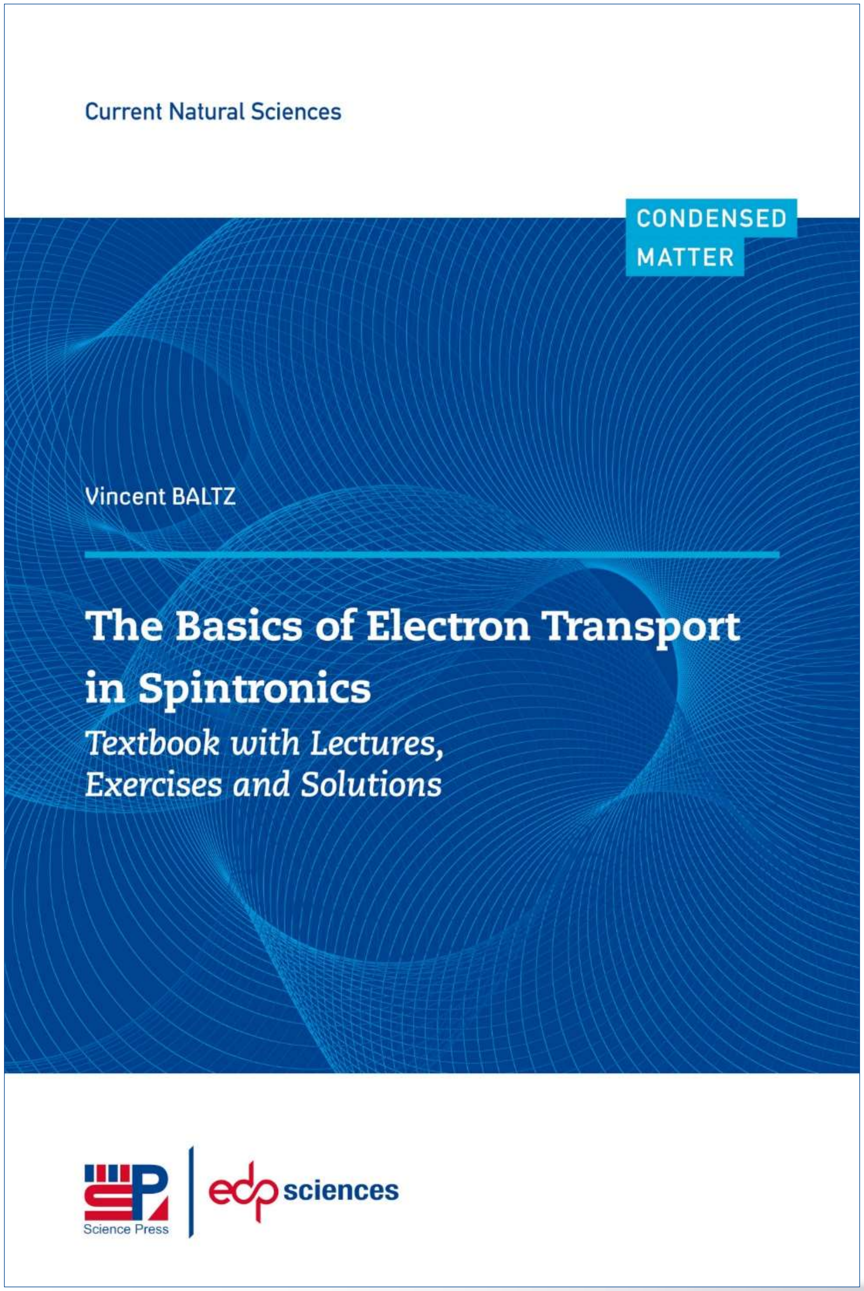

More on electron transport in spintronics:

- magnetoelectronic circuit theory
- spin-orbit torques
- skyrmion Hall angle
- spin Hall magnetoresistance
- intrinsic and extrinsic damping
- anomalous Hall harmonic analysis
- …

https://bit.ly/3oScD5p

Lectures on spintronics

Master 2 Univ. Grenoble Alpes

Vincent Baltz
CNRS Researcher at SPINTEC

Lecture 1	–	04 Dec.
Lecture 2	–	07 Dec.
Lecture 3	–	11 Dec.
Lecture 4	–	14 Dec.
Exercises 1 & 2	–	21 Dec.

vincent.baltz@cea.fr
https://fr.linkedin.com/in/vincentbaltz
www.spintec.fr/af-spintronics/

1h30

I. Brief overview of the field of spintronics and its applications

II. First notions to describe electron and spin transport – AMR, CIP-GMR

1h30

III. Spin accumulation – CPP-GMR

1h30

IV. Transfer of angular momentum – STT

1h30

V. Berry curvature, parity and time symmetries – AHE

VI. Brief non-exhaustive introduction to current topics

1h30

Exercise 1 - Anisotropic magnetoresistance (AMR)

Exercise 2 – The spin pumping (SP) and inverse spin Hall effects (ISHE)

Exercises 1 & 2

1. Anisotropic magnetoresistance (AMR)

Introduction / Reminder

The anisotropic magnetoresistance (AMR) effect refers to the dependence of the electrical resistivity ρ on the relative angle θ between the applied electrical current ***I*** and the magnetization ***M*** of a magnetic material [W. Thomson, Proc. Roy. Soc. **8**, 546 (1857); T. McGuire and R. Potter, IEEE Trans.Magn. **11**, 1018 (1975)]. It is a bulk property caused by anisotropic mixing of majority moment(↑)–spin(⇓) electrons and minority moment(↓)–spin(⇑) electrons conduction bands, induced by the spin-orbit interaction.

In the reference frame set by ***M*** (FIG. 1), the electric field $\boldsymbol{E}$ and the current density $\boldsymbol{J_e}$ are linked by the resistivity tensor $\bar{\bar{\rho}}$

$$\boldsymbol{E} = \bar{\bar{\rho}}\boldsymbol{J_e}$$

$$\text{with } \begin{pmatrix} E_{\parallel} \\ E_{\perp} \end{pmatrix} = \begin{pmatrix} \rho_{\parallel} & 0 \\ 0 & \rho_{\perp} \end{pmatrix} \begin{pmatrix} J_{\parallel} \\ J_{\perp} \end{pmatrix} \tag{1}$$

with $\rho_{\parallel}$ and $\rho_{\perp}$, the resistivities for $\boldsymbol{J_e} \parallel \boldsymbol{M}$ and $\boldsymbol{J_e} \perp \boldsymbol{M}$, respectively.

Questions

a) Find the expressions of E_x and E_y vs. J_x, J_y, $\rho_{\parallel}$, $\rho_{\perp}$ and θ, in the experimental reference frame defined by $(\hat{\boldsymbol{x}}, \hat{\boldsymbol{y}})$, (FIG. 1).

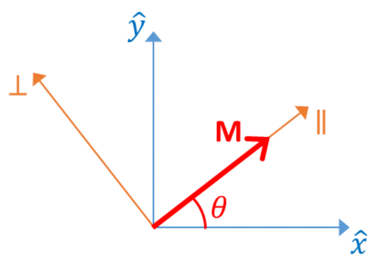

FIG. 1. Illustration showing the two reference frames considered.

b) In practice, how would you proceed experimentally to measure $\rho_{\parallel}$ and $\rho_{\perp}$? What is the order of magnitude of the values of field, current, voltage etc that you think you would use or measure ?

c) Experimental measurements of Ni films at room temperature returned $\rho_{\parallel}$ = 8.2 $\mu\Omega.cm$ and $\rho_{\perp}$ = 8 $\mu\Omega.cm$. Calculate the AMR ratio $\frac{\Delta\rho}{\rho} = \frac{\rho_{\parallel} - \rho_{\perp}}{\rho_{\perp}}$ for Ni. Can you think of any practical use of the AMR effect ?

d) We now consider a 'Union Jack' device shown in FIG. 2, a magnetization pointing along $\hat{\boldsymbol{x}}$, a film of thickness d, and a time-dependent square wave current density $J_{ij}(t)$. Plot the time(t)-variation of: V_{15}, and V_{37} for J_{15} ; V_{84}, and V_{26} for J_{84} ; V_{73}, and V_{15} for J_{73} ; V_{62}, and V_{84} for J_{62}.

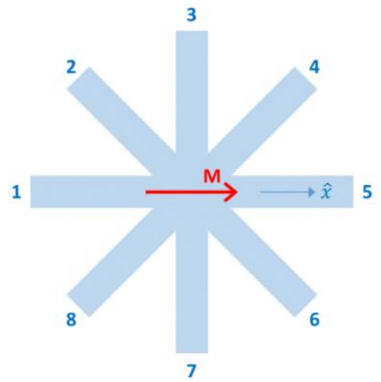

FIG. 2. Illustration of the 'Union Jack' device considered.

e) An antiferromagnet is used instead of a ferromagnet. This antiferromagnet has two collinear sublattices with magnetizations pointing towards opposite directions (M_1=-M_2). The total magnetization is M=M_1+M_2=0. Do you think that using AMR is appropriate to characterize this type of magnetic material ?

2. Spin pumping (SP) and inverse spin Hall effect (ISHE)

Introduction / Reminder

The spin pumping effect [Y. Tserkovnyak *et al*, Rev. Mod. Phys. **77**, 1375 (2005)] refers to the ability of a magnetic material to generate a spin current $\boldsymbol{J}_s^0$ when brought out-of-equilibrium. The technique usually involves inducing resonance in a ferromagnetic (F) spin injector – *e.g.* a NiFe layer – which is adjacent to a non-magnetic material (N) known as the spin sink – *e.g.* a Pt layer (FIG. 3). Spin pumping and spin transfer torque are reciprocal effect. An intuitive picture consists in comparing spin transfer torque to a water flow (spin current) moving the blades of a watermill (magnetization) and spin pumping to moving blades (magnetization) creating a water flow (spin current).

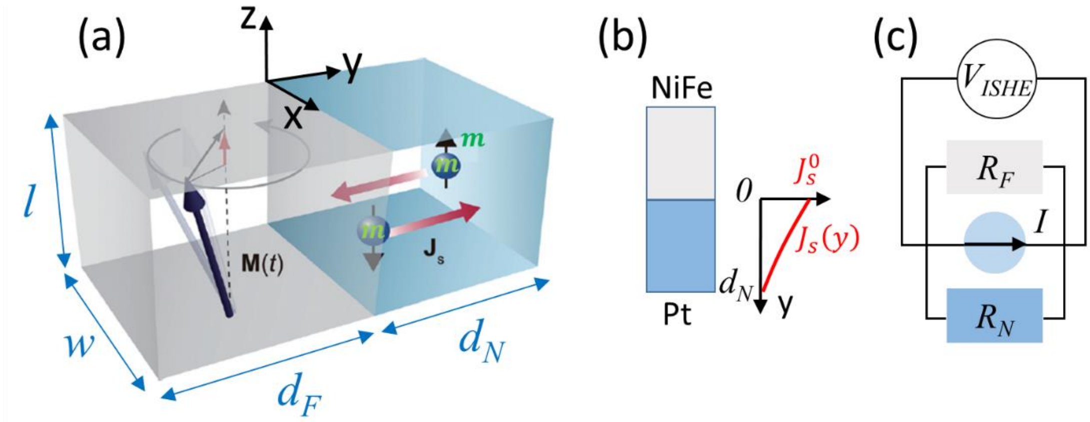

FIG. 3. (a) Illustration of the spin pumping effect due to sustained out-of-equilibrium magnetization dynamics. (b) Illustration of spin current diffusion across the non-magnetic layer (here, Pt). (c) Equivalent circuit considering spin-charge conversion due to the inverse spin Hall effect in the non-magnetic layer. Adapted from K. Ando *et al*, J. Appl. Phys. **109**, 103913 (2011).

Questions

a) Because the system is out-of-equilibrium, spins accumulate at the F/N interface and diffuse across the N layer [FIG. 3(b)]. The time-varying spin density (nonequilibrium chemical-potential imbalance) can be written as follows: $\widetilde{\mu_s} = \mu_s e^{i\omega t}$. In this part, you will calculate the y-dependence of the spin current in the N layer: $J_s(y)$.

a1) Write the relation between J_s and μ_s.
This will be Eq. (a1).

a2) Write the transport equation that regulates μ_s and show that

$$\frac{d^2\mu_s}{dy^2} - \frac{1}{{l_{sf}^{\#}}^2}\mu_s = 0, \qquad \text{(a2)}$$

with $l_{sf}^{\#} = \frac{l_{sf}^*}{\sqrt{1+i\omega\tau_{sf}^*}}$ and $l_{sf}^* = \sqrt{D\tau_{sf}^*}$, where D is the diffusive constant, and τ_{sf}^* is the average spin flip scattering rate in the N layer. Here, $l_{sf}^* = l_{sf,N}^*$ and $l_{sf}^{\#} = l_{sf,N}^{\#}$.

a3) Is it realistic to consider that $l_{sf}^{\#} \sim l_{sf}^*$?

a4) Write the boundary conditions at $y = 0$ and $y = d_N$.

a5) Use the result of question a4) and the fact that the solution of Eq. (a2) takes the following form: $\mu_s(y) = Ae^{y/l_{sf}^*} + Be^{-y/l_{sf}^*}$, to explicit $\mu_s(y)$ vs y, d_N, l_{sf}^*, e, and ρ_N.

a6) Use the result of question a5) and Eq. (a1) to explicit $J_s(y)$ vs y, d_N, l_{sf}^*, and J_s^0. This will be Eq. (a6).

b) Due to the inverse spin Hall effect (ISHE) (§V), the spin current is converted in a transverse charge current J_e along x. The N layer then becomes a 'source' of charge current. The spin-charge conversion is expressed as $J_e(y) = \theta_{SHE} J_s(y)$, where θ_{SHE} is called the spin Hall angle.

b1) Use Eq. (a6) and the indications above to explicit the average charge current density $J_e = \langle J_e(y) \rangle = \frac{1}{d_N}\int_0^{d_N} J_e(y)dy$ vs y, d_N, l_{sf}, and J_s^0.

b2) Plot the charge current I vs d_N. Comment the trend for $d_N \ll l_{sf}^*$ and for $d_N \gg l_{sf}^*$.

b3) The equivalent circuit of the F/N bilayer is illustrated in FIG. 3(c). Explicit the electromotive force (voltage V_{ISHE}) due to the inverse spin Hall effect in the N layer induced by spin pumping in a F/N bilayer.

b4) Calculate the value of the 'spin-charge conversion efficiency': $\theta_{SHE} l_{sf}^*$, considering that $d_N\sigma_N \gg d_F\sigma_F$, and for V_{ISHE}=4 *µV*, d_N=10 *nm*, l_{sf}^*=3 *nm*, σ_N=4 x 10^6 *S.m*$^{-1}$, *w*=0.5 *mm*, and J_s^0=4.8 x 10^5 *A.m*$^{-2}$.

b5) A contribution to the spin Hall angle is due to extrinsic *sd* scattering on defects. Given this specific contribution – intrinsic contributions are not considered here - how would you proceed to increase the value of the spin Hall angle in a material ? Will the options you propose improve the 'spin-charge conversion efficiency' ?

c) It is possible to show that the angular dependence of the inverse spin Hall voltage is

$$V_{ISHE} = \frac{w\theta_{SHE} l_{sf}^* \tanh\left(d_N/(2l_{sf}^*)\right)}{d_N\sigma_N + d_F\sigma_F} \frac{e g_r^{\uparrow\downarrow}\gamma^2\left(\mu_0 h_{rf}\right)^2}{8\pi\alpha^2\omega} \sin(\theta_M)\,\bar{\Gamma}, \quad \text{(c)}$$

with $\bar{\Gamma} = 2\omega \frac{\mu_0 M_S|\gamma|\sin^2(\theta_M)+\sqrt{(\mu_0 M_S\gamma\sin^2(\theta_M))^2+4\omega^2}}{(\mu_0 M_S\gamma\sin^2(\theta_M))^2+4\omega^2}$, w the width of the layers, θ_{SHE} the spin-Hall angle, h_{rf} the *rf* excitation field used to reach F resonance, and ω the resonance angular frequency. θ_M is defined in FIG. 4. $\bar{\Gamma}$ is a parameter accounting for the trajectory of the magnetization precession in the (xy) plane. It can be viewed as the elliptic- to circular-trajectory ratio. $g_r^{\uparrow\downarrow}$ is the real part of the spin mixing conductance per unit area per quantum conductance per spin channel, accounting for the ability of the F/N interface and N layer to absorb the spin component along $\boldsymbol{M} \times (\boldsymbol{m} \times \boldsymbol{M})$.

c1) Show that $\bar{\Gamma}$ is a dimensionless parameter.

c2) What is the trajectory of the magnetization precession for θ_M=0 ? Why is it so ? And should it always be the case ?

c3) The angular(θ_H)-dependence of the magnetization's tilt θ_M deduced from experimental data for the case of a 8 nm-thick NiFe film is given in FIG. 4. θ_H is the angle between the applied magnetic field ***H*** and the normal to the sample's surface ***y***. Comment this behaviour: what governs it ? Use Eq. (c) and FIG. 4, to hand-sketch the θ_H-dependence of V_{ISHE}. Comment the symmetry of V_{ISHE} with ***H***.

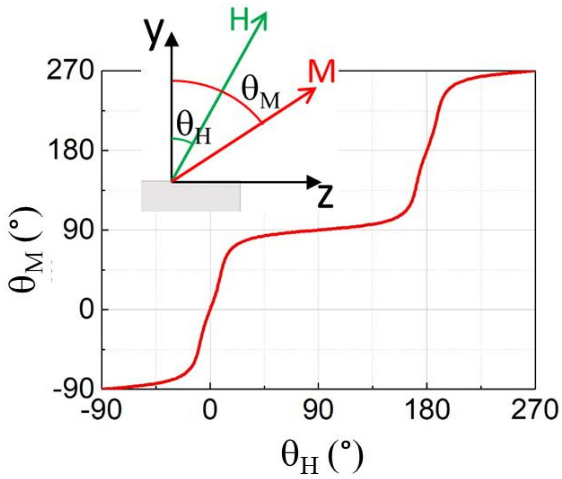

FIG. 4. Typical angular(θ_H)-dependence of the magnetization's tilt θ_M. From O. Gladii *et al*, Phys. Rev. B 100, 174409 (2019).

Solutions to exercise 1

a) A change of basis can be done by using the appropriate rotation matrix

$$\begin{pmatrix} E_{\parallel} \\ E_{\perp} \end{pmatrix} = \begin{pmatrix} \cos\theta & \sin\theta \\ -\sin\theta & \cos\theta \end{pmatrix} \begin{pmatrix} E_x \\ E_y \end{pmatrix} \text{ and } \begin{pmatrix} J_{\parallel} \\ J_{\perp} \end{pmatrix} = \begin{pmatrix} \cos\theta & \sin\theta \\ -\sin\theta & \cos\theta \end{pmatrix} \begin{pmatrix} J_x \\ J_y \end{pmatrix} \quad (2)$$

Combining Eqs. (1) (see text of exercise 1) and (2) gives

$$\begin{pmatrix} \cos\theta & \sin\theta \\ -\sin\theta & \cos\theta \end{pmatrix} \begin{pmatrix} E_x \\ E_y \end{pmatrix} = \begin{pmatrix} \rho_{\parallel} & 0 \\ 0 & \rho_{\perp} \end{pmatrix} \begin{pmatrix} \cos\theta & \sin\theta \\ -\sin\theta & \cos\theta \end{pmatrix} \begin{pmatrix} J_x \\ J_y \end{pmatrix},$$

$$\begin{pmatrix} E_x \\ E_y \end{pmatrix} = \begin{pmatrix} \cos\theta & \sin\theta \\ -\sin\theta & \cos\theta \end{pmatrix}^{-1} \begin{pmatrix} \rho_{\parallel} & 0 \\ 0 & \rho_{\perp} \end{pmatrix} \begin{pmatrix} \cos\theta & \sin\theta \\ -\sin\theta & \cos\theta \end{pmatrix} \begin{pmatrix} J_x \\ J_y \end{pmatrix},$$

$$\begin{pmatrix} E_x \\ E_y \end{pmatrix} = \frac{1}{\cos^2\theta + \sin^2\theta} \begin{pmatrix} \cos\theta & -\sin\theta \\ \sin\theta & \cos\theta \end{pmatrix} \begin{pmatrix} \rho_{\parallel} & 0 \\ 0 & \rho_{\perp} \end{pmatrix} \begin{pmatrix} \cos\theta & \sin\theta \\ -\sin\theta & \cos\theta \end{pmatrix} \begin{pmatrix} J_x \\ J_y \end{pmatrix},$$

$$\begin{pmatrix} E_x \\ E_y \end{pmatrix} = \begin{pmatrix} \cos\theta\,\rho_{\parallel} & -\sin\theta\,\rho_{\perp} \\ \sin\theta\,\rho_{\parallel} & \cos\theta\,\rho_{\perp} \end{pmatrix} \begin{pmatrix} \cos\theta & \sin\theta \\ -\sin\theta & \cos\theta \end{pmatrix} \begin{pmatrix} J_x \\ J_y \end{pmatrix},$$

$$\begin{pmatrix} E_x \\ E_y \end{pmatrix} = \begin{pmatrix} \cos^2\theta\,\rho_{\parallel} + \sin^2\theta\,\rho_{\perp} & \cos\theta\sin\theta\,(\rho_{\parallel} - \rho_{\perp}) \\ \cos\theta\sin\theta\,(\rho_{\parallel} - \rho_{\perp}) & \sin^2\theta\,\rho_{\parallel} + \cos^2\theta\,\rho_{\perp} \end{pmatrix} \begin{pmatrix} J_x \\ J_y \end{pmatrix},$$

$$\begin{pmatrix} E_x \\ E_y \end{pmatrix} = \begin{pmatrix} \rho_{\parallel} - (\rho_{\parallel} - \rho_{\perp})\sin^2\theta & \cos\theta\sin\theta\,(\rho_{\parallel} - \rho_{\perp}) \\ \cos\theta\sin\theta\,(\rho_{\parallel} - \rho_{\perp}) & \rho_{\perp} - (\rho_{\perp} - \rho_{\parallel})\sin^2\theta \end{pmatrix} \begin{pmatrix} J_x \\ J_y \end{pmatrix} \quad (3)$$

For $J_y = 0$, we obtain

$$E_x = [\rho_{\parallel} - (\rho_{\parallel} - \rho_{\perp})\sin^2\theta] J_x,$$

$$E_y = (\rho_{\parallel} - \rho_{\perp}) \cos\theta \sin\theta\, J_x.$$

Note that, in this case, a transversal voltage drop $\propto E_y$ is obtained when $\theta \neq 0$ and $\theta \neq \pi/2$. By analogy, this effect is called the planar Hall effect. It is noteworthy that the terminology planar Hall effect is misleading because the phenomenon at play is unrelated to Hall effects. The terminology transverse AMR is sometimes preferred.

b) Use 4-point resistance measurements and a known geometry [I. Miccoli *et al*, J. Phys. Cond. Mat. **27**, 223201 (2015)].

Set $I_x \neq 0$ and $I_y = 0$.

Monitor V_x, to get R_x.

Use a magnet to apply an external magnetic field at $\theta = 0$ and get $\rho_\parallel$; and at $\theta = 90°$ and get $\rho_\perp$.

Use 4-point resistance measurements and a known geometry.

Use a magnet to apply an external magnetic field and set $\theta = 0$.

Set $I_x \neq 0$ and $I_y = 0$ and monitor V_x, to get R_x and then $\rho_\parallel$.

Set $I_x = 0$ and $I_y \neq 0$ and monitor V_y, to get R_y and then $\rho_\perp$.

Orders of magnitude: *mm* device, *mA*, tenth of *Ohms*, *mV*

c) For Ni, $\frac{\Delta\rho}{\rho} \sim 2.5\%$ at room temperature.

The AMR effect was used in the first generation of sensors, like read heads in hard disk drives. Nowadays, most sensors are based on tunnel magnetoresistance with orbital filtering. Typical values of magnetoresistance are now greater than 100%. The temperature-dependence of AMR sensors can still be a plus for some applications.

d) From Eq. (3) we can deduce the following:

For J_{15}, we have θ=0

$V_{15} = \rho_\parallel J_{15}/d$

$V_{37} = 0$

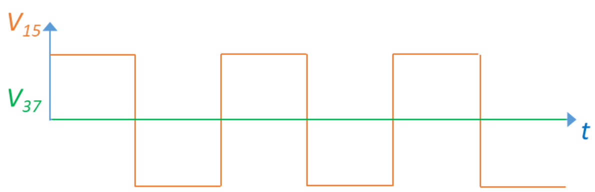

For J_{84}, we have θ=-45°

$V_{84} = (\rho_\parallel + \rho_\perp)J_{84}/(2d)$

$V_{26} = -(\rho_\parallel - \rho_\perp)J_{84}/(2d)$

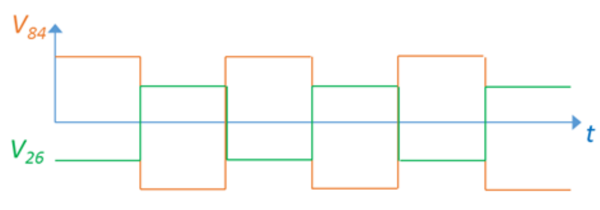

For J_{73}, we have θ=-90°

$V_{73} = \rho_{\perp} J_{73}/d$

$V_{15} = 0$

For J_{62}, we have θ=-135°

$V_{62} = (\rho_{\parallel} + \rho_{\perp}) J_{84}/(2d)$

$V_{84} = (\rho_{\parallel} - \rho_{\perp}) J_{62}/(2d)$

e) The AMR effect is even in magnetization, *i.e.* it is invariant on magnetization reversal. It can be shown that $\frac{\Delta\rho}{\rho} \propto (\boldsymbol{M}.\boldsymbol{J_e})^2$. The AMR responses from the two sublatices add up. Using the AMR effect is hence appropriate for characterizing/detecting a collinear antiferromagnet [P. Wadley *et al*, Science **351**, 587 (2016)].

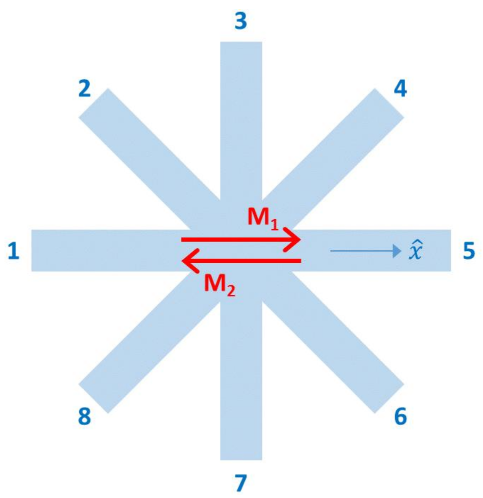

Solutions to exercise 2

a1) The relation between J_s and μ_s is

$$J_s = \frac{1}{2e\rho_N}\frac{d\mu_s}{dy} \qquad (a1)$$

Note: take $\sigma^{\uparrow} = \sigma^{\downarrow} = \sigma_N/2$

a2) The time-variation of the spin density $\widetilde{\mu_s}$ results in spin diffusion, which is balanced by spin scattering. The transport equation becomes

$$\frac{d\widetilde{\mu_s}}{dt} = D\frac{d^2\widetilde{\mu_s}}{dy^2} - \frac{\widetilde{\mu_s}}{\tau_{sf}^*},$$

$$i\omega\mu_s = D\frac{d^2\mu_s}{dy^2} - \frac{\mu_s}{\tau_{sf}^*},$$

$$\frac{d^2\mu_s}{dy^2} - \frac{1}{{l_{sf}^{\#}}^2}\mu_s = 0 \qquad (a2)$$

with $l_{sf}^{\#} = \frac{l_{sf}^*}{\sqrt{1+i\omega\tau_{sf}^*}}$ and $l_{sf}^* = \sqrt{D\tau_{sf}^*}$, where D is the diffusive constant and τ_{sf}^* is the average spin-flip scattering rate.

a3) We have $l_{sf}^{\#} = \frac{l_{sf}^*}{\sqrt{1+i\omega\tau_{sf}^*}}$ with $\omega\tau_{sf} = 2\pi f\tau_{sf}^*$. The typical value of the resonance frequency for a ferromagnet is $f \sim 10\ GHz$ (with $\mu_0 H$~0.1 T), and the typical value of spin-flip scattering rate is $\tau_{sf}^* \sim 1\ ps$, so $\omega\tau_{sf}^* \sim 10^{11} \times 10^{-14} \ll 1$ => $l_{sf}^{\#} \sim l_{sf}^*$. Note that this condition is no longer true in the THz regime, for example for antiferromagnetic resonance. In the following, we consider that $l_{sf}^{\#} = l_{sf}^*$.

a4) At the boundaries, we have:

for $y = 0, J_s = \frac{1}{2e\rho_N}\frac{d\mu_s}{dy}(0) = J_s^0,$

for $y = d_N, J_s = \frac{1}{2e\rho_N}\frac{d\mu_s}{dy}(d_N) = 0.$

a5) The solution of Eq. (a2) takes the form

$$\mu_s(y) = Ae^{y/l_{sf}^*} + Be^{-y/l_{sf}^*},$$

for $y = 0, \frac{1}{2e\rho_N}\frac{d\mu_s}{dy} = J_s^0$ => $A - B = 2e\rho_N J_s^0 l_{sf}^*$

for $y = d_N, \frac{1}{2e\rho_N}\frac{d\mu_s}{dy} = 0$ => $B = Ae^{2d_N/l_{sf}^*}$

$$\mu_s(y) = 2e\rho_N J_s^0 \frac{l_{sf}^*}{1-e^{2d_N/l_{sf}^*}}\left(e^{y/l_{sf}^*} + e^{-y/l_{sf}^*}e^{2d_N/l_{sf}^*}\right)$$

$$\mu_s(y) = 2e\rho_N J_s^0 \frac{e^{-d_N/l_{sf}^*}}{e^{-d_N/l_{sf}^*}} \frac{l_{sf}^*}{1-e^{2d_N/l_{sf}^*}} \left(e^{y/l_{sf}^*} + e^{-y/l_{sf}^*} e^{2d_N/l_{sf}^*}\right)$$

$$\mu_s(y) = -2e\rho_N J_s^0 l_{sf}^* \frac{\cosh\left((y-d_N)/l_{sf}^*\right)}{\sinh\left(d_N/l_{sf}^*\right)}$$

a6) Using the result of question a5) and Eq. (a1), we obtain

$$J_s(y) = -J_s^0 \frac{\sinh\left((y-d_N)/l_{sf}^*\right)}{\sinh\left(d_N/l_{sf}^*\right)} \qquad \text{(a6)}$$

b1) $J_e = \langle J_e(y)\rangle = \frac{1}{d_N}\int_0^{d_N} \theta_{SHE} J_s(y)dy = -\frac{1}{d_N}\int_0^{d_N} \theta_{SHE} J_s^0 \frac{\sinh\left((y-d_N)/l_{sf}^*\right)}{\sinh\left(d_N/l_{sf}^*\right)}\, dy$

$$J_e = -\theta_{SHE} J_s^0 \frac{1}{d_N} \frac{1}{\sinh\left(d_N/l_{sf}^*\right)} \int_0^{d_N} \sinh\left((y-d_N)/l_{sf}^*\right)dy$$

$$J_e = -\theta_{SHE} J_s^0 \frac{l_{sf}^*}{d_N} \frac{1-\cosh\left(d_N/l_{sf}^*\right)}{\sinh\left(d_N/l_{sf}^*\right)} = -\theta_{SHE} J_s^0 \frac{l_{sf}^*}{d_N} \frac{1-2\sinh^2\left(d_N/\left(2l_{sf}^*\right)\right)+1}{2\sinh\left(d_N/(2l_{sf})\right)\cosh\left(d_N/\left(2l_{sf}^*\right)\right)}$$

$$J_e = \theta_{SHE} \frac{l_{sf}^*}{d_N} \tanh\left(\frac{d_N}{2l_{sf}^*}\right) J_s^0$$

$$J_e = \theta_{SHE} \frac{l_{sf}^*}{d_N} \tanh\left(\frac{d_N}{2l_{sf}^*}\right) J_s^0$$

b2) $I = J_e l d_N = \theta_{SHE} l l_{sf}^* \tanh\left(\frac{d_N}{2l_{sf}^*}\right) J_s^0$

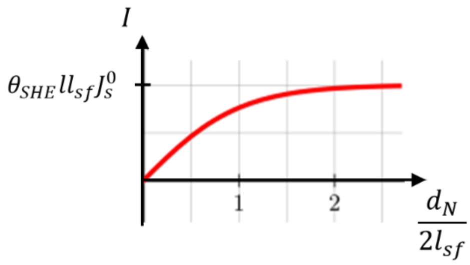

For $d_N \ll l_{sf}^*$, $I \sim \theta_{SHE} l \frac{d_N}{2} J_s^0$. Spins are still coherent and get converted efficiently in the N layer. The thicker the layer, the more spins are converted.

For $d_N \gg l_{sf}^*$, $I = \theta_{SHE} l l_{sf}^* J_s^0$. The signal levels out. The part of the N layer in contact with the F layer ($d_N < 2 - 3l_{sf}^*$) converts spins. Above $d_N \sim 2 - 3l_{sf}^*$ spin-charge conversion becomes inefficient because the spins are depolarized.

b2) $V_{ISHE} = \frac{R_F R_N}{R_{F+}R_N} I = \frac{\frac{\rho_F w}{l d_F}\frac{\rho_N w}{l d_N}}{\frac{\rho_F w}{l d_F}+\frac{\rho_N w}{l d_N}} J_e l d_N$

$$V_{ISHE} = \frac{w d_N}{d_N \sigma_N + d_F \sigma_F} J_e$$

$$V_{ISHE} = \theta_{SHE} \frac{w l_{sf}^*}{d_N \sigma_N + d_F \sigma_F} \tanh\left(\frac{d_N}{2 l_{sf}^*}\right) J_s^0$$

b3) The Hall angle is $\theta_{SHE} \sim 6\%$ and the 'spin-charge conversion efficiency' is $\theta_{SHE} l_{sf}^* \sim 0.18\ nm$ [J. C. Rojas-Sanchez *et al*, Phys. Rev. Lett. **112**, 106602 (2014)].

b4) Increasing the number of scattering centers will increase the extrinsic contribution to θ_{SHE}, because for this extrinsic contribution $\theta_{SHE} \propto \frac{1}{l_{sf}^*}$, and increasing the number of scatterers will reduce l_{sf}^*. This solution is however not appropriate to increase the 'spin-charge conversion efficiency' because $\theta_{SHE} l_{sf}^*$ will remain unchanged.

Increasing the scattering efficiency by using heavier materials, with a large atomic number *Z*, is another solution to increase θ_{SHE}. Because spin-orbit interactions roughly vary as Z^4, this solution will results in a large increase of 'spin-charge conversion efficiency'. Note however that other effects contribute to θ_{SHE} and the picture presented above is certainly more complicated. In particular, intrinsic contributions do matter.

c1) $\bar{\Gamma} = 2\omega \frac{\mu_0 M_S |\gamma| \sin^2(\theta_M) + \sqrt{(\mu_0 M_S \gamma \sin^2(\theta_M))^2 + 4\omega^2}}{(\mu_0 M_S \gamma \sin^2(\theta_M))^2 + 4\omega^2}$

γ is in unit of *Hz.T*$^{-1}$; $\mu_0 M_S$ is in *T*; and ω is in *Hz*, so we can conclude that $\bar{\Gamma}$ is a dimensionless parameter.

c2) For θ_M=0, $\bar{\Gamma} = 1$. By definition, the magnetization trajectory in the *(x,y)* plane is circular. In this case, the magnetization rotates about the out-of-plane direction. If there is no in-plane anisotropy, it is expected that the trajectory is circular. It would not be the case in the presence of an in-plane anisotropy.

c3) The magnetization is mostly in-plane, whatever the angle of the applied field. This is because of the demagnetizing field.

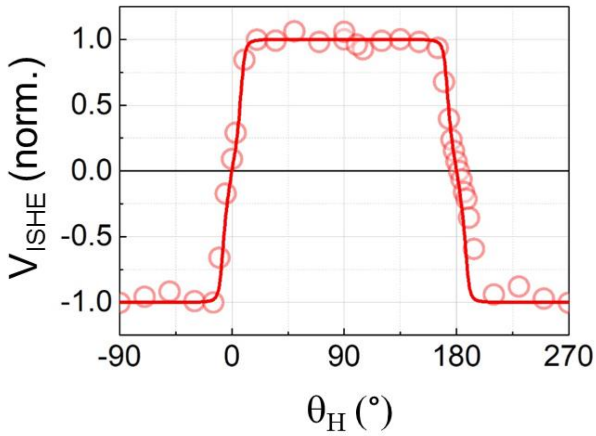

From O. Gladii *et al*, Phys. Rev. B **100**, 174409 (2019).

V_{ISHE} is an odd function of ***H***. Angular-dependent symmetries are useful to disentangle the inverse spin Hall effect and several others that may occur concurrently [M. Harder *et al*, Phys. Rep. **661**, 1 (2016)]. When two effects share the same angular-dependent symmetries, frequency-, temperature-, stacking order- etc. dependences are used to unravel the contributions.